32 5
6/24/64

ORNL-3617
UC-25 – Metals, Ceramics, and Materials
TID-4500 (30th ed.)

DIFFUSION IN BODY-CENTERED CUBIC METALS ZIRCONIUM, VANADIUM, NIOBIUM, AND TANTALUM

Ted Sadler Lundy

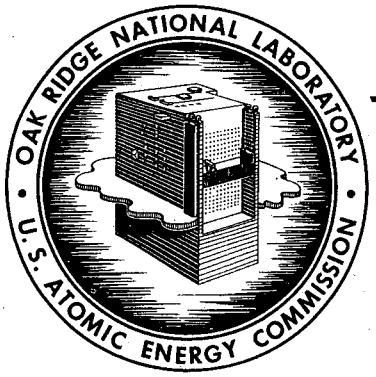

OAK RIDGE NATIONAL LABORATORY
operated by
UNION CARBIDE CORPORATION
for the
U.S. ATOMIC ENERGY COMMISSION

DISCLAIMER

ORNL-3617

Contract No. W-7405-eng-26

Metals and Ceramics Division

DIFFUSION IN BODY-CENTERED CUBIC METALS ZIRCONIUM, VANADIUM, NIOBIUM, AND TANTALUM

Ted Sadler Lundy

Submitted as a dissertation to the Graduate Council of The University of Tennessee in partial fulfillment of the requirements for the degree of Doctor of Philosophy

JUNE 1964

OAK RIDGE NATIONAL LABORATORY
Oak Ridge, Tennessee
operated by
UNION CARBIDE CORPORATION
for the
U. S. ATOMIC ENERGY COMMISSION

ACKNOWLEDGMENTS

The author is deeply indebted to many members of the staff of the Oak Ridge National Laboratory for guidance and assistance during the course of this work. Special thanks are due Dr. C. J. McHargue, Dr. E. E. Stansbury, and Dr. J. H Frye, Jr., for their encouragement and interest.

Members of the Metals and Ceramics Division who have actively participated in the experimental work are Drs. R. E. Pawel and F. R. Winslow, T. L. Boswell, J. I. Federer, J. F. Murdock, R. A. Padgett, and J. H. Terry. Contributions by two summer employees, F. G. Arcella and J. J. Arcella, were invaluable. Drs. W. K. Biermann and D. Heitkamp, temporary employees from Germany, assisted in evaluating the significance of the experimental findings.

Dr. J. J. Pinajian and others of the Isotopes Division and Dr. W. Laing of the Analytical Chemistry Division contributed to this work in supplying the radioactive tracers and in preparing materials analyses, respectively.

The author wishes to thank W. C. Colwell for assistance in preparing the figures and Dolores Poe for typing the rough draft. Special thanks are extended to Geneva Harris for her superb performance in typing the final manuscript.

Finally, the author thanks the Oak Ridge National Laboratory for allowing him to participate in its educational assistance program.

ABSTRACT

The importance of refractory, body-centered cubic metals and alloys has increased rapidly with the development of high-temperature nuclear reactors and space vehicles. Prior to about 1960 only a small amount of data was available on atomic mobilities within metals and alloys of this type. Designers had to rely principally on empirical rules obtained from investigations of face-centered cubic metals when they were faced with problems requiring a knowledge of diffusion. This study was initiated with the objective of defining the characteristics of diffusion in body-centered cubic metals with particular attention being given to the temperature dependence of the diffusion coefficient and the applicability of various empirical relationships.

The first experiments were directed to the resolution of large differences in self-diffusion coefficients reported by several investigators for beta zirconium. These differences as reported in terms of D_o and Q in the Arrhenius-type expression,

$$D = D_o \exp\left(-\frac{Q}{RT}\right),$$

have been explained in terms of the failure of this equation to describe such data over large temperature intervals. Both D_o and Q were found to be temperature dependent for diffusion in this system. The empirical rules involving melting point, heat of fusion, etc., were therefore found to be inapplicable because they assume the activation energy Q to be constant with temperature. This study has shown that the pre-exponential factor D_o varies with a power of temperature and that Q

varies linearly with temperature for diffusion of both zirconium-95 and niobium-95 in beta zirconium.

Since the discovery that the Arrhenius equation does not adequately describe the temperature dependence of the diffusion coefficient in beta zirconium has far-reaching implications, it was important to study other systems over wide temperature intervals to find if the equation is, in general, inapplicable. Similar results were obtained for diffusion of vanadium-48 in vanadium. This work was done to check the possibility that the phase transformation in zirconium might somehow be responsible for the unusual results. It clearly shows that such is not the explanation.

Then, an experimental study of the diffusion of niobium-95 in niobium was begun. For the high-temperature diffusion anneals ($T > 1500°C$), it was possible to use standard sectioning techniques to obtain diffusion coefficients. For the lower temperature work, it was necessary to develop a new technique of sectioning. This method, based on anodizing and stripping of the thin anodic layers, permits measurement of diffusion coefficients as low as 10^{-20} square centimeters per second for diffusion in both niobium and tantalum. This resolution is at least five orders of magnitude smaller than those previously obtained by a direct method. Using this technique, measurements were made down to about 1000°C. These precision measurements permitted a detailed study of the so-called near-surface effect previously reported and showed that a penetration plot for diffusion from a thin source of isotope has three regions associated with it — a

near-surface region, a normal region, and a short-circuiting region. The surface effects were shown to be much more common than had been generally realized. Upon analyzing the normal regions of each penetration plot, diffusion coefficients for niobium-95 in niobium were found to follow the Arrhenius-type expression over nearly seven orders of magnitude from 2450 to about 1200°C. Deviations occurred at lower temperatures, but these deviations may be due to interaction of the different regions of diffusion. Oxygen content variations were found to have little effect on the diffusion of niobium-95 in niobium. Cursory data were also obtained for the diffusion of tantalum-182 in niobium.

A few experiments have been done on the diffusion of niobium-95 in tantalum at low temperatures. These tests, accomplished by using the anodizing and stripping technique, clearly show the near-surface region at temperatures of 1050 to 1250°C.

TABLE OF CONTENTS

LIST OF TABLES

LIST OF FIGURES

FIGURE PAGE

CHAPTER I

INTRODUCTION

The importance of refractory, body-centered cubic metals and alloys has increased rapidly with the development of high-temperature nuclear reactors and space vehicles. Prior to about 1960, only a small amount of data was available on atomic mobilities within metals and alloys of this type. Designers had to rely principally on empirical rules obtained from investigations of face-centered cubic metals when they were faced with problems requiring a knowledge of diffusion.

This study represents an attempt to supply information that is needed not only for practical purposes but for basic understandings of diffusion in body-centered cubic systems. Diffusion coefficients were determined over wide ranges of temperatures for several systems — zirconium-95 and niobium-95 in beta zirconium, vanadium-48 in vanadium, and niobium-95 in niobium. Data were also obtained on diffusion of tantalum-182 in niobium and niobium-95 in tantalum.

I. GENERAL

According to the dictionary (1), diffusion is "a spontaneous process of equalization of physical states, as of temperature by heat conduction or of gases when one gas is liberated in another." Crank (2) has defined diffusion as "the process by which matter is transported from one part of a system to another as a result of random molecular motions," while Jost (3) has stated that "diffusion is a process which

leads to an equalization of concentration within a single phase." An example given by Seith (4) of the mixing that occurs with time after one pours water onto a $CuSO_4$ solution gives an intuitive picture of the physical significance of the process of diffusion.

Man has long been interested in the role of diffusion in natural processes. For example, in the first systematic study of diffusion in the solid state, Roberts-Austen (5) discussed the history of diffusion by referring to such observations as "kernel roasting used as early as 1692" and "cementation processes described in the eighth century by Gerber." In recent years there has been considerable effort to relate such things as the rates of solid-state transformations, creep in metals and alloys, and corrosion phenomena to atomic and/or molecular diffusion processes.

Ostwald's statement published in 1891 and quoted by Roberts-Austen (5) that "to make accurate experiments on diffusion is one of the most difficult problems in practical physics" certainly held true until after World War II when radioactive tracers became readily available. In fact, even today wide differences are sometimes reported (6,7) in diffusion data obtained by different investigators presumably using similar techniques. The large discrepancies can usually be traced to some anomalous behavior not understood by the investigators (8); but still the problems of temperature calibration and measurement exist and often cause large differences in data obtained by different investigators.

In this thesis, consideration will be given only to diffusion that occurs in the crystalline state. Three principal mechanisms by which diffusion can take place have been suggested. The first and most widely advocated of these mechanisms, at least for a substitutional-type process, involves migration of vacant lattice sites within the crystalline lattice. Naturally, as vacancies move in one direction, atoms move in the opposite direction so that a net flow of atoms results. An interstitial mechanism whereby relatively small atoms move by way of the natural spacings between atoms in the lattice is accepted as being the primary mechanism for diffusion where there are extreme differences in sizes of the solvent and solute atoms (i.e., carbon in iron). A third possible mechanism involves interchange of atoms by a simultaneous jump process. This ring mechanism might involve two, as in the case of a simple interchange, or more atoms for a basic event. Calculations (9) involving energies required for the ring mechanism to take place have shown that the four-atom jump is more likely to occur than is the more easily visualized two-atom interchange.

The diffusion coefficient D is generally defined in terms of the first law of Fick which in a one-dimensional isotropic system is

$$J = - D \frac{\partial c}{\partial x} \qquad (1)$$

where J is the quantity of substance diffusing per unit time perpendicularly through a unit cross-sectional area under a concentration gradient $\partial c/\partial x$ in the direction of J. In this equation, the negative sign is introduced so that the quantity D will have a positive sign.

This is necessary because J is positive when $\partial c/\partial x$ is negative. Since it is usually inconvenient and often experimentally difficult to measure J and $\partial c/\partial x$, one generally uses a solution to the second law of Fick, which describes the non-steady state. The second law,

$$\frac{\partial c}{\partial t} = \frac{\partial}{\partial x}\left(D \frac{\partial c}{\partial x}\right), \tag{2}$$

may be obtained from the first by applying the law of conservation of matter over a volume element into and out of which matter is being transferred by the diffusion process.

If, as will be the case throughout this study, the diffusion coefficient can be considered independent of both species concentration and position in the specimen, the second law of Fick becomes

$$\frac{\partial c}{\partial t} = D \frac{\partial^2 c}{\partial x^2} . \tag{3}$$

Solutions to this equation are then found for the boundary conditions encountered in the experiments and diffusion coefficients are calculated from the data.

For the present work, two particular solutions to equation 3 are important. If an infinitesimally thin film of radioactive isotope is deposited on the flat surface of a specimen having a thickness greater than the ensuing penetration and if the specimen is held at a temperature T for a time t, the resulting distribution of activity is given by (2)

$$A(x) = \frac{M}{\sqrt{\pi D t}} \exp\left(-\frac{x^2}{4Dt}\right) \tag{4}$$

where

$A(x)$ = the specific activity at a distance x from the original isotope layer, and

M = the total activity originally deposited on the specimen per unit surface area.

If the stated boundary conditions are obeyed, plots of the experimental data as $\ell n\ A(x)$ versus x^2 should yield straight lines having slopes equal to $-(4Dt)^{-1}$.

Since measurements of thicknesses of deposited layers of activity are usually difficult and uncertain, it is important to examine the situation where the thicknesses are not "infinitesimally thin." If the thickness of the deposited isotope layer is h, the solution to the second law becomes (2)

$$A(x) = \frac{A_o}{2}\left[\ \mathrm{erf}\left(\frac{h-x}{2\sqrt{Dt}}\right) + \mathrm{erf}\left(\frac{h+x}{2\sqrt{Dt}}\right)\right] \qquad (5)$$

where A_o represents the specific activity in the deposited layer and $\mathrm{erf}\ u \equiv 2/\sqrt{\pi}\ \int_o^u \exp\ (-\xi^2)\ d\xi$. Examination of equation 5 reveals that, for large values of h relative to values of $0.1\sqrt{Dt}$, plots of $\ell n\ A(x)$ versus x^2 become concave downward near $x = 0$. Thus, a criterion for the deposit thickness being too large for application of equation 4, page 4, might be such a deviation from linearity on this type plot.

There are three general methods of measuring the diffusion coefficient of a radioactive isotope in a solid. These three

methods — sectioning, surface decrease, and autoradiographic — will be described even though only the sectioning method was used in these experiments.

The sectioning method gives a direct measurement of the redistribution of the radioactive tracer in the samples. A series of sections is removed parallel to the original layer of isotope. The specific activity distribution from these sections is determined, and its analysis in terms of the proper solution to Fick's second law yields a value of the diffusion coefficient. The sections may be removed by a lathe, a microtome, a grinding apparatus, chemical methods, etc., depending on materials and diffusion distances. Prior to this study, the lowest diffusion coefficients that could be accurately determined by the sectioning method were about 10^{-15} square centimeters per second.

In the surface-decrease method, activity on the specimen surface is measured before and after a diffusion anneal. The decrease in surface activity with time at a given temperature can be related to the diffusion coefficient through appropriate solutions to the diffusion laws. This decrease stems from the fact that the radiation emitted by an atom is absorbed by the intervening mass of the specimen. The method thus requires an accurate knowledge of the radiation absorption properties of the specimen material. It is also necessary to show that the tracer is not lost by other means, such as evaporation. In theory, the lowest diffusion coefficient that can be found by this method or by modifications of it is about 10^{-18} square centimeters per second.

However, the data obtained by this technique have not generally been accepted as being reliable.

Autoradiographic techniques have become increasingly popular in the last few years. In particular, they have been used in several studies of diffusion in body-centered cubic metals (10–13). The method is facilitated by carefully sectioning the specimen at a small angle to the original active surface and placing a film against this new surface for exposure to the radiation. The exposure of the film is related to the specific activity of the specimen at various distances from the original isotope layer. The primary difficulty is one of correcting for the effects of exposure by unwanted radiations. With good technique, the method can give answers to within ten per cent of those obtained by sectioning methods (13).

II. THEORY

According to LeClaire (14), the diffusion coefficient is the product of two factors – one a mobility term and the other a term expressing the departure of the solution under consideration from ideality. This latter term multiplied by the concentration gradient is proportional to the so-called diffusion force acting on an atom. If the elementary process involves the net movement of only one atom, the diffusion coefficient D_i takes the form

$$D_i = G_i \, kT \left(1 + \frac{\partial \, \ell n \, \gamma_i}{\partial \, \ell n \, N_i} \right) \tag{6}$$

where

G_i = the mobility of the i^{th} particle (i.e., its average velocity under unit force),

γ_i = the activity coefficient, and

N_i = the mole fraction of the i^{th} component.

For the case of self-diffusion in a pure metal or for an ideal solution where $a_i = KN_i$, equation 6, page 7, reduces to the Einstein form

$$D_i = G_i kT , \tag{7}$$

so that measurement of the diffusion coefficient is also a direct measurement of the atomic mobility. In this study, either self-diffusion or impurity diffusion at very small solute concentrations was measured. The assumption may therefore be made that deviations from ideality are negligible and that equation 7 is applicable. Thus, measurements were made only of the mobility term in the diffusion coefficient, and the departure of the solution from ideality was not considered.

Now let us consider, following LeClaire (14), that ρ is the probability of migration and that n is the probability per second that a migration occurs along the direction of the free energy gradient. Then, G_i is the average velocity of a migrating atom under unit free energy gradient and v is the average velocity of an atom between equilibrium positions spaced the distance a apart. Then, $v = an$ and ρ is proportional to n and therefore v. So, the problem of arriving at

expressions for the atomic mobility G_i reduces to one of either determining reasonable expressions describing the probability of migration ρ or directly finding expressions for D. To this problem, there are three general approaches: (1) statistical, (2) reaction rate, and (3) kinetic. These will be described in the following three sections.

Simple Statistical Theory

In this approach given by Seitz (15), the statistical fluctuations of the atom are related directly to the diffusion coefficient D through an expression involving the concentration of vacant sites in the lattice; that is, a vacancy mechanism of diffusion is assumed. Consider an atom or molecule that is in position to move to an adjoining equilibrium lattice site. This atom has thermal energy and will be oscillating about an equilibrium position with a vibrational frequency f, whose exact value depends on the mass of the atom and the elastic forces. The amplitude of vibration depends on the amount of thermal energy possessed by the atom and varies because of thermal fluctuations. If the atom moves from one equilibrium position to another, the change in energy with position varies in a manner suggested by the schematic drawing in Figure 1. It is necessary that the atom pass over a potential barrier of height ϵ'. Application of Boltzmann's statistics suggests that the relative probability of finding the atom at the top of the barrier instead of in an equilibrium position such as 1 or 2 at any given time is

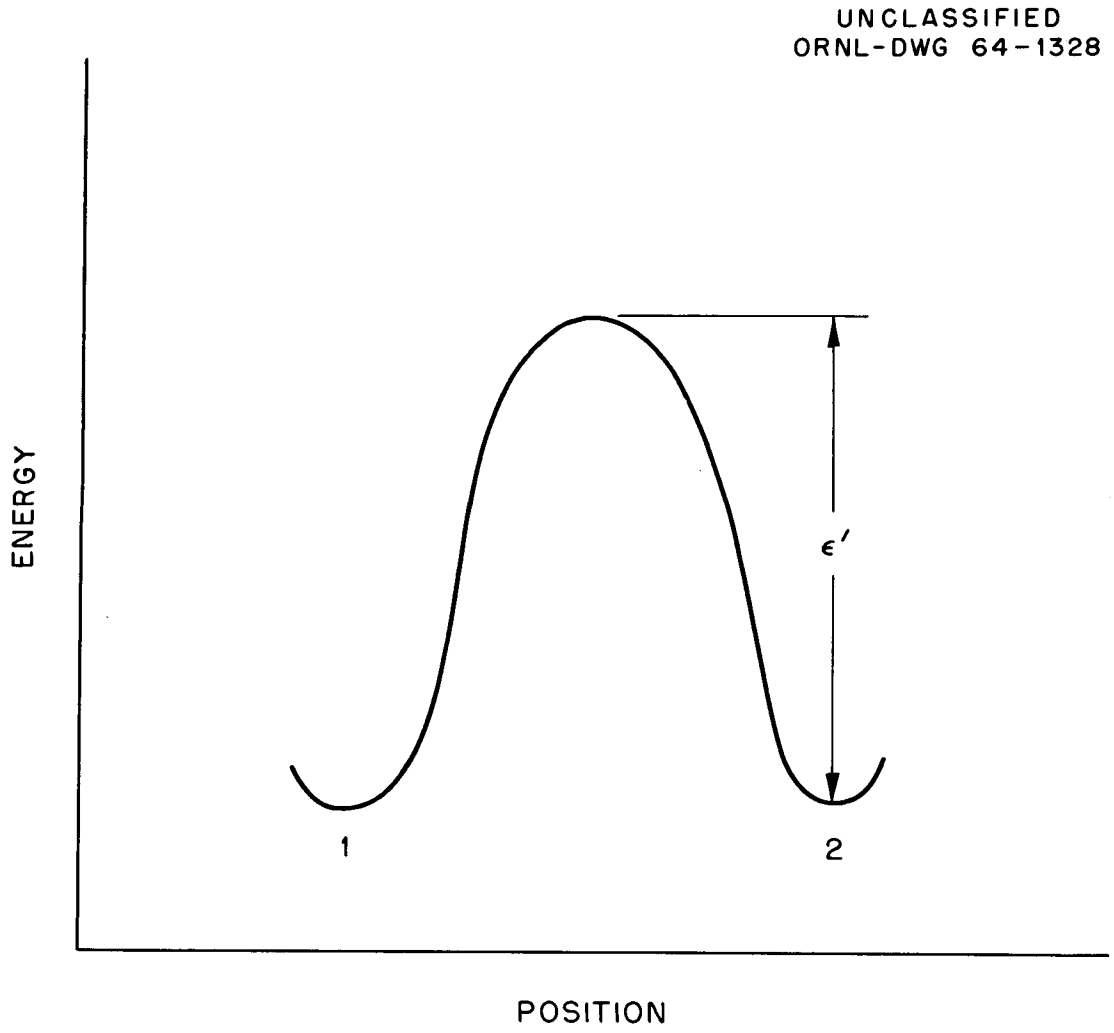

Figure 1. Schematic drawing of the energy of the atom versus position in the crystalline lattice relative to equilibrium positions 1 and 2.

$$p = \exp\ (-\epsilon'/kT) \tag{8}$$

where ϵ' is called the activation energy.

Each time the atom oscillates about its equilibrium lattice position there is a chance (given by equation 8) that it will cross the barrier. Thus, the probability per unit time or the jump frequency is

$$\nu = f \exp\ (-\epsilon'/kT)\ . \tag{9}$$

In the simple case, the diffusion coefficient is related to the jump frequency by

$$D = \nu a^2 \tag{10}$$

where a is the distance between equilibrium positions. If the mechanism involves a vacancy, ν must be multiplied by the probability of finding a vacancy in the adjacent lattice site. It can be shown by statistical mechanics that the number of vacancies n_v in a crystal having N lattice sites in thermal equilibrium at temperature T is given by

$$n_v/N = C \exp\ (-\epsilon_v/kT)\ , \tag{11}$$

where ϵ_v is the energy of formation of a vacant lattice site and C has a value of approximately unity and is almost temperature independent (16). Thus, for vacancy diffusion

$$D = a^2 f(n_v/N) \exp\ (-\epsilon'/kT) = a^2 fC \exp\ (-[\epsilon' + \epsilon_v]/kT)\ . \tag{12}$$

If the pre-exponential factor is taken to be constant, these expressions take the form

$$D = D_o \exp(-\epsilon/kT) = D_o \exp(-Q/RT) \qquad (13)$$

which, of course, is the form of the Arrhenius equation. In this application of simple statistical theory, no description of the barrier is made; hence, there is no justification for the assumption often made that equation 13 will accurately describe the temperature dependence of the diffusion coefficient.

Reaction Rate Theory

The diffusion process can be described in terms of the Wigner-Eyring treatment of reaction rates which is described in detail in the book by Glasstone, Laidler, and Eyring (17). In this treatment, diffusion is considered as a chemical reaction in the sense that the system is changed as a result of the diffusion processes. Seitz (15) has summarized the basic assumptions of the reaction rate theory as:

1. Whenever an atom moves in a chemical reaction, the accelerations of the nucleus are small enough that the electrons remain in the same state of motion at each instant of time. This is the same as if the nucleus were at rest. This assumption makes it possible to treat the energy of any group of atoms as if composed of a kinetic energy of nuclei motion and a configurational energy. The latter can be considered as the potential energy of interaction of the nuclei.

2. Quantum mechanics may be used to describe the motion of the nuclei.

3. The distribution of chemically identical units will be described by laws of statistical mechanics. This is equivalent to assuming that the kinetic and potential energy of the nuclei are distributed according to equilibrium statistics at each instant.

4. During the unit process of reaction, the coordinates of the nuclei change from one minimum of potential energy to another and pass through a maximum during the change. This gives the concept of the activated state shown in Figure 2.

According to statistical mechanics, the relative probability that one group of atoms will be in a given state at temperature T is

$$P = \overline{N} \exp (- \epsilon/kT) \tag{14}$$

where $\overline{N}$ is the number of different ways of putting the given group of atoms in the given state and ϵ is the energy of that state. The free energy per mole A is related to the molar energy E and molar entropy S by the expression

$$A = E - TS \tag{15}$$

where

$$S = N_o \, k \, \ell n \, \overline{N} \text{ and}$$

$$E = N_o \, \epsilon.$$

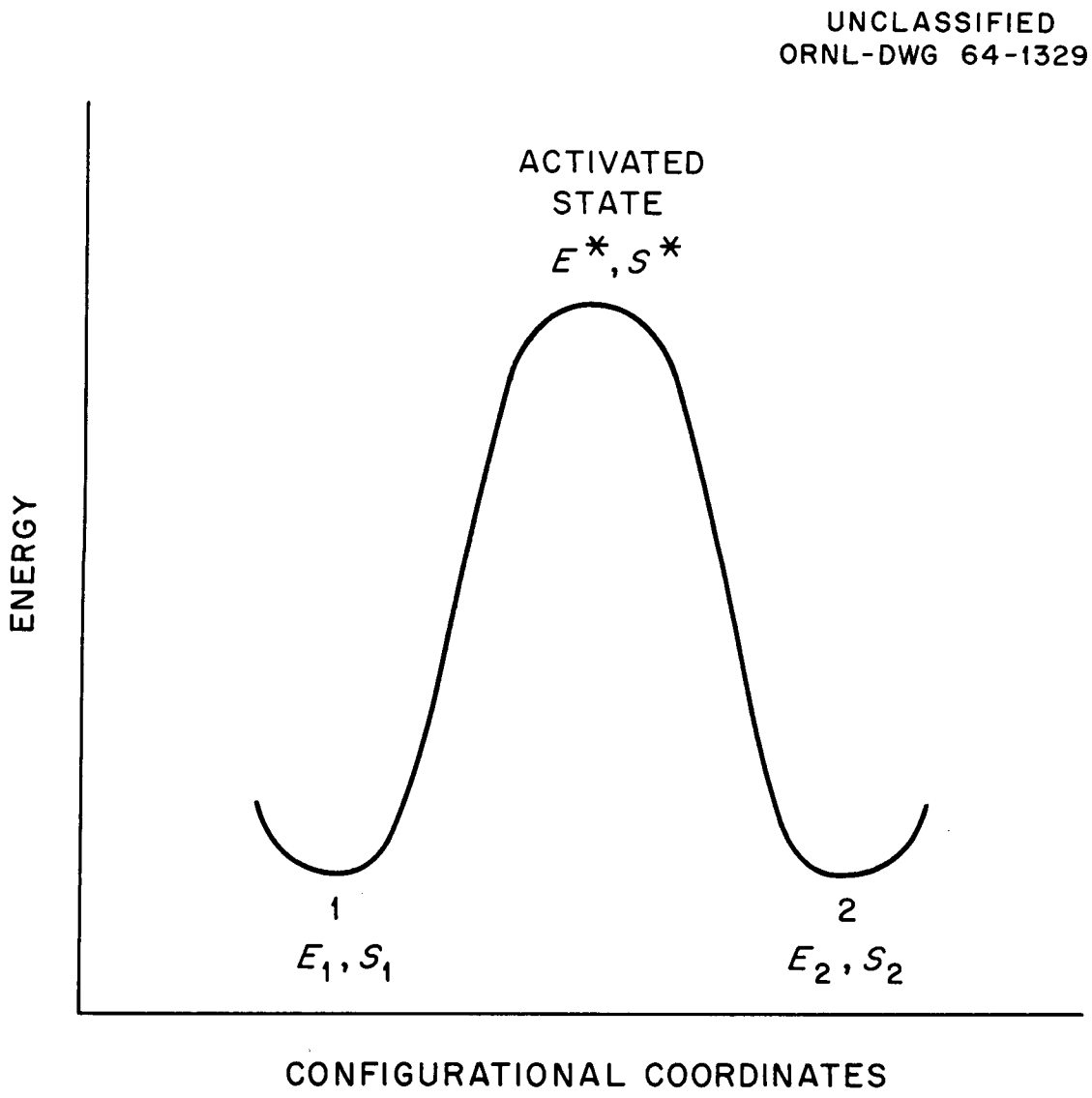

Figure 2. Schematic drawing of the energy of the atom versus configurational coordinates represented as molar energy E and molar entropy S for equilibrium lattice positions 1 and 2 and for the position of the activated state.

Equation 14, page 13, can be written in the form

$$P = \exp\left[-(E - RT\,\ell n\,\bar{N})/RT\right] = \exp\left(-A/RT\right) . \tag{16}$$

The ratio of the probabilities of finding groups in the stable positions 1 and 2 is

$$\frac{P_1}{P_2} = \exp\left[-(A_1 - A_2)/RT\right] . \tag{17}$$

The average rate at which groups pass from state 1 to state 2 is determined by the probability of finding a group at the saddle point of the energy surface (or in the activated state) multiplied by the velocity with which it moves past the saddle point. An exact calculation of these quantities requires a description of the energy surface. Under the conditions assumed by Seitz (15), the probability per unit time that a given group makes the transition over the saddle point to state 2 is given by

$$(1-R)\left(\frac{kT}{h\nu_s}\right)^2 \frac{(2\pi MkT)^{1/2}}{h}\left(\frac{kT}{2\pi M}\right)^{1/2} \exp\left[-(A^* - A_1)/RT\right] . \tag{18}$$

The factors in this expression have the following meaning: (1) R is the probability that the system will be diffracted or reflected back in attempting to pass the barrier even if it has sufficient energy, and is determined by the wave properties of matter; (2) $(kT/h\nu_s)^2$ represents the probability of finding the group at the saddle point because of vibration in a direction normal to the direction of flow over the saddle, ν_s is the frequency of oscillation normal to the saddle point;

(3) $(2\pi MkT)^{1/2}/h$ represents the probability associated with the motion of the group in the direction of flow, M being the reduced mass;

(4) $(kT/2\pi M)^{1/2}$ is the velocity of motion over the barrier; and

(5) $A^* = E^* - TS^*$ is the free energy per mole of the unit groups under consideration when existing at the saddle point.

The usual form of jump frequency for a unit process is $\nu = f \exp(-\Delta E/RT)$ and equation 18, page 15, may be put into the form (15)

$$\nu_{12} = f_1 \exp\left[-(E^*-E_1)/RT\right] \tag{19}$$

where

$$f_1 = R\left(\frac{kT}{h}\right)^2 \frac{(2\pi MkT)^{1/2}}{h}\left(\frac{kT}{2\pi M}\right)^{1/2} \exp\left[(S^*-S_1)/R\right] \tag{20}$$

in which f_1 represents the vibrational frequency. The jump frequency for the reverse process is

$$\nu_{21} = f_2 \exp\left[-(E^*-E_2)/RT\right] . \tag{21}$$

If equilibrium is achieved and if n_1 and n_2 are the number of atoms in two successive planes of atoms, then

$$n_1\nu_{12} = n_2\nu_{21} \tag{22}$$

so that

$$\frac{n_1}{n_2} = \frac{f_2}{f_1}\exp\left(-\frac{E_1-E_2}{RT}\right) = \exp\left(-\frac{A_1-A_2}{RT}\right) . \tag{23}$$

This concentration will be uniform; that is, $n_1 = n_2$ only when $A_1 = A_2$. Note that equation 23, page 16, contains no terms descriptive of the activated state.

An alternate way of finding the rate of migration is to assume that an equilibrium exists between atoms in their normal positions and those in the activated state at the top of the barrier. The rate of passage of atoms from 1 to 2 is then determined by the rate at which atoms in this activated state pass along the top of the barrier. The diffusion coefficient is given by (17)

$$D = a^2 \frac{kT}{h} \frac{F^*}{F} \exp\left(-\frac{E_o}{RT}\right) = a^2 \frac{kT}{h} \exp(\Delta S/R) \exp(-\Delta H/RT) \qquad (24)$$

where F and F^* are partition functions for the equilibrium and activated states, respectively, and ΔS and ΔH are differences in entropy and enthalpy for those states.

In order for there to be a net flux of atoms in one direction, there must be a free energy gradient or force per atom due to a concentration gradient or vacancy current. The force per atom is given by (14)

$$\frac{1}{N_o} \frac{\partial \mu_i}{\partial x} = kT \frac{\partial N_i}{\partial x} \frac{1}{N_i} \qquad (25)$$

for ideal solutions, where N_i is the mole fraction of i and μ_i is its chemical potential. The effect of this will be to shift the potential barrier by an amount of δE relative to each equilibrium position

(increasing it relative to one and decreasing it relative to the other). This change is equal to

$$\delta E = \frac{1}{N_o} \frac{\partial \mu}{\partial x} \frac{a}{2} . \tag{26}$$

The probability of migration from 1 to 2 now exceeds that of 2 to 1 so that there is a net flow of atoms. The number of migrations per second is given by

$$n = \frac{1}{m} A \exp [- (\Delta E - \delta E)/kT] \exp [- (\Delta E + \delta E)/kT] . \tag{27}$$

When $\delta E << kT$, then

$$n = \frac{1}{m} 2A \frac{\delta E}{kT} \exp [- \Delta E/kT] = \frac{1}{kT} \frac{A}{m} a \exp [- \Delta E/kT] \frac{1}{N_o} \frac{\partial \mu}{\partial x} \tag{28}$$

where A is related to the probability of migration and 1/m is a geometrical factor.

Since the average velocity of a diffusing atom is the probability per second of a migration times the distance between equilibrium positions, or (14)

$$v = na , \tag{29}$$

then

$$v = \frac{1}{kT} \frac{A}{m} a^2 \exp (-\Delta E/kT) \frac{1}{N_o} \frac{\partial \mu}{\partial x} . \tag{30}$$

The factor $\frac{1}{N_o} \frac{\partial \mu}{\partial x}$ is a force; hence the mobility is

$$G = \frac{1}{kT} \frac{A}{m} a^2 \exp (- \Delta E/kT)$$

or (31)

$$GkT = \frac{A}{m} a^2 \exp (- \Delta E/kT) = \frac{a^2}{m} \rho \ .$$

According to equation 7, page 8, the diffusion coefficient for self-diffusion in an ideal solution is equal to GkT.

Kinetic Theory

Another way of developing the diffusion coefficient from the above concepts of reaction rates is based on the assumption that the rate of crossing the barrier is very much more rapid than the rate at which the activation energy is accumulated. In this case, the probability ρ of migration is proportional to the probability per unit time that the atom or atoms participating in the unit process possess energy greater than or equal to ΔE and is given by (14)

$$\rho = P\nu \frac{1}{(s-1)!} \left(\frac{\Delta E}{kT} \right)^{s-1} \exp (- \Delta E/kT) \qquad (32)$$

where ν is the average frequency of thermal vibrations and s is the number of degrees of freedom over which ΔE is accumulated.
When s = 1, this reduces to

$$\rho = P\nu \exp (- \Delta E/kT) \ . \qquad (33)$$

In these treatments, based on the reaction rate theory, it is necessary to have some detailed description of the activated state in order to calculate the diffusion coefficient from first principles. The attempt by Fisher, Hollomon, and Turnbull (18) is based on the assumption that the reactants combine to form an activated complex with which they are in equilibrium and that this complex decomposes to give the products. A specific reaction rate constant is developed which has the form

$$K = \frac{kT}{h} \frac{\gamma_1 \gamma_2 \cdots \gamma_i}{\gamma_M} \left(\frac{n}{V} \right)^{1-i} \exp\ (-\Delta F/RT) \tag{34}$$

where

γ_i = the activity of the i^{th} component,

γ_M = the activated complex,

n/V = the number of particles per unit volume, and

ΔF = the free energy of activation.

To proceed further, a model for the diffusion process must be adopted.

Random Walk Theory

Shewmon (19) has considered the problem of relating the large number of atomic jumps per atom in a lattice (about 10^8 jumps per second near the melting point) to the observed macroscopic diffusion phenomena by, first, vectorially tracing the movement of an atom from an origin. Here, the final position vector after n jumps is

$$\vec{R}_n = \vec{r}_1 + \vec{r}_2 + \ldots + \vec{r}_n = \sum_{i=1}^{n} \vec{r}_i \tag{35}$$

where $\vec{r}_i$ represents an individual jump vector.

From this equation, the magnitude of $\vec{R}_n$ is found to be given by

$$R_n^2 = |\vec{R}_n|^2 = \sum_{i=1}^{n} r_i^2 + 2 \sum_{j=1}^{n-1} \sum_{i=1}^{n-j} |\vec{r}_i| \cdot |\vec{r}_{i+j}| \cos \theta_{i,\, i+j} \,. \tag{36}$$

If it is now assumed that all the jump vectors are equal in magnitude to a, then

$$R_n^2 = na^2 \left(1 + \frac{2}{n} \sum_{j=1}^{n-1} \sum_{i=1}^{n-j} \cos \theta_{i,\, i+j} \right). \tag{37}$$

In this expression, the magnitude of $\vec{R}_n$ is given for one atom after n successive jumps. To consider the average value of R_n^2, many atoms must be considered, each with n jumps. The average is

$$\overline{R_n^2} = na^2 \left(1 + \frac{2}{n} \overline{\sum_j \sum_i \cos \theta_{i,\, i+j}} \right). \tag{38}$$

If the process is truly random, the positive and negative values of $\cos \theta_{i,\, i+j}$ will occur with equal frequency and

$$\overline{R_n^2} = na^2 \,. \tag{39}$$

This equation would, of course, be incorrect if the jumps were not random. The so-called "correlation effects" where the jumps are not random will be discussed in the next section.

Let us now consider the diffusion of tracer atoms in a face-centered cubic metal by a pure vacancy mechanism. If Γ is the average number of jumps per second for each tracer atom and n_1 is the number of tracer atoms on plane 1, then $n_1 \Gamma \delta t$ atoms of the tracer on plane 1 will jump in a time increment δt. $\Gamma \delta t$ is proportional to the number of nearest neighbor sites, to the probability that any given neighboring

site is vacant (P_v), and to the probability $w\delta t$ that the tracer will jump into a particular vacant site

or

$$\Gamma\delta t = 12 P_v w \delta t \ . \tag{40}$$

Since four of the nearest neighbor sites are on plane 2, the flux from 1 to 2 is

$$J_{12} = 4 n_1 P_{v2} w_{12}$$

where P_{v2} is the probability that any site on plane 2 is vacant. The inverse flux is

$$J_{21} = 4 n_2 P_{v1} w_{21} \ .$$

In a pure metal $w_{12} = w_{21}$ and $P_{v1} = P_{v2}$, so

$$J = \alpha P_v w \ (C_1 - C_2) = \alpha N_v w \ (C_1 - C_2) \tag{41}$$

where

$$n_1 = \alpha C_1 = \left(\frac{a_o}{2} \right) C_1 \ .$$

Thus, the net flux is

$$J = - a_o^2 N_v w \frac{\partial c}{\partial x} \ , \tag{42}$$

and

$$D = a_o^2 N_v w \tag{43}$$

by comparison with Fick's first law. The problem of calculating D in a pure face-centered cubic metal is then reduced to one of calculating the mole fraction N_v of vacancies and the jump frequency w of an atom into an adjacent vacancy.

Correlation Effects (20)

If one considers atomic jumps that occur between two adjacent lattice planes normal to the concentration gradient, then J, the difference in the numbers of atoms jumping per unit time in opposite directions between unit areas, is given by Fick's first law in equation 1, page 3. In this expression, $\partial c/\partial x$ is the concentration gradient and D is the diffusion coefficient. If the atomic jumps are random,

$$D = \frac{1}{2} \Gamma' \, d^2 \qquad (44)$$

where Γ' is the probability per unit time that an atom will make any one of the possible jumps that will take it out of its plane and d is the interplanar spacing. If the jumps are not random, that is, if the probabilities are not equal for the atom to move in either direction from the plane, then the factor 1/2 in equation 44 will be incorrect. If the atomic jump process occurs by a vacancy mechanism, the probability of each jump depends on the direction of the previous jump and the jump directions are said to be "correlated."

Using the random walk method for vacancy-type diffusion, LeClaire and Lidiard (20) showed that the average square of the displacement after a time t is given by

$$\overline{R^2(t)} = na^2 + 2a^2 \sum_{j=1}^{n-1} (n-j)\ \overline{\cos\ \theta_j}\ , \tag{45}$$

where $\overline{\cos\ \theta_j}$ is the average value of the cosine of the angle between the i^{th} and $(i+j)^{th}$ jump of an atom. Use of this expression and the relation,

$$\overline{\cos\ \theta_j} = \overline{\cos\ \theta_{j-1}} \cdot \overline{\cos\ \theta_1}\ , \tag{46}$$

with θ_1 being the angle between consecutive jumps, gives

$$D = \frac{1}{6}\ \Gamma\ a^2\ \frac{(1+C)}{(1-C)} \tag{47}$$

where $C = \overline{\cos\ \theta_1}$. In this formula, $\frac{1+C}{1-C}$ is called the "correlation factor."

A detailed analysis of the vacancy self-diffusion correlation factors for body-centered cubic and face-centered cubic lattices yields values of 0.72 and 0.78, respectively (19). Thus, the D's are reduced by about 20 per cent for the self-diffusion process. Solute or impurity diffusion, where the solute atoms have a different attraction for vacancies than do solvent atoms, may alter the diffusion coefficient considerably — making it either larger or smaller than the self-diffusion coefficient.

III. AREAS OF SPECIAL INTEREST

The Temperature Dependence of the Diffusion Coefficient

In the above discussion, several expressions for the diffusion coefficient were obtained. For the most part, to proceed further requires that a model for diffusion be proposed.

For the simple statistical theory, the vacancy model gives an expression

$$D = a^2 f C \exp [- (\epsilon' + \epsilon_v)/kT] . \tag{48}$$

The reaction rate theory when applied to the direct interchange mechanism gives an expression for an ideal solution,

$$D = \frac{1}{m} a^2 \frac{kT}{h} \exp (\Delta S/R) \exp (-\Delta H/RT) \approx D_o \exp \left(- \frac{Q}{RT} \right) , \tag{49}$$

where D_o is not strongly dependent upon T. This theory gives the following expression for vacancy diffusion where there are N′ vacancies:

$$D = \frac{1}{m} a^2 \frac{N'}{N} \frac{kT}{h} (1 - \exp [- h\nu/kT]) \exp [-\Delta E/RT] . \tag{50}$$

If the value for vacancy concentration is substituted,

$$D = \frac{1}{m} a^2 \nu C \exp [- (\Delta E + U)/RT] \tag{51}$$

where U is the energy of formation of a vacancy and ΔE corresponds to its energy of migration.

The kinetic theory as applied to the direct interchange mechanism gives an expression:

$$D = \frac{1}{m} a^2 \nu \frac{1}{(s-1)!} \left(\frac{\Delta E}{RT} \right)^{s-1} \exp (-\Delta E/RT) . \quad (52)$$

Since the smallest value of s should be 2, corresponding to one degree of freedom for each atom,

$$D = \frac{1}{m} a^2 \nu \left(\frac{\Delta E}{RT} \right) \exp (-\Delta E/RT) . \quad (53)$$

This model applied to vacancy diffusion yields

$$D = \frac{1}{m} a^2 \nu \frac{N'}{N} \frac{1}{(s-1)!} \left(\frac{\Delta E}{RT} \right)^{s-1} \exp (-\Delta E/RT) \quad (54)$$

where ΔE is the energy required for an atom to move into an adjacent hole. If s = 1,

$$D = \frac{1}{m} a^2 \nu C \exp [- (\Delta E + U)/RT] , \quad (55)$$

which is the same as equation 51, page 25, obtained from the reaction rate treatment.

It is characteristic of all these models that the diffusion coefficient can be written as a pre-exponential term which is not strongly dependent on temperature and an exponential term containing an activation energy. Hence, the use of the Arrhenius expression contains the approximation that the pre-exponential term is constant and that the activation energy term is independent of temperature.

Prior to this investigation, the general opinion of people engaged in diffusion studies was that the simple Arrhenius-type equation

$$D = D_o \exp (-Q/RT) \quad (56)$$

with D_o and Q constant must be followed by the experimental data. Thus, in previous works in which small deviations from this expression were noted, attempts were made to explain the deviations in terms of some changing mechanism. For example, in the work of Mackliet (21), the "experimental data yielded unexpectedly large diffusion coefficients at low temperatures." In this case, the explanation for this "anomalous" behavior of the temperature dependence of the diffusion coefficient was that the cobalt and iron isotopes had an appreciable degree of misfit with the lattice (low solubilities) and therefore the contribution of diffusion down dislocation pipes might be accentuated at low temperatures. During the course of the present study, pronounced deviations from equation 56, page 26, were found and no longer could the usual "hand-waving" type explanation suffice. Instead, a detailed study of the history of the Arrhenius-type equation in describing diffusion data was found to be needed. From this study, it became evident that the equation was used more as a matter of convenience than as a theoretically rigorous law. The following discussion traces this history and, it is hoped, gives the reader an insight as to the evolution of the Arrhenius concept.

In 1889, Svante Arrhenius (22) presented his famous paper in which he proposed that an equation of the form

$$\frac{d\ \ell n\ k}{dT} = \frac{\Delta H}{RT^2}$$

could be used to describe the temperature dependence of the specific reaction rate parameter k. In this equation, ΔH is the heat released

during the reaction, R is the gas constant, and T is the absolute temperature. In order to derive this expression, Arrhenius used the previous work of van't Hoff (23) on the temperature dependence of equilibrium constants and introduced some new assumptions that did not appear to be too unreasonable.

van't Hoff had assumed the existence of an equilibrium between four quantities, A, B, C, and D, of which A and B are reactants and C and D are products. He then defined forward and reverse specific reaction rate constants k_1 and k_2 in terms of concentration of the i^{th} component c_i by the equilibrium condition that

$$k_1 c_A c_B = k_2 c_C c_D . \tag{57}$$

The equilibrium constant K was defined as k_1/k_2 for such a reaction.

Using a thermodynamic approach, van't Hoff had shown that

$$\frac{d \ell n K}{dT} = \frac{\Delta H_o}{RT^2} . \tag{58}$$

The van't Hoff equation used with the relation $K = k_1/k_2$ gives

$$\frac{d \ell n k_1}{dT} - \frac{d \ell n k_2}{dT} = \frac{\Delta H}{RT^2} . \tag{59}$$

Equation 59 implies that if the temperature dependence of k_1 and k_2 are of the same form, then

$$\frac{d \ell n k}{dT} = \frac{A}{T^2} + B \tag{60}$$

where A and B may both be functions of temperature.

In order to determine B, Arrhenius (22) introduced the idea of an activated state in equilibrium with the reactants. The overall reaction rate was then assumed to be proportional to the concentration of substance in this activated state. Then the van't Hoff equation with k, the reaction rate parameter, substituted for K, the equilibrium constant, would be applicable or

$$\frac{d\ \ell n\ k}{dT} = \frac{\Delta H}{RT^2} \ . \tag{61}$$

Arrhenius (22) indicated that small deviations from equation 61 can be explained because the reaction heat ΔH must, in general, be regarded as a function of temperature. He wrote that ΔH is constant with temperature only in the first approximation.

In 1919, Perrin (24) published an article in which he used Planck's radiation law and considered that the activated molecules received their energies from radiant energy. Using this approach, he was able to show, after making certain assumptions, that the temperature dependence of the reaction rate constant was the same as that given by Arrhenius. In 1920, Tolman (25) used statistical mechanics to again arrive at the so-called Arrhenius-type expression. In neither of these approaches was an assumption made about the constancy of the energy of activation. Tolman (25) did make the statement that "it should not vary much with temperature, since neither the energy of the activated molecules and modes of vibration, nor their average energy will change rapidly with temperature."

In 1921, Daniels and Johnston (26) in an article on "The Thermal Decomposition of Gaseous Nitrogen Pentoxide: A Monomolecular Reaction" discussed the temperature dependence of the rate constant. The authors said: "The important thing about these calculations is that E (or ΔH) is shown experimentally to be practically constant with a wider range of temperature than has been possible hitherto." This statement, concerning data obtained between 0 and 65°C, illustrates and perhaps initiated the trend which was ultimately to lead to the common belief that some natural law required the activation energy to be constant with temperature.

In the first systematic study (5) of diffusion in the solid state, no mention was made of an expression for writing the temperature dependence of the diffusion coefficient. The coefficients were simply listed in tabular form in the paper.

In 1922, Dushman and Langmuir (27) considered the question of the temperature dependence of diffusion coefficients in solids and concluded that "the velocity of such reactions is approximately given by the semi-empirical relation"

$$D = \frac{Qd^2}{N_o h} \exp\left(-\frac{Q}{RT}\right) , \qquad (62)$$

where Q is a characteristic of the reaction and d is the distance between layers of the lattice. They further concluded that, since Q could be calculated from only one measurement of the diffusion coefficient, one measurement would completely describe diffusion for the system. In 1923, however, Langmuir (28) concluded that "the natural

logarithm of the diffusion coefficient is a linear function of the reciprocal of the temperature, the slope of this line being equal to Q_D/R where Q_D represents the 'heat of diffusion.'" Thus, using these considerations, D would have to be determined at two temperatures to completely describe its temperature dependence. Until recent work on diffusion in body-centered cubic metals, investigators have determined several data points, plotted ℓn D versus $1/T$, and found Q as accurately as warranted by the data. The pre-exponential factor D_o, in equation 56, page 26, is also calculated from these same data.

It should be pointed out that equation 56, page 26, is obtained from Arrhenius' equation 61, page 29, by simply integrating under the assumptions that k is proportional to D and that the activation energy ΔH or Q is constant with temperature. Use of the differential form by plotting ℓn D versus the inverse absolute temperature gives, in the general case, a curve whose slope at any one temperature is, by definition, proportional to the activation energy at that temperature.

In 1949, Wert and Zener (29) attempted to clarify the meaning of D_o and Q in equation 56, page 26, by applying reaction rate theory to a simple model of self-diffusion. Using this model, one finds

$$D = \frac{\alpha a_o^2}{\tau} \tag{63}$$

where

α = a geometrical factor related to possible jumping sites,

a_o = the lattice parameter, and

τ = the average time between jumps.

Application of absolute rate theory then gives

$$D = q \alpha a_o^2 \nu \exp (\Delta S/R) \exp (-\Delta H/RT) \qquad (64)$$

where

q = the number of equivalent diffusion paths,

ν = the frequency of vibration along the direction leading to diffusion, and

ΔS = the entropy change associated with the diffusion process.

It is possible to compare experimentally determined D_o and ΔH (or Q) values with those obtained by assuming a mechanism of diffusion and by substituting reasonable values into equation 64. Such comparisons have been made for several systems by using possible mechanisms such as vacancy, ring, and interstitial movements. Results have generally supported the vacancy mechanism for diffusion in face-centered cubic metals. Since it has not been possible to experimentally demonstrate the existence of vacancies in body-centered cubic metals, the situation for identification of the diffusion mechanism is still one of uncertainty.

Near-Surface Diffusion

It was previously stated that one method of determining diffusion coefficients is based on the decrease in specimen surface activity with time at a given temperature. This method is valid only if the penetration behavior is well known; but, prior to this study, such behavior could not be determined accurately for very small

diffusion coefficients. Thus, the usual assumption that penetration is "normal" (i.e., plots of $\ell n\ A$ versus x^2 are linear for diffusion from a very thin source) was made without experimental verification. Recent work has demonstrated that "normal" Gaussian behavior is not always achieved in practice; therefore, the validity of surface-decrease methods for determination of coefficients of diffusion is now questioned.

Since the start of the present study, non-Gaussian penetration plots have been reported by several investigators (30–33) for unidirectional diffusion from a plane source. This behavior reveals itself as an enhanced relative activity in two different regions of the penetration plot – near the surface and deep into the specimen. The overall picture is illustrated in Figure 3 where the penetration profile is divided into three regions with the normal volume diffusion portion identified as region II.

The work by Williams and Slifkin (30) on the diffusion of rare earths (cerium, niobium, and promethium) in mono- and polycrystalline silver and in lead probably illustrates the presence of regions I and III with a masking of the normal region II. In their work, the penetration plots consisted "of two regions: (a) a steep segment near the surface, corresponding to diffusion coefficients of the order of 10^{-12} to 10^{-13} cm^2/sec even at temperatures near the melting point; and (b) a deep segment, corresponding to diffusion coefficients of the order of 10^{-9} to 10^{-11} cm^2/sec." (30) It is felt that the second portion of their plots was not due to volume diffusion because it was

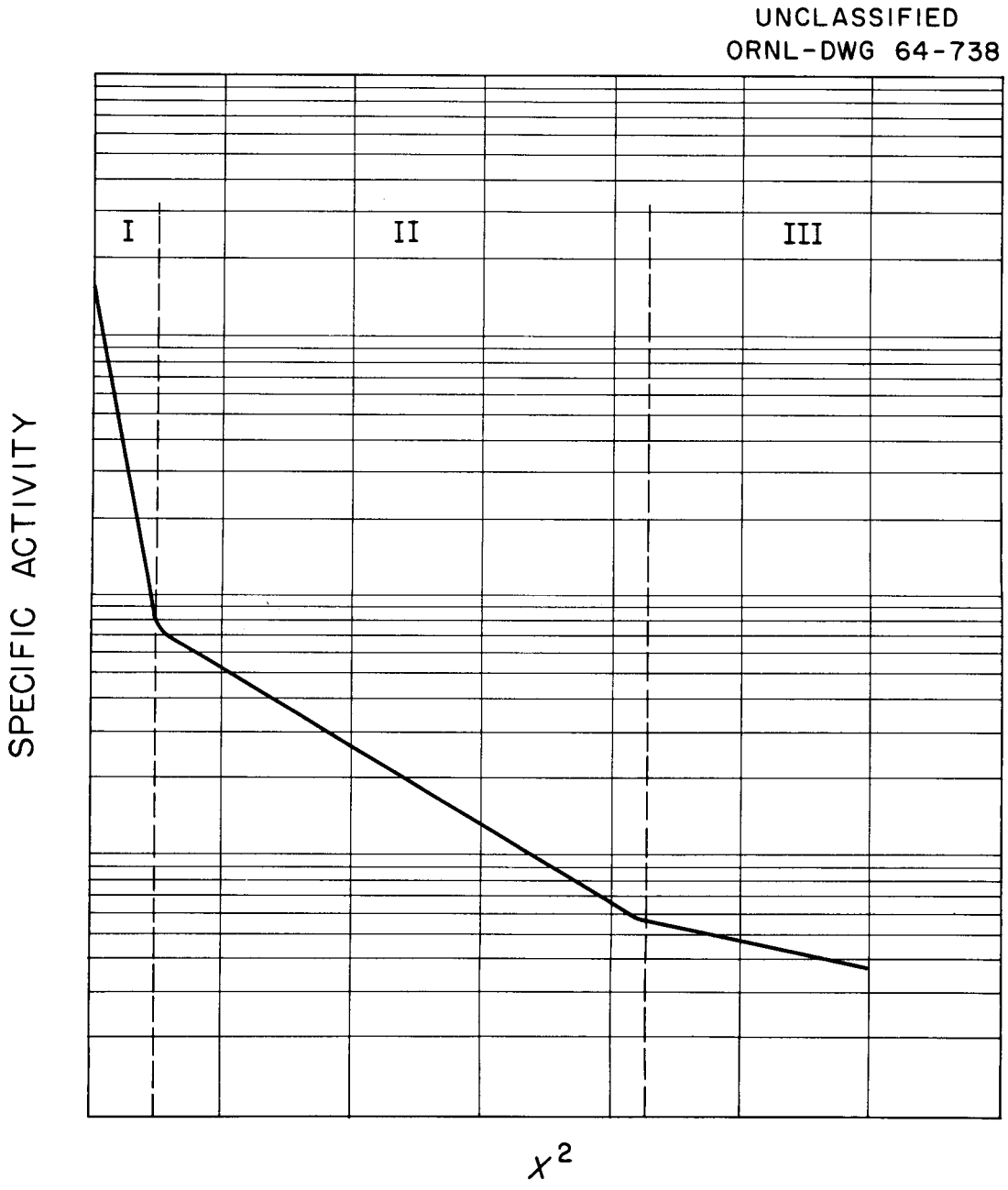

Figure 3. Schematic penetration plot showing near-surface, normal, and deep behavior for unidirectional diffusion from a plane source.

extremely structure sensitive as one would expect if the enhancement were caused by preferential diffusion along dislocation-pipe networks. They attributed the overall behavior of the penetration of rare earths into silver to the extremely low solubilities of the tracers in silver and lead lattices (30).

Subsequent work by Styris and Tomizuka (31) on the diffusion of zinc-65 in single crystals of copper also showed unusual penetration behavior. The two regions in their penetration plots may be labeled as being due to near-surface effects and to normal volume diffusion. Masking of the normal regions of diffusion by region III did not occur because the solubility of zinc-65 in copper is quite large. This work clearly shows that region I in Figure 3, page 34, is not due to low solubility effects.

Ignatkov and Kosenko (33) found all three regions in their penetration plots for the diffusion of tellurium in germanium.

In the present study, all three regions of diffusion were also observed. However, little effort was made to characterize region III which is found where very little total activity remains in the specimen and is probably due to short-circuiting penetration by the isotope. As will be seen, development of the anodizing and stripping technique for sectioning diffusion specimens has allowed accurate characterization of region I for diffusion in tantalum.

IV. LITERATURE SURVEY

Information reported prior to 1960 on both interstitial and substitutional diffusion in refractory body-centered cubic metals has been adequately summarized by Peterson (34) and only later data will be discussed. This approach will allow inclusion of almost all important works on substitutional diffusion in beta zirconium, beta titanium, vanadium, niobium, and tantalum. Recent work on self-diffusion in chromium and molybdenum will be discussed for completeness.

Several studies (35–39) on diffusion of zirconium-95 in beta zirconium had been reported prior to initiation of this work. Results of these studies are summarized in Table I. Also included are activation energies computed from three empirical rules derived for face-centered cubic metals. Two important facts are illustrated by these data. First, there are large differences in reported D_o and Q values; this occurs in spite of the fact that each work had reasonable internal consistency. A second point is that the activation energies computed by the empirical relationships are considerably larger than those determined experimentally. Examination of the data in all these works reveals unusually large diffusion coefficients – even at temperatures hundreds of degrees below the melting point of zirconium (1852°C). The "rule-of-thumb" that the self-diffusion coefficient should be about 10^{-8} square centimeters per second at the melting point certainly does not hold for zirconium. It is also important to note that the data

TABLE I

PREVIOUS RESULTS ON DIFFUSION OF ZIRCONIUM-95 IN ZIRCONIUM

D_o (cm^2/sec)	Q (kcal/mole)	Reference
	EXPERIMENTAL	
4×10^{-5}	26.0	(35)
2.4×10^{-4}	30.1	(36)
2.4×10^{-3}	38.0	(37)
4.2×10^{-5}	24.0	(38)
1×10^{-4}	27.0	(39)
	EMPIRICAL	
$Q = 40\ T_m = 85.0$	(T_m = 2125°K)	
$Q = 16.5\ \Delta H_f = 90.8$	(ΔH_f = 5.5 kcal/mole)	
$Q = 0.67\ \Delta H_s = 73.7$	(ΔH_s = 110.0 kcal/mole)	

for each paper were gathered over temperature ranges of only a few hundred degrees.

Several papers (10,12,13) have been published on the diffusion of solute elements in beta titanium. Mortlock and Tomlin (10) investigated the diffusion of chromium-51 in iodide titanium and in titanium alloys with up to 18 per cent chromium. Peart and Tomlin (12) measured the diffusion of iron-55, iron-59, niobium-95, nickel-65, cobalt-60, and manganese-54 in beta titanium between 900 and 1300°C. In both of these works, no apparent anomalies in Arrhenius-type plots were reported. Then, after the first results of the present work became public (40), Gibbs, Graham, and Tomlin (13) reported nonlinear Arrhenius behavior for a large number of solutes diffusing in beta titanium for the temperature interval 900 to 1650°C. As will be seen, their results are in substantial agreement with those for beta zirconium reported herein. In addition, Murdock and Lundy (41) have reported diffusion coefficients of titanium-44 and vanadium-48 in beta titanium between 900 and 1550°C. For both these systems, Arrhenius-type plots were nonlinear with the apparent activation energies varying by about a factor of two over the temperature interval investigated.

Little, if any, experimental work has been published on diffusion in vanadium. In addition to the work in this report, however, Peart (42) is currently engaged in measuring the diffusion of vanadium-48 in both mono- and polycrystalline vanadium.

Resnick and Castleman (43) have determined diffusion coefficients of niobium-95 in niobium between 1535 and 2120°C. There was large

scatter in the data, but no apparent curvature was noted in the Arrhenius-type plot. The temperature dependence of the diffusion coefficient was described by D = 12.4 exp (−105,000/RT) square centimeters per second. Peart, Graham, and Tomlin (44) have reported good agreement with Resnick and Castlemen (43) on the diffusion of niobium-95 in niobium, but give D_o and Q as 1.3 square centimeters per second and 95,000 calories per mole, respectively, for the temperature range of 1700 to 2150°C. They (44) also report D = 0.74 exp (−70,500/RT) square centimeters per second for cobalt-60 in niobium between 1550 and 2050°C and D = 1.5 exp (−77,700/RT) square centimeters per second for iron-55 in niobium between 1400 and 2100°C. Curvature was absent in all Arrhenius-type plots for diffusion in niobium.

No recent data have been forthcoming on self-diffusion in tantalum. Gruzin and Meshkov (45) previously measured the migration of tantalum-182 into tantalum disks at 1200 and 1300°C and reported the diffusion coefficient as $D = 1.3 \times 10^3$ exp (−110,000/RT) square centimeters per second.

Hagel (46) has recently reported that diffusion of chromium-51 in chromium is described by D = 0.28 exp (−73,200/RT) square centimeters per second. His work covered the temperature range of 1200 to 1600°C and his results are in sharp contrast to those of Paxton and Gondolf (47) who reported $D = 1.51 \times 10^{-4}$ exp (−52,700/RT) square centimeters per second for the same system. The latter work covered a lower temperature interval and, if one plots all the data on the same Arrhenius-type plot, he finds that there is either a sharp break in the

plot at about 1200°C or small curvature over the whole temperature range. It would be appropriate for one investigator to cover the whole temperature range to examine this point further.

Askill and Tomlin (48) have determined diffusion coefficients of molybdenum-99 in molybdenum between 1850 and 2350°C. They found significant differences for diffusion in mono- and polycrystalline materials. For the former, they report $D = 0.5 \exp(-96{,}900/RT)$ square centimeters per second, while, for the latter, $D = 0.1 \exp(-92{,}200/RT)$ square centimeters per second. In both cases, diffusion anneals were accomplished in vacuum, and lathe-sectioning techniques were used. Difficulties in studying this system at lower temperatures would be compounded by the short half-life (67 hours) of the isotope.

CHAPTER II

EXPERIMENTAL PROCEDURES

I. SPECIAL MATERIALS

The materials used were of two general types — inactive base metals and radioactive tracers. The base metals were usually either mono- or polycrystalline with a large grain size. The radioactive tracers were either stock items from the Isotopes Division at the Oak Ridge National Laboratory or special preparations from the same source.

The zirconium base metal used in these experiments was reactor-grade-1 crystal-bar ingot of 99.94 per cent minimum purity. The ingot was arc melted, forged to a one and one-half inch diameter rod, and swaged to three-fourths inch diameter. From this rod, specimens one-half inch long by five-eighths inch diameter were machined. The major impurities in the zirconium are given in Table II in units of parts per million.

The vanadium was a one-half inch diameter single crystal purchased from Linde Company. Analyses of major impurities by the vendor and by W. Laing of the Analytical Chemistry Division at the Oak Ridge National Laboratory are summarized in Table III.

The niobium was obtained from three sources. The initial experiments were performed using material originally obtained from Shieldalloy Corporation. The as-received niobium was electron-beam

TABLE II

MAJOR IMPURITY CONTENT OF THE ZIRCONIUM BASE METAL

Element	Content (ppm)
Carbon	50
Copper	25
Iron	242
Hydrogen	53
Hafnium	135
Nitrogen	10
Nickel	24
Oxygen	19
Silicon	22

TABLE III

MAJOR IMPURITY CONTENT OF THE VANADIUM

Element	Analysis by Linde (ppm)	Analysis at ORNL of Specimen V-7 After Diffusion Runs (ppm)
Oxygen	880	860
Carbon	600	420
Nitrogen	800	220
Hydrogen	120	ND*
Iron	250	ND
Silicon	100	ND
Manganese	10	ND
Chromium	Trace	ND
Calcium	Trace	ND
Aluminum	Trace	ND
Silver	Trace	ND

*ND means "not determined."

melted into a bar three inches in diameter by three feet long. About forty specimens, five-eighths inch diameter by one-half inch long, were then machined from the central portion of the rod. The analysis supplied by the vendor for the starting material and interstitial analysis for one of the specimens are given in Table IV.

Two 8-inch-long single crystals of niobium were purchased from Semi-Elements, Incorporated. These crystals were about one-half inch diameter and were cut to give specimen lengths of about three-eighths inch. The material was specified by the vendor to have less than 25 parts per million interstitial content. The analyses at the Oak Ridge National Laboratory, as given in Table V, showed the as-received material to have an interstitial content considerably higher than that specified. Material from the first bar (SE-I) was used for the low-temperature ($T < 1500°C$) runs where the technique of sectioning was that of anodizing and stripping.

Small-diameter (about one-fourth inch) niobium single crystals intentionally doped with certain amounts of oxygen were received from Materials Research Corporation. The oxygen content, nominally 250 and 500 parts per million, and other interstitial contents, as determined at the Oak Ridge National Laboratory, are summarized in Table VI. These crystals were used at low temperatures to determine the effect of increasing oxygen content on the diffusion coefficient.

Two batches of tantalum single crystals were purchased from Materials Research Corporation. These crystals had diameters of approximately three-eighths and one-half inch and were cut into

TABLE IV

MAJOR IMPURITY CONTENT OF SHIELDALLOY NIOBIUM

Element	Vendor Analysis (ppm)	ORNL Analysis (ppm)
Tantalum	1200	ND*
Titanium	100	ND
Iron	300	ND
Tungsten	400	ND
Carbon	100	50
Nitrogen	100	79
Oxygen	200	63
Hydrogen	15	13

*ND means "not determined."

TABLE V

INTERSTITIAL CONTENT OF NIOBIUM SINGLE CRYSTALS FROM SEMI-ELEMENTS, INCORPORATED

Element	Bar SE-I Analysis (ppm)	Bar SE-II Analysis (ppm)
Carbon	20	20
Nitrogen	14	16
Oxygen	100	85
Hydrogen	2	3

TABLE VI

INTERSTITIAL CONTENT OF NIOBIUM SINGLE CRYSTALS FROM MATERIALS RESEARCH CORPORATION

Element	Rod I Analysis (ppm)	Rod II Analysis (ppm)
Nitrogen	15	20
Oxygen	250	420
Hydrogen	3	7

specimens about three-eighths inch long. According to the vendor, the interstitial content was less than 25 parts per million and the metallic content less than 60 parts per million. Table VII gives the results of an analysis performed at the Oak Ridge National Laboratory.

Radioactive isotopes used in the experiments were zirconium-95, niobium-95, vanadium-48, and tantalum-182. All were obtained from the Isotopes Division of the Oak Ridge National Laboratory.

The zirconium-95 was received as a freshly separated oxalate complex in oxalic acid solution. The solution was diluted with distilled water to yield a specific activity of about 120 counts per lambda per second ($1\lambda = 10^{-6}$ liters). Zirconium-95 decays with a half-life of 65 days and with the emission of gamma rays of 0.75 million electron volts. The daughter product, niobium-95, also emits decay gammas of essentially the same energy; so, for these experiments using gamma counting techniques, it was necessary to work with freshly prepared zirconium-95. All diffusion anneals were completed within two days of the chemical separation.

Several shipments of niobium-95 were obtained for experiments involving this isotope. Niobium-95 has a half-life of 35 days and decay gammas have an energy of 0.76 million electron volts. In each shipment, the isotope was in an oxalate form with a specific activity of one to ten millicuries per milliliter. The zirconium-95 contamination was about 0.0002 millicuries per milliliter, and the ruthenium-103 contamination was less than 0.001 millicuries per milliliter.

TABLE VII

INTERSTITIAL CONTENT OF TANTALUM SINGLE CRYSTALS FROM MATERIALS RESEARCH CORPORATION

Element	Three-Eighths Inch Rod Analysis (ppm)
Nitrogen	5
Oxygen	10
Hydrogen	2

The vanadium-48 was made by special preparation by proton bombardment of a titanium target in the 86-Inch Oak Ridge National Laboratory Cyclotron. A carrier-free chemical separation was done by the Isotopes Division of the Oak Ridge National Laboratory and the isotope was received in nitric acid solution. Vanadium-48 has a half-life of 16.2 days and emits decay gammas of 0.99, 1.32, and 2.23 million electron volts.

Two shipments of tantalum-182 were obtained. The first order was for a shipment from stock of the isotope in a tantalate solution. Subsequent experimental difficulties in deposition of the isotope onto specimens made it necessary to order a special preparation so that the tantalum-182 would be in oxalate solution. Tantalum-182 decays with a 112-day half-life and emits decay gammas of 1.1 and 1.2 million electron volts.

II. PREPARATION OF SPECIMENS

The as-machined zirconium specimens were degreased with acetone, heavily etched with 46 per cent nitric acid–46 per cent water–8 per cent hydrofluoric acid solution, homogenized at 1150°C for 48 hours in a vacuum of 3×10^{-5} torr or better, and furnace cooled. In order to prevent possible contamination from the mullite furnace tube during homogenization, the specimens were contained within a tantalum box inside a tantalum tube. The large beta grain size produced by this treatment (body-centered cubic beta exists above 865°C, close-packed hexagonal alpha below) is illustrated in Figures 4 and 5. The hydrogen

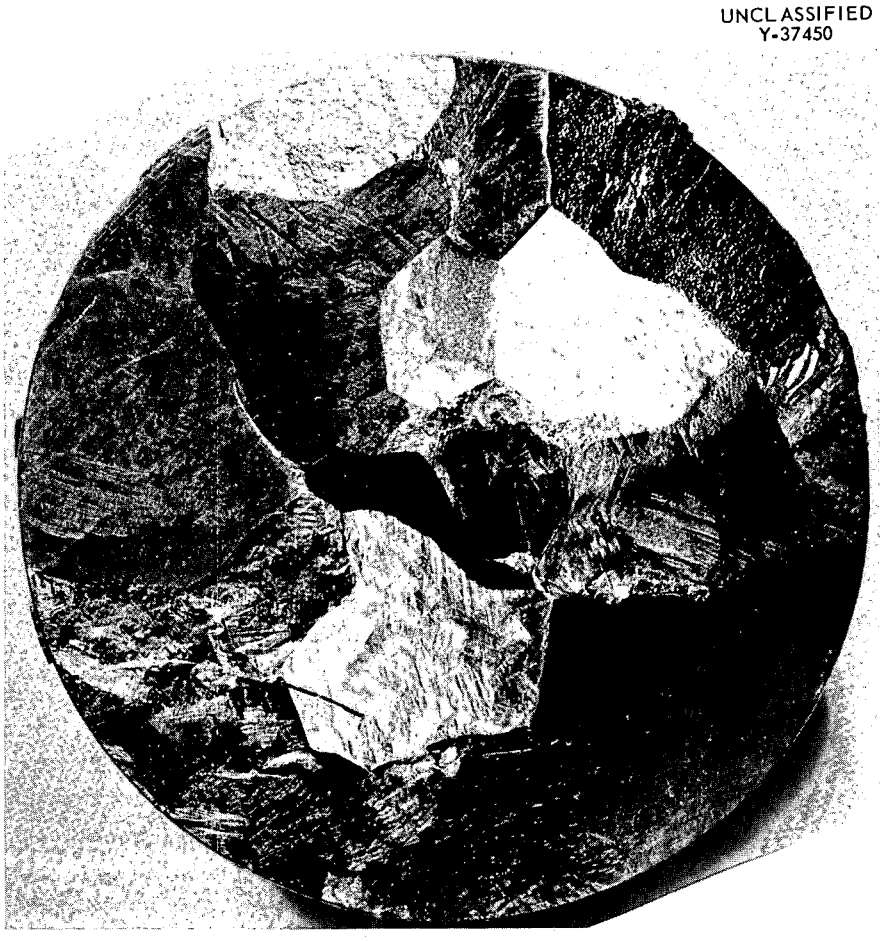

Figure 4. Typical zirconium specimen after vacuum annealing at 1150°C for 48 hours. 7X.

Figure 5. Same zirconium specimen shown in Figure 4, page 51, after polishing and etching. 7X.

content of the specimens was probably decreased to less than 10 parts per million by this vacuum anneal (49). The specimens were then abraded through 4/0 metallographic polishing papers to produce a smooth flat surface on one end of each cylinder. This was followed by heavy etching in 46 per cent nitric acid–46 per cent water–8 per cent hydrofluoric acid solution, light polishing with 4/0 paper, and another etching with the above solution. Then a small portion (about ten lambda) of the oxalate solution containing either freshly prepared zirconium-95 or niobium-95 was deposited dropwise onto the prepared surface. The solution was evaporated to dryness by means of a heat lamp. On subsequent heating of the specimens to diffusion temperatures, the residue decomposed to leave a thin layer of oxide or metal from which the isotope diffused into the specimen.

The electron-beam-melted niobium specimens were degreased by alternate bathing in acetone and alcohol. They were etched in 80 per cent nitric acid–20 per cent hydrofluoric acid and rinsed in water. At this stage they appeared to have ten to twenty grains on the five-eighths inch diameter surface. The specimens were then remachined to improve the surface and the etching process was repeated. Each of these specimens was given a high-temperature anneal at 2400°C in an argon atmosphere for one hour. After this treatment, there were one to five grains on the flat faces of the specimens. The specimens were then abraded through 4/0 metallographic paper and then etched with 85 per cent nitric acid–15 per cent hydrofluoric acid. The polishing and etching were repeated until no evidence of previous machining was

observed. Then three to ten lambda of niobium-95 solution was deposited dropwise onto the prepared surface and the solution was evaporated to dryness.

For the niobium (either the polycrystalline electron-beam-melted metal or the single crystals) used in low-temperature diffusion anneals, where very thin sectioning was done by anodizing and stripping of layers, it was necessary to prepare highly polished surfaces. This was done by electropolishing the specimens after the previously described abrading and etching procedures. Niobium was successfully electropolished in a 90 per cent sulphuric acid–10 per cent hydrofluoric acid solution at a current density of 1–2 amperes per square centimeter for about thirty minutes. Then the isotope was deposited dropwise as previously described or was electrodeposited in one instance to determine the effect, if any, of the method of isotope deposition on the results. No such effect was observed.

Nineteen specimens one-half inch in diameter and three-eighths inch long were cut from the as-received vanadium single crystal. Each specimen was lightly machined to make the flat face perpendicular to the longitudinal axis. The specimens were polished through 1/0 metallographic paper and chemically etched with 25 per cent hydrofluoric acid–10 per cent sulphuric acid–10 per cent nitric acid–55 per cent water. The polishing and etching were repeated until a satisfactory surface finish was achieved. An attempt was made to deposit the vanadium-48 onto the crystals in a dropwise manner. Severe pitting resulted, however, and the technique was abandoned. Next, the isotope solution was neutralized with ammonium hydroxide and deposited dropwise.

No pitting of the vanadium resulted, but the isotope was contained in a nonadherent white residue. Then it was found that the isotope could be electroplated from neutral solution. This was accomplished by applying about five volts between a platinum electrode and the specimen immersed in the solution. Maximum counting rates of the vanadium-48 for each specimen were about 100 counts per second.

All of the work on diffusion in tantalum was done using single crystals at low temperatures where the anodizing and stripping method of sectioning was necessary. The specimens were abraded, etched, and electropolished in the same manner as that used for niobium. The radioactive niobium-95 was deposited dropwise from oxalate solutions and evaporated to dryness in preparation for the diffusion anneals.

III. DIFFUSION ANNEALS

The diffusion anneals may be divided into two types — high temperature and low temperature — with the dividing line at about 1200°C. Most of the high-temperature anneals were done in either a Brew or an Abar tantalum resistance furnace. Both of these furnaces were equipped to operate either with a vacuum of about 10^{-5} torr or with an inert atmosphere of high-purity argon up to about 15 pounds per square inch gauge pressure. The argon atmosphere was used in all cases where specimen evaporation might be a problem. The temperatures — a maximum of about 2400°C — were controlled manually by adjusting the input voltage to the furnace elements by a "powerized" variac. This method proved to be highly satisfactory because line voltage variations were

quite small. The specimens were placed in a small tantalum box inside the heating element. They usually were in contact with tungsten which was compatible with all specimens. This experimental arrangement is illustrated in Figure 6. The Pyro micro-optical pyrometers were calibrated with platinum versus platinum–10 per cent rhodium thermocouples to about 1600°C and extrapolations of these calibrations were made to higher temperatures. In some instances, both an optical pyrometer and a thermocouple were used to determine specimen temperatures during diffusion anneals, but usually only the calibrated optical pyrometers were used.

For the low-temperature treatments, the specimens were either sealed off in evacuated quartz ampoules and annealed in Kanthal wire-wound horizontal-tube furnaces or placed in a similar furnace equipped with a mullite tube through the hot zone so that dynamic vacuums of about 10^{-7} torr could be achieved. In both cases, the temperatures were controlled by Wheelco 402 units and were determined to within ±1°C by using calibrated platinum versus platinum–10 per cent rhodium thermocouples.

The diffusion anneals lasted from fifteen minutes to about three months, depending on the temperature and sectioning method. For the experiments involving zirconium-95, the time was a maximum of about two days so that errors introduced by the increase in activity of the daughter isotope niobium-95 would be minimized.

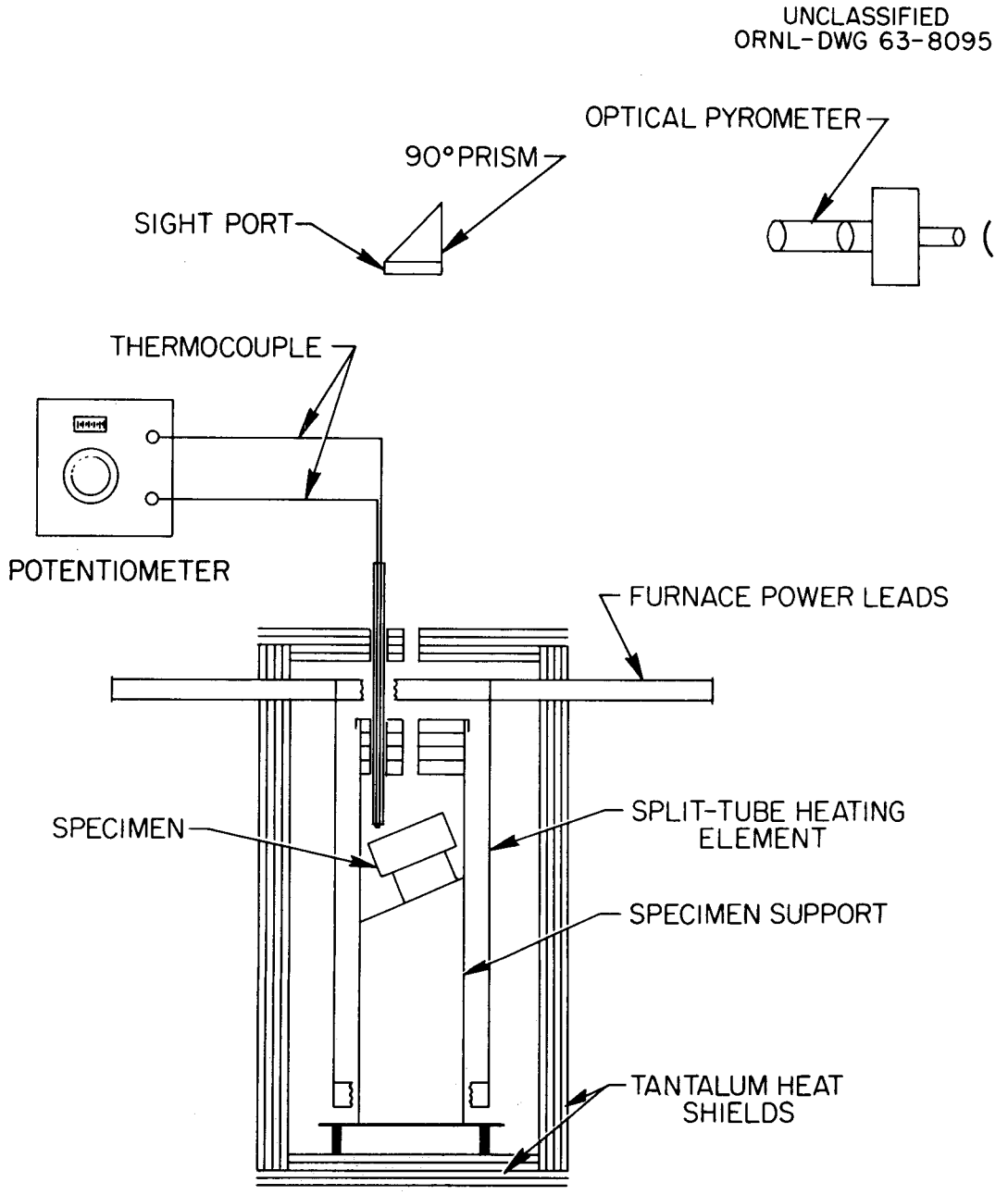

Figure 6. Experimental arrangements for diffusion anneals in tantalum resistance furnaces.

IV. SPECIMEN SECTIONING

On completion of a diffusion anneal, the problem was reduced to one of determining the penetration profile of the isotope in the specimen and relating this to the diffusion coefficient by the appropriate solution of Fick's second law. Sectioning of the specimen perpendicular to the direction of diffusion (after lathe reduction of the diameter to remove possible surface effects) was accomplished by one of three methods: (1) lathe turning, (2) grinding, or (3) anodizing and stripping the anodic layers. The first two methods have been frequently used in diffusion studies, while the last method was developed during the course of these experiments.

Lathe sectioning was done by standard machining techniques with the additional feature that the turnings for each section were retained for counting purposes. This was accomplished by using a specially designed plastic chip catcher. The turnings were placed in previously weighed bottles and reweighed (using an Ainsworth semi-micro balance) so that the thickness of removed material could be accurately calculated. The turnings were then placed on tape on cardboard cards for counting purposes.

Sectioning by grinding was done on a grade of emery paper, dependent on the desired section thickness. This was done by hand on a marked-off area of paper by using "figure-8" strokes to keep the specimen face flat and parallel to the original surface. After each section, the paper was folded to retain the radioactive particles and

wrapped with masking tape. The amount of material removed was found by weighing the specimen before and after each section. This was converted to thickness removed by appropriate use of density and diameter values.

As previously stated, the technique of anodizing and stripping the anodic layer from a diffusion specimen was developed during these studies. The method allows accurate sectioning of both niobium and tantalum in thicknesses at least an order of magnitude smaller than was previously possible with conventional methods. Thin sectioning (down to about 150 angstroms) allows determination of diffusion coefficients, at least in theory, as small as 10^{-20} square centimeters per second by a direct method. Previously, this was possible only by using the surface-decrease method which depends on an accurate knowledge of the radiation absorption properties of the material and on the absence of any peculiar penetration behavior, such as the near-surface effect previously discussed. This new method is based on the fact that, for the refractory metals tantalum and niobium, very uniform anodic oxide films can be formed on and mechanically stripped from suitably prepared surfaces. The details of the anodization process are well known (50). If a small amount of fluoride ion is present in the anodizing solution, the oxide layer is less adherent than otherwise. In these studies, the specimens were anodized for two minutes at low current in a 0.5 per cent solution of Na_2SO_4 to which about two drops of 48 per cent hydrofluoric acid per 100 cubic centimeters had been added. Thickness-voltage relationships, as determined by weighing, anodizing, and

reweighing strips with large surface areas, showed that 6.54 and 9.51 angstroms of metal were anodized per applied volt for tantalum and niobium, respectively. After anodizing, the specimens were washed in distilled water and dried either in an oxygen blast or with a hair dryer. Stripping was then done, using Scotch Brand Magic Tape, by placing the tape on the specimen and pulling. The tape was then folded back on itself and marked for identification. Each strip was subsequently transferred to the counting facility for determining the relative activity associated with it. This technique may be applicable to metals other than niobium and tantalum.

V. COUNTING

For determining the relative radioactivity of the sections, a single-channel gamma analyzer was used in conjunction with a three inch diameter by three inch long NaI(Tl) crystal. The crystal was contained within a top-opening lead cask with a three inch wall thickness. This cask reduced the background level of radiation — especially for activities of low energies. By calibrating the analyzer with known radiation sources, such as cesium-137, adjustments could be made to count only gamma rays within a certain known energy interval.

The sections from each specimen, whether they were obtained by lathe turning, grinding, or anodizing and stripping, were placed one at a time over the center of a one-half inch thick aluminum plate on top of the NaI(Tl) crystal. The aluminum plate shielded the crystal from unwanted beta radiation. The activity of each section for the

particular gamma radiation of interest was then found in terms of counts per second with the total counts being enough to give three per cent or better counting statistics. During the last experiments, the counting equipment had a timer using a 10,000 cycles per second quartz crystal so that variations from the 60 cycles per second line power would not affect the accuracy of the counting data.

As previously stated, zirconium-95 decays to niobium-95 and both isotopes have decay gammas of about 0.76 million electron volts. The diffusion anneals for zirconium-95 specimens were therefore completed within two days of the purification of the isotope. However, the niobium-95 built in after the diffusion anneals by zirconium-95 decay was proportional to the amount of zirconium-95 that had diffused as zirconium-95. Thus, no particular timetable had to be followed for counting these specimens. For both zirconium-95 and niobium-95, the single-channel analyzer was set to count gamma rays having energies between either 0.56 and 0.96 million electron volts or 0.66 and 0.86 million electron volts. The latter setting was used when niobium-95 was being counted in a background that contained the higher energy gammas from tantalum-182. Backgrounds for the two settings were about 1.5 and 0.6 counts per second, respectively.

Vanadium-48 decays with a half-life of 16.2 days by emission of gamma rays of energies 0.99, 1.32, and 2.23 million electron volts. The analyzer was set to count gammas with energies between 0.75 and 1.75 million electron volts. The background for this particular setting was about 1.5 counts per second.

Tantalum-182 decays with a half-life of 112 days and emits decay gammas of 1.1 and 1.2 million electron volts. In order to span both gamma peaks, the analyzer was set to count gammas with energies between 1.0 and 1.4 million electron volts. For this energy range, the background was generally about 0.6 counts per second.

VI. DATA TREATMENT

All the data obtained by the techniques described were of the same general character in that they represented the final isotope distribution after unidirectional diffusion from a plane source during an isothermal diffusion anneal. The form of the raw data was dependent upon the method used in analyzing the specimens.

For lathe sectioning, the weight of the turnings was determined and related to the section thickness at the annealing temperature by appropriate use of the room-temperature density, thermal expansion data, and specimen diameter. The distance from the specimen surface was set equal to the sum of all prior section thicknesses plus one-half of the thickness of the section under consideration. The counting data were treated by subtracting the background counting rate and dividing the result by the section weight to give the relative specific activity. Then, in accordance with the appropriate solution to Fick's second law, the data were plotted as $\ell n\ A(x)$ versus x^2. The slope of the resulting straight line equals $(-\ 4\ Dt)^{-1}$ and the diffusion coefficient may be readily computed for the given time t of the diffusion anneal.

As an example of this procedure, consider the data for specimen V-5 which was a vanadium-48 in vanadium specimen diffusion annealed at 1802°C for 18,120 seconds. The reduced diameter of the specimen at room temperature was 1.1412 centimeters. Table VIII contains the raw data and illustrates its treatment to give information for plotting. Note that, in this case, the conversion to normal distance units (centimeters) was not done until after the data were plotted and the diffusion coefficient calculated in square milligrams per second. The conversion could have been made earlier but this method was more convenient. The plot of $\ell n\ A(x)$ versus x^2 for V-5 is shown in Figure 7. By considering the line through these data over exactly one order of magnitude (from 40 to 400) of specific activity, one finds the slope S to be

$$S = - \frac{\ell n\ 10}{106{,}000 - 10{,}500} = - 2.411 \times 10^{-5} .$$

Setting this slope equal to $(- 4\ Dt)^{-1}$, one finds D = 0.5722 square milligrams per second. If the room-temperature density is ρ_o and the thermal expansion to T is $\frac{\ell + \Delta\ell}{\ell}$, the conversion factor to change D to units of square centimeter per second is

$$\left(\frac{1}{\rho A}\right)_T^2 = \left(\frac{1}{\rho_T A_T}\right)^2 = \left(\frac{\rho_o}{\left(\frac{\ell + \Delta\ell}{\ell}\right)^3} \left[\frac{\pi}{4} d_o^2 \left(\frac{\ell + \Delta\ell}{\ell}\right)^2\right]\right)^{-2}$$

$$= \left(\frac{\rho_o}{\left(\frac{\ell + \Delta\ell}{\ell}\right)} \frac{\pi}{4} d_o^2\right)^{-2} .$$

TABLE VIII

SECTIONING AND COUNTING DATA FOR SPECIMEN V-5 ANNEALED AT 1802°C FOR 18,120 SECONDS*

Section Number	w, Section Weight (mg)	x, Distance from Surface (mg)	$x^2 \cdot 10^{-2}$ (mg^2)	Counts (C)	Time (t, sec)	$\frac{C}{t}$	$\frac{C - B}{t}$	$\frac{C - B}{t \cdot w}$
Background (B)	--	--	--	12,513	9,900	1.234	--	--
1	8.52	4.26	0.18	2,589	440	5.884	4.620	0.542
2	26.81	21.92	4.81	2,838	190	14.937	13.673	0.510
3	32.52	51.59	26.62	2,927	170	17.218	15.954	0.491
4	27.94	81.82	66.94	2,729	200	13.645	12.381	0.443
5	19.81	105.69	111.7	2,986	330	9.048	7.784	0.393
6	28.66	129.93	168.8	2,810	250	11.240	9.976	0.348
7	34.42	161.47	260.7	2,563	240	10.638	9.374	0.272
8	28.64	193.00	372.5	2,716	380	7.147	5.883	0.205
9	27.70	221.17	489.2	2,724	480	5.645	4.411	0.1592
10	31.58	250.81	629.1	2,946	600	4.910	3.646	0.1155
11	33.27	283.23	802.2	1,870	500	3.740	2.476	0.0744
12	28.97	314.35	988.2	1,931	700	2.759	1.495	0.0516
13	33.36	345.52	1193.8	2,013	900	2.237	0.973	0.0291

*Reduced specimen diameter at room temperature = 1.1412 centimeters.

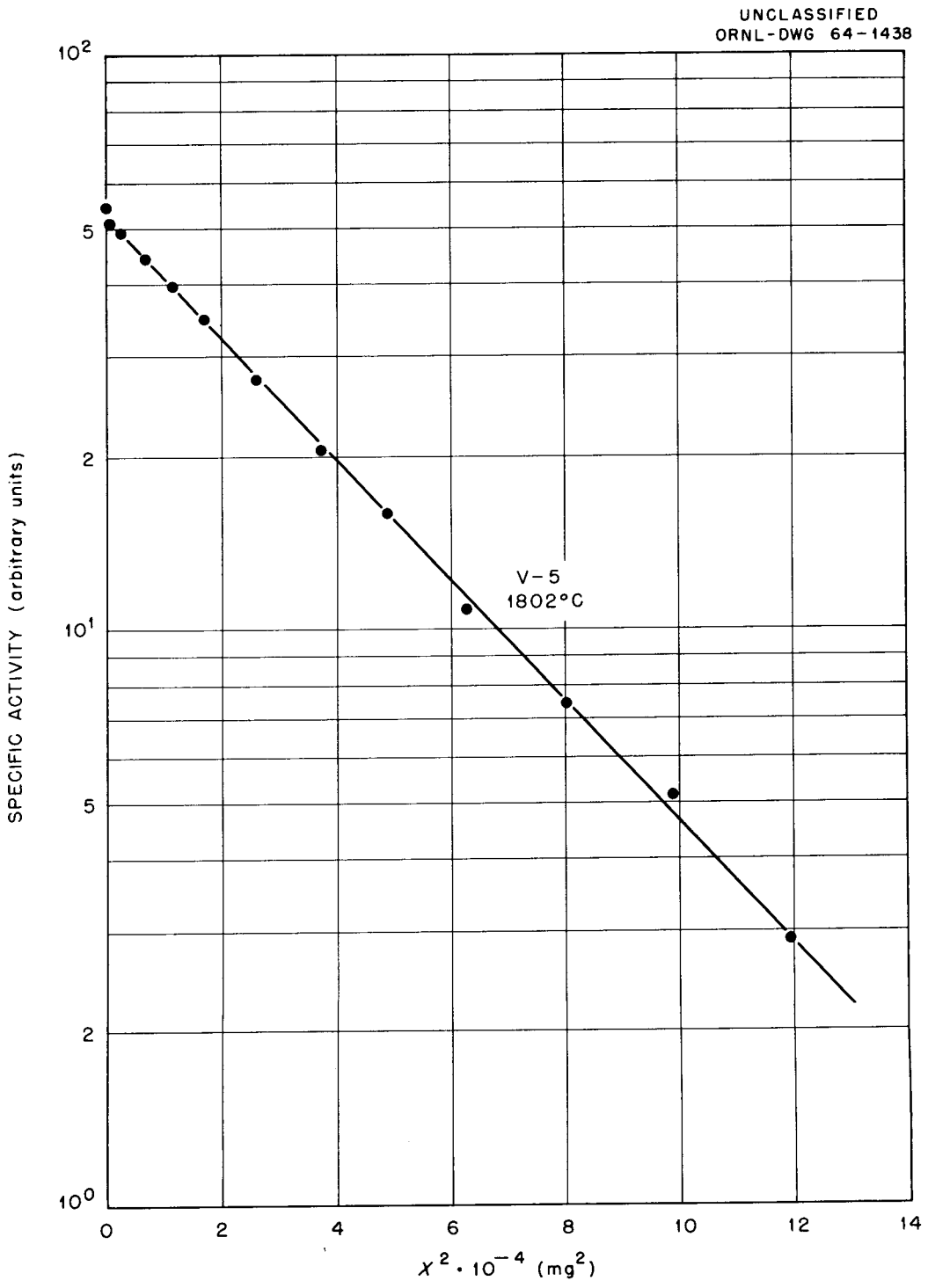

Figure 7. Penetration profile for specimen V-5 for diffusion of vanadium-48 in vanadium at 1802°C for 18,120 seconds.

For specimen V-5,

$\left(\frac{1}{\rho A}\right)_T^2 = 2.667 \times 10^{-8}$ square centimeters per square milligram.

So, $D = 1.53 \times 10^{-8}$ square centimeters per second.

The procedure for treating grinding data is similar to that described above. However, when anodizing and stripping was used, the distances were given directly in normal distance units (centimeters); therefore, the only correction was that of thermal expansion of the specimens from room to diffusion annealing temperatures. Division of the counting rates by section thickness was necessary only when different anodizing voltages were used in the same specimen.

Some of the data were treated by using a computer program written by F. R. Winslow (51). The input data were the background counting rate (counts per second), annealing time (seconds) and temperature (°C), thermal expansion $\left(\frac{\ell + \Delta\ell}{\ell}\right)$, specimen diameter (inches), room-temperature density (grams per cubic centimeter), and half-life of the isotope if a decay correction was to be made. The computer determines the least-squares value of D and the 90 per cent confidence limits on this value and automatically plots the data and results on a graph. Figure 8 shows the resulting plot for specimen V-5. The value of the diffusion coefficient as determined by this method is $D = (1.54 \pm 0.02) \times 10^{-8}$ square centimeters per second.

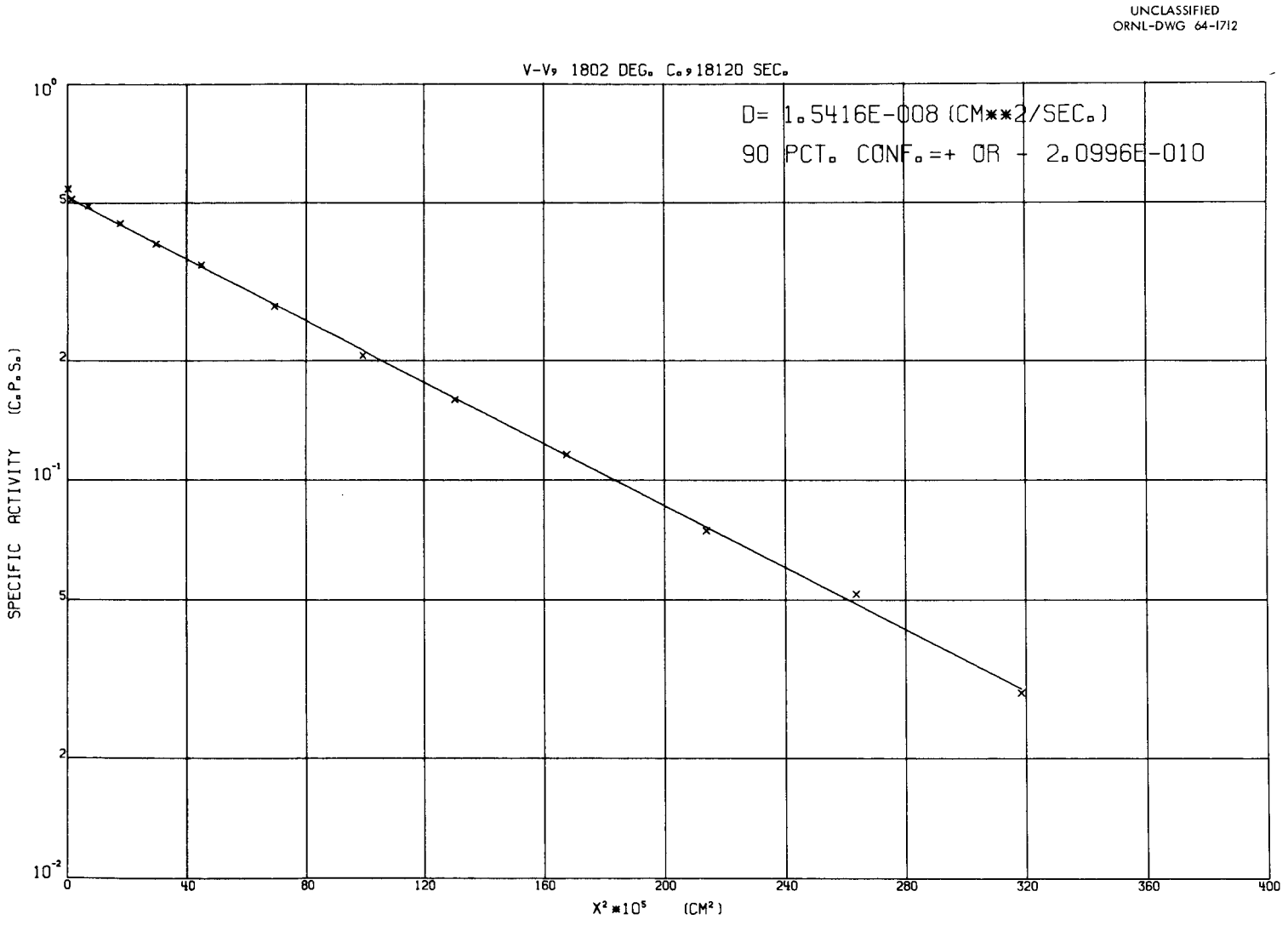

Figure 8. Computer plot (CALCOMP) of the penetration for specimen V-5.

CHAPTER III

RESULTS

Activity penetration profiles for all specimens studied are presented in the figures in the Appendixes. Diffusion coefficients calculated from such plots are summarized in tabular form and graphically. Subsequent evaluation of the temperature dependence of the determined diffusion coefficients will be made in Chapter V.

I. ZIRCONIUM-95 AND NIOBIUM-95 IN BETA ZIRCONIUM

The figures in Appendix A show activity penetration profiles for the diffusion of zirconium-95 in body-centered cubic beta zirconium. The logarithm of the relative specific activity is plotted versus the square of the distance into the specimen in square milligrams. As previously discussed, the diffusion coefficient was first calculated in square milligrams per second and then converted to the standard units of square centimeters per second. These calculated diffusion coefficients are listed in Table IX along with the temperature in degrees centigrade and the inverse absolute temperature. A graph of $\ell n\ D$ versus T^{-1} for these data is found in Figure 9.

The figures in Appendix B illustrate the activity penetration profiles for the diffusion of niobium-95 in beta zirconium. Here, the abscissa is given in square centimeters; therefore, the diffusion coefficients were computed directly in square centimeters per second. These diffusion coefficients are summarized in Table X and Figure 9.

TABLE IX

SUMMARY OF RESULTS FOR ZIRCONIUM-95 IN BETA ZIRCONIUM

T (°C)	$\frac{10^4}{T}$ ($°K^{-1}$)	D (cm^2/sec)
901	8.517	7.27×10^{-10}
947	8.197	1.03×10^{-9}
1000	7.855	1.44×10^{-9}
1053	7.541	2.26×10^{-9}
1098	7.294	3.06×10^{-9}
1148	7.037	4.38×10^{-9}
1200	6.789	6.81×10^{-9}
1252	6.557	8.81×10^{-9}
1302	6.349	1.38×10^{-8}
1355	6.143	1.74×10^{-8}
1403	5.967	2.45×10^{-8}
1457	5.780	3.40×10^{-8}
1504	5.627	4.62×10^{-8}
1551	5.482	6.08×10^{-8}
1605	5.325	8.44×10^{-8}
1647	5.208	1.09×10^{-7}
1698	5.074	1.51×10^{-7}
1747	4.950	2.05×10^{-7}

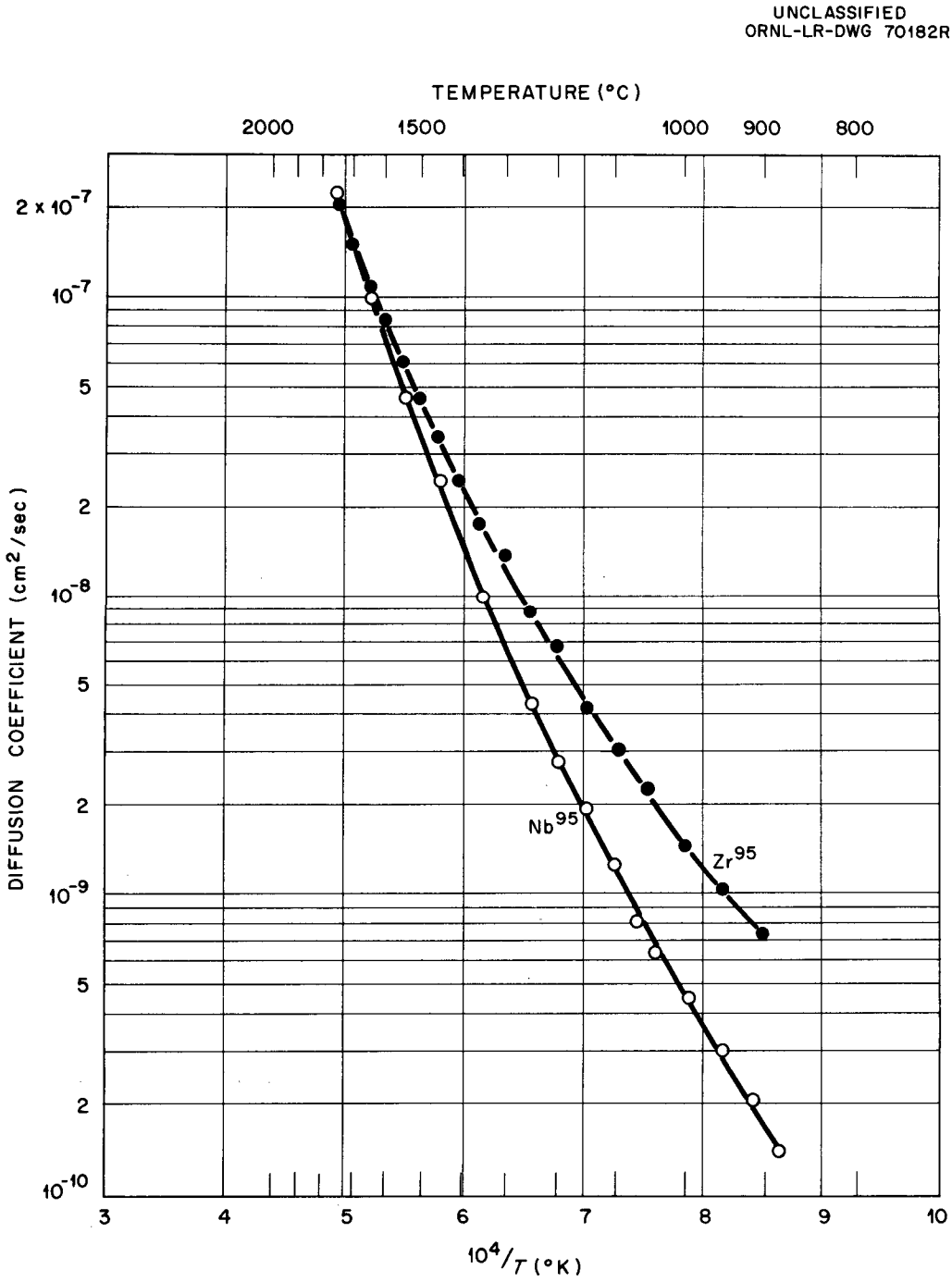

Figure 9. Temperature dependence of diffusion of zirconium-95 and niobium-95 in beta zirconium.

TABLE X

SUMMARY OF RESULTS FOR NIOBIUM-95 IN BETA ZIRCONIUM

T (°C)	$\frac{10^4}{T}$ ($°K^{-1}$)	D (cm^2/sec)
882	8.658	1.39×10^{-10}
911	8.446	2.04×10^{-10}
949	8.183	3.00×10^{-10}
993	7.899	4.52×10^{-10}
1039	7.622	6.29×10^{-10}
1067	7.463	8.10×10^{-10}
1100	7.283	1.26×10^{-9}
1149	7.032	1.93×10^{-9}
1198	6.798	2.74×10^{-9}
1246	6.583	4.32×10^{-9}
1350	6.161	1.00×10^{-8}
1450	5.804	2.44×10^{-8}
1545	5.501	4.61×10^{-8}
1645	5.214	9.90×10^{-8}
1758	4.924	2.26×10^{-7}

Figure 10 compares the plots obtained in this work for both zirconium-95 and niobium-95 in beta zirconium with data from previous studies (35–39) on diffusion of zirconium-95 in beta zirconium.

II. VANADIUM-48 IN VANADIUM

The figures in Appendix C show the activity penetration profiles for diffusion of vanadium-48 in vanadium. Diffusion coefficients calculated from these plots by hand and calculated using the computer are summarized in Table XI and Figure 11. Limits of error are seen to be quite large for the low-temperature data.

III. NIOBIUM-95 AND TANTALUM-182 IN NIOBIUM

The figures in Appendix D show the activity penetration plots for diffusion of niobium-95 and tantalum-182 in niobium. Table XII summarizes the diffusion coefficients determined for niobium-95 in niobium having less than 100 parts per million oxygen. Results for niobium doped with oxygen to nominal contents of 250 and 500 parts per million are given in Tables XIII and XIV. Results for two experiments on tantalum-182 diffusion in niobium are given in Table XV. The data are plotted as a function of temperature for diffusion of niobium-95 in niobium in Figure 12. Also plotted are data by Resnick and Castleman (43) on the same system but in the limited temperature interval of about 1600 to 2150°C.

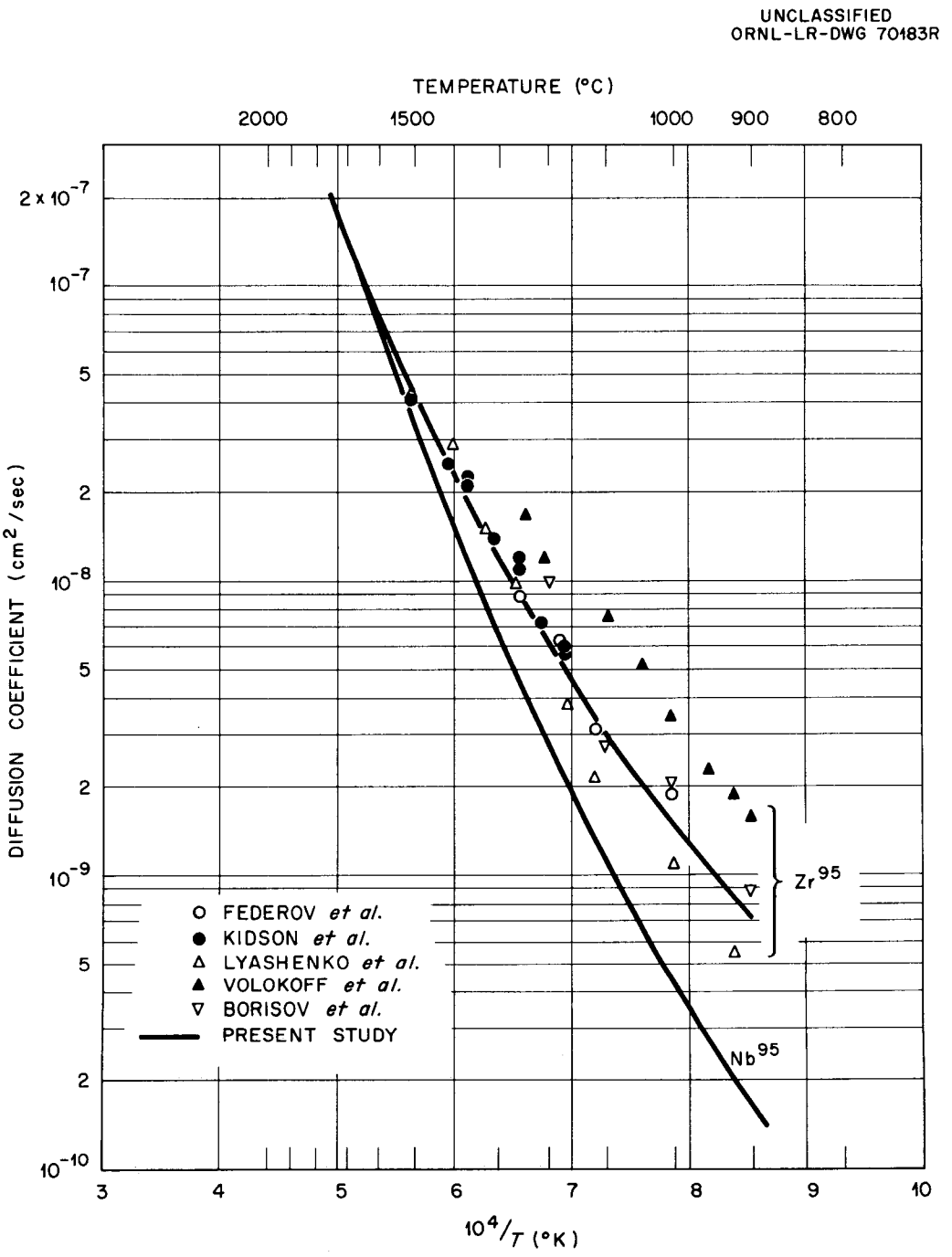

Figure 10. Comparison of present results on diffusion of zirconium-95 and niobium-95 in beta zirconium with results by other investigators.

TABLE XI

SUMMARY OF RESULTS FOR VANADIUM-48 IN VANADIUM

T (°C)	$\frac{10^4}{T}$ ($°K^{-1}$)	D (cm^2/sec) Hand Calculated	D (cm^2/sec) Computer
1002	7.843	3×10^{-13}	$(4.14 \pm 1.74)^* \times 10^{-13}$
1101	7.278	1.95×10^{-12}	$(2.09 \pm 0.28) \times 10^{-12}$
1200	6.789	1.98×10^{-12}	$(2.43 \pm 0.64) \times 10^{-12}$
1200	6.789	3.58×10^{-12}	$(3.39 \pm 0.41) \times 10^{-12}$
1200	6.789	1.61×10^{-12}	$(1.64 \pm 0.07) \times 10^{-12}$
1300	6.357	3.38×10^{-11}	$(4.15 \pm 0.89) \times 10^{-11}$
1401	5.974	1.10×10^{-10}	$(1.16 \pm 0.06) \times 10^{-10}$
1498	5.646	3.32×10^{-10}	$(3.43 \pm 0.29) \times 10^{-10}$
1610	5.311	1.53×10^{-9}	$(1.59 \pm 0.03) \times 10^{-9}$
1652	5.195	2.22×10^{-9}	$(2.15 \pm 0.06) \times 10^{-9}$
1702	5.063	4.97×10^{-9}	$(5.03 \pm 0.17) \times 10^{-9}$
1752	4.938	7.84×10^{-9}	$(7.90 \pm 0.08) \times 10^{-9}$
1802	4.819	1.53×10^{-8}	$(1.54 \pm 0.02) \times 10^{-8}$
1848	4.715	2.17×10^{-8}	$(2.25 \pm 0.07) \times 10^{-8}$
1888	4.627	3.57×10^{-8}	$(3.54 \pm 0.05) \times 10^{-8}$

*The deviations in parentheses represent the 90 per cent confidence limits calculated using student's t distribution.

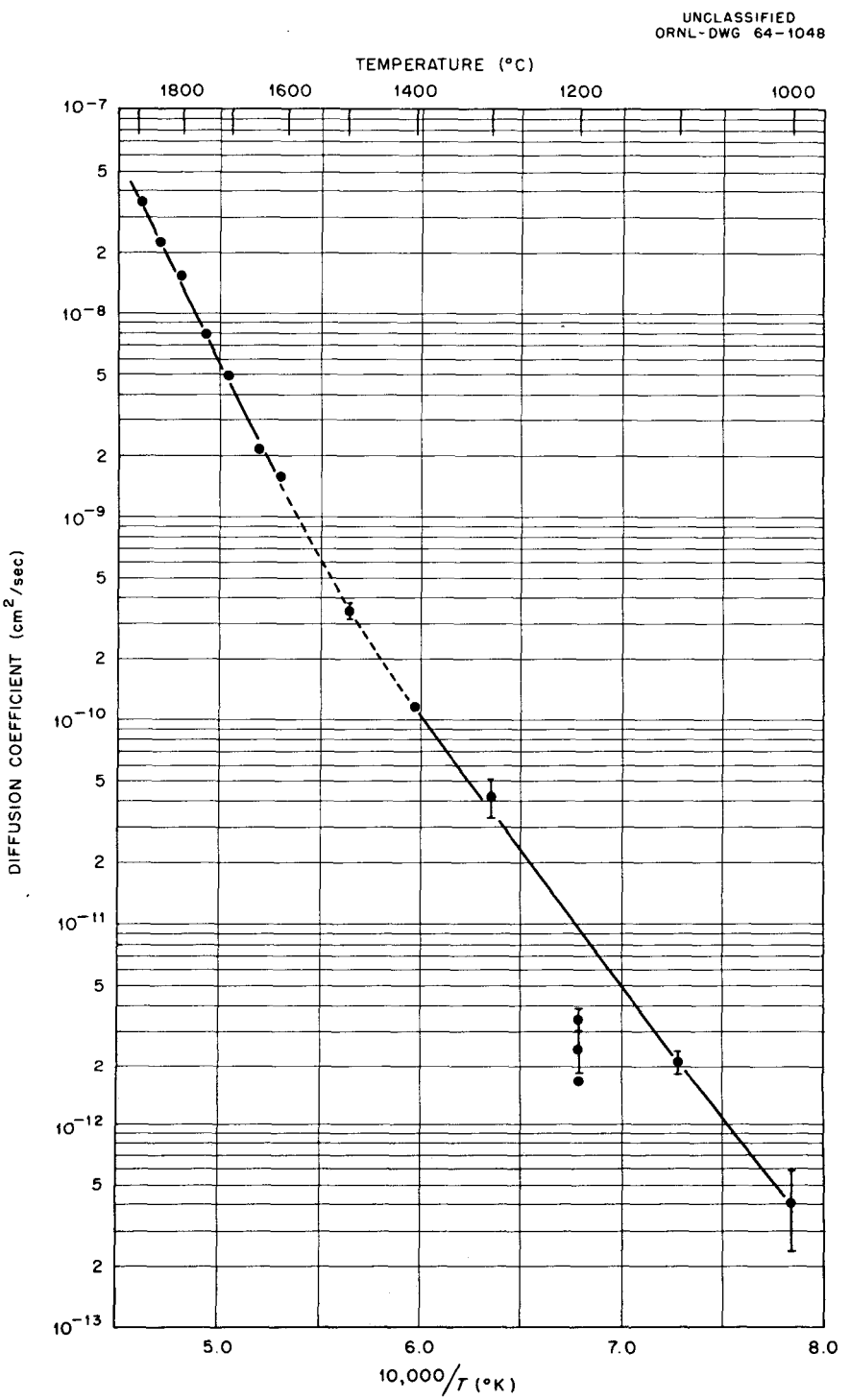

Figure 11. Temperature dependence of diffusion of vanadium-48 in vanadium.

TABLE XII

SUMMARY OF RESULTS FOR NIOBIUM-95 IN NIOBIUM

T (°C)	$\frac{10^4}{T}$ (°K^{-1})	D (cm^2/sec) Hand Calculated	D (cm^2/sec) Computer
1003	7.837	6.92×10^{-16}	
1103	7.267	2.73×10^{-15}	
1200	6.789	6.29×10^{-15}	
1312	6.309	7.40×10^{-14}	
1315	6.297	7.75×10^{-14}	
1408	5.949	2.24×10^{-13}	
1502	5.634	5.26×10^{-12}	
1601	5.336	1.21×10^{-11}	
1691	5.092	2.50×10^{-11}	
1799	4.826	6.44×10^{-11}	
1900	4.602	1.12×10^{-10}	
1999	4.401	5.55×10^{-10}	$(7.08 \pm 1.36)^* \times 10^{-10}$
2000	4.400	8.34×10^{-10}	$(8.95 \pm 0.48) \times 10^{-10}$
2106	4.203	1.24×10^{-9}	$(1.45 \pm 0.04) \times 10^{-9}$
2140	4.144	2.33×10^{-9}	$(2.55 \pm 0.15) \times 10^{-9}$
2200	4.044	4.06×10^{-9}	$(4.04 \pm 0.21) \times 10^{-9}$
2320	3.856	9.72×10^{-9}	$(9.99 \pm 0.22) \times 10^{-9}$
2395	3.748	1.90×10^{-8}	$(1.90 \pm 0.03) \times 10^{-8}$

*The deviations in parentheses represent the 90 per cent confidence limits calculated using student's t distribution.

TABLE XIII

SUMMARY OF RESULTS FOR NIOBIUM-95 IN NIOBIUM DOPED WITH OXYGEN TO 250 PARTS PER MILLION

T (°C)	$\frac{10^4}{T}$ ($°K^{-1}$)	D (cm^2/sec)
1200	6.789	6.29×10^{-15}
1298	6.365	4.70×10^{-14}
1501	5.643	1.16×10^{-12}

TABLE XIV

SUMMARY OF RESULTS FOR NIOBIUM-95 IN NIOBIUM DOPED WITH OXYGEN TO 500 PARTS PER MILLION

T (°C)	$\frac{10^4}{T}$ ($°K^{-1}$)	D (cm^2/sec)
1200	6.789	6.29×10^{-15}
1298	6.365	4.70×10^{-14}
1501	5.643	1.16×10^{-12}

TABLE XV

SUMMARY OF RESULTS FOR TANTALUM-182 IN NIOBIUM

T (°C)	$\frac{10^4}{T}$ ($°K^{-1}$)	D (cm^2/sec)
1103	7.267	1.52×10^{-15}
1408	5.949	9.03×10^{-14}

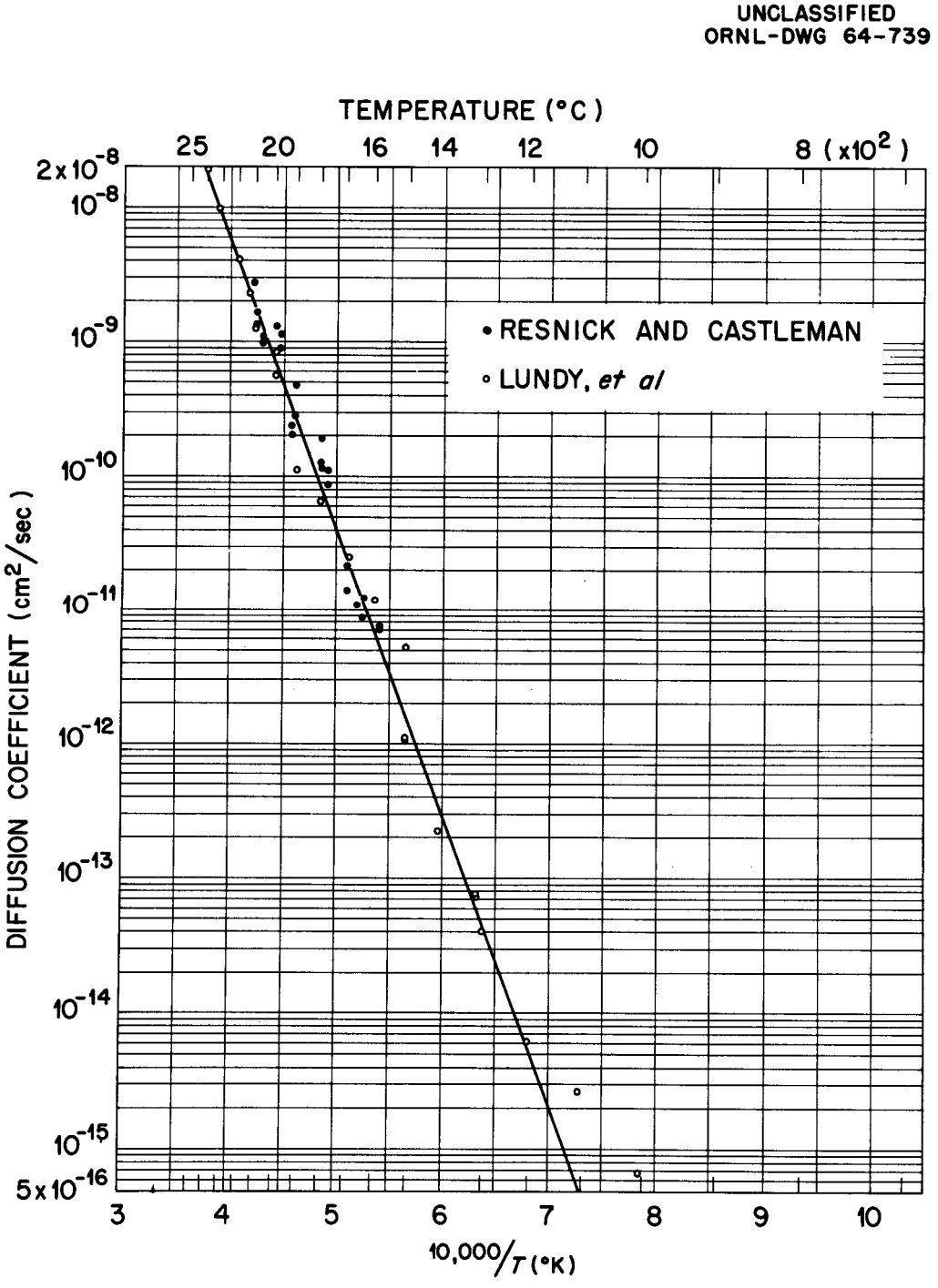

Figure 12. Temperature dependence of diffusion of niobium-95 in niobium.

IV. NIOBIUM-95 IN TANTALUM

Penetration plots for the diffusion of niobium-95 in tantalum are given in the figures in Appendix E. Diffusion coefficients were determined both in the near-surface regions and in the volume regions. Results of these determinations are found in Table XVI. A comparison of these data with data by Gruzin and Meshkov (45) on tantalum-182 diffusion in tantalum and with one point by Peterson (34) on inter-diffusion of niobium and tantalum as analyzed using an electron microprobe is given in Figure 13.

TABLE XVI

SUMMARY OF RESULTS FOR NIOBIUM-95 IN TANTALUM

T (°C)	$\frac{10^4}{T}$ ($°K^{-1}$)	D (cm^2/sec) Near-Surface	D (cm^2/sec) Volume
1050	7.559	3.12×10^{-17}	1.15×10^{-15}
1170	6.930	1.04×10^{-15}	3.12×10^{-14}
1250	6.566	1.71×10^{-15}	1.47×10^{-13}

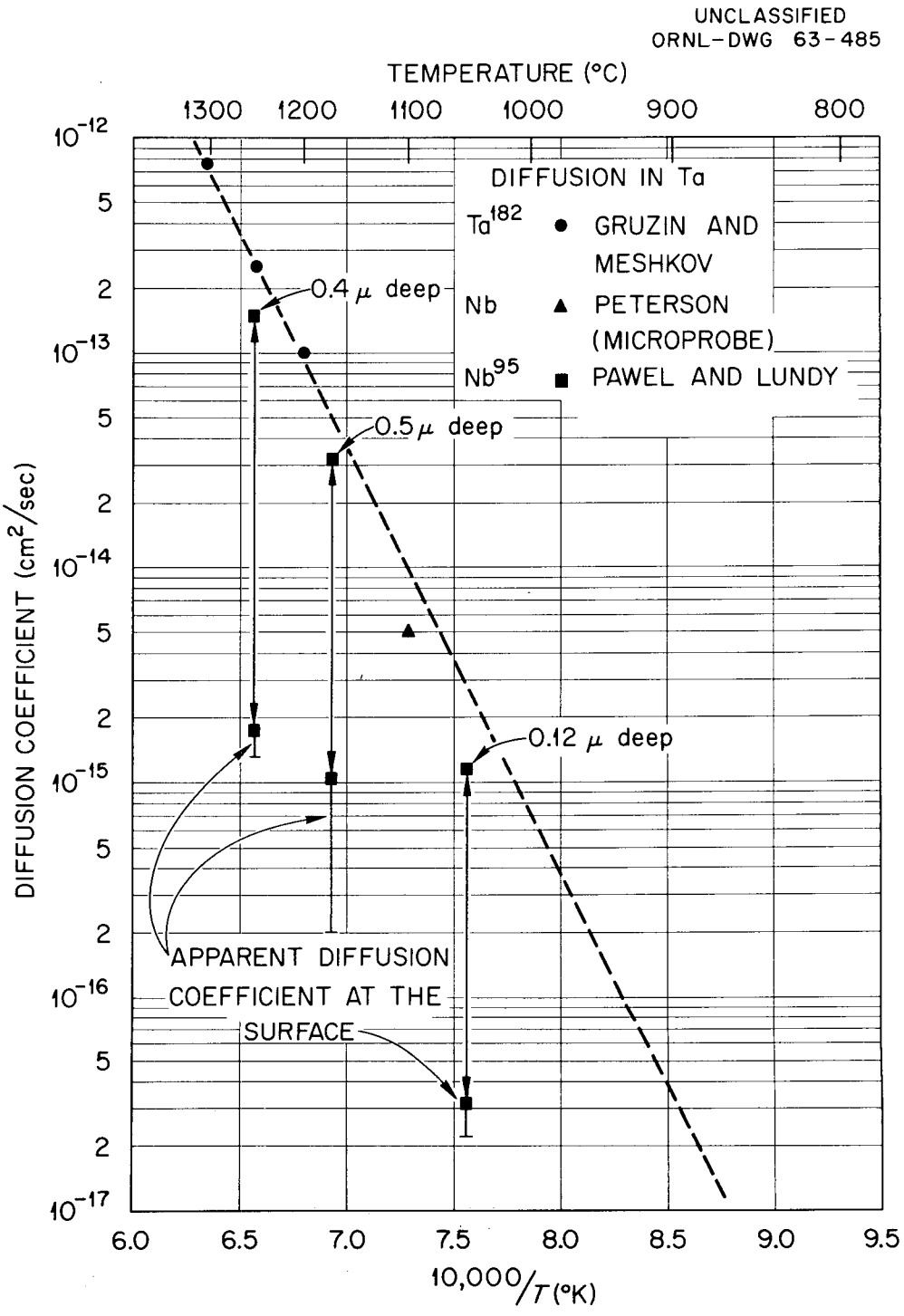

Figure 13. Temperature dependence of diffusion of niobium-95 in tantalum showing data from near-surface and volume regions of diffusion.

CHAPTER IV

DISCUSSION OF RESULTS

Results of this study will be discussed principally in terms of the observed temperature dependences of the diffusion coefficients for the different systems. The fact that much of the data cannot be described in terms of the usual Arrhenius-type equation has led to considerable speculation as to the reason or reasons involved. These various possibilities will be thoroughly examined. Development of the anodizing and stripping technique has allowed accurate measurement of diffusion coefficients in niobium and tantalum at very low temperatures. The resulting characterization of the near-surface regions will be discussed. Models of diffusion will be discussed in the last section. Important conclusions from this study will be summarized in Chapter V.

I. ZIRCONIUM-95 AND NIOBIUM-95 IN BETA ZIRCONIUM

Penetration profiles for diffusion of zirconium-95 in beta zirconium at temperatures between the transformation temperature and about 1100°C are characterized by an enhanced activity near the surface, as shown in Figure 16, Appendix A. Other profiles for both zirconium-95 and niobium-95 in zirconium, however, have the normal Gaussian distribution (Figures 17–19, Appendix A; Figures 20–23, Appendix B). These other profiles include ones for niobium-95 diffusion in the low-temperature range. As previously stated,

zirconium-95 decays with a half-life of 65 days to niobium-95 which has a half-life of 35 days (both decay with gamma emissions of 0.75 million electron volts). The zirconium-95 isotope was purified shortly before the experiments were begun. However, during the two days of diffusion annealing of the low-temperature specimens, a significant amount of niobium-95 was formed. This niobium-95 was responsible for the non-Gaussian penetration behavior shown in Figure 16, Appendix A. The effects at low temperatures were accentuated because of the longer diffusion anneals required and the greater differences in diffusion coefficients of the two isotopes as shown in Figure 9, page 70. Diffusion coefficients of zirconium-95 in zirconium in the low-temperature range were calculated from the penetration profiles in Figure 16, Appendix A, by neglecting the first few data points which were influenced by presence of niobium-95. All other penetration profiles for diffusion in beta zirconium were of normal character.

The non-Arrhenius-type behavior for diffusion of both zirconium-95 and niobium-95 in beta zirconium is quite pronounced. This is illustrated by the lack of linearity of the data plotted in Figure 9, page 70. Previous discrepancies (35–39) for self-diffusion in this system may now be readily explained in terms of this nonlinearity. The calculated pre-exponential and activation energy terms in the Arrhenius-type expression simply were dependent on the particular temperature interval accentuated by the investigators. Lyashenko et al. (37) and Kidson and McGurn (36) covered higher temperatures and obtained larger D_o and Q values than did the other

investigators (35,38,39). Figure 10, page 73, illustrates that, in fact, there is reasonably good agreement between data obtained by different investigators. The apparent disagreement was due to use of a nonapplicable equation. This illustrates the significance of the very important results of the present study. One cannot, in general, extrapolate diffusion data from one temperature interval to another by using the Arrhenius-type equation.

One of the early objectives of this study was to determine if the usual empirical rules related to diffusion coefficients for face-centered cubic metals could be extended generally to body-centered cubic systems. One "rule-of-thumb" is that the self-diffusion coefficient should be about 10^{-8} square centimeters per second at the melting point. For zirconium this is almost 10^{-6}, so the rule does not apply. Other empirical formulas have been used to relate the activation energy for diffusion to melting temperature, heat of melting, and heat of sublimation as seen in Table I, page 37. Since these rules give unique values of activation energy and since, for zirconium, the apparent activation energy changes with temperature, such rules cannot apply.

Several approaches may be taken to explain the curvature in the Arrhenius-type plots for diffusion in beta zirconium. The first and probably the best approach is simply that curvature is to be expected when wide temperature ranges are covered by diffusion data — even if a single mechanism of diffusion operates. There is no theoretical reason requiring the activation energy to be constant with changing

temperature. Arrhenius (22) was first to point out that, in the general case, one must consider the activation energy to be temperature dependent. Jost (3) considered the case where the activation energy is a linear function of temperature. However, he erroneously applied this assumption to the integrated form of the Arrhenius-type expression instead of to the differential form. If one assumes that the activation energy is a linear function of temperature and applies this assumption to the expression

$$\frac{d\ \ell n\ D}{d\left(\frac{1}{T}\right)} = -\frac{Q}{R} \quad , \tag{65}$$

then it may be easily shown that

$$D = AT^{B} \exp\left(\frac{C}{T}\right) \quad . \tag{66}$$

An equation of this same form has been previously suggested as describing vapor pressure data more accurately than the widely used Clausius-Clapeyron equation (52). If one assumes equation 65 to be the defining equation for the activation energy Q of diffusion, then Q can be found as a function of temperature from plots of ℓn D versus T^{-1}. Such a procedure was followed for the zirconium diffusion data and Q was found to vary, at least within the accuracy of the procedure, linearly with temperature as illustrated in Figure 14. If one makes the further assumption that the pre-exponential factor D_o is given at any temperature by the usual extrapolation to $T^{-1} = 0$, then D_o may be calculated as a function of temperature. It is found to vary, as

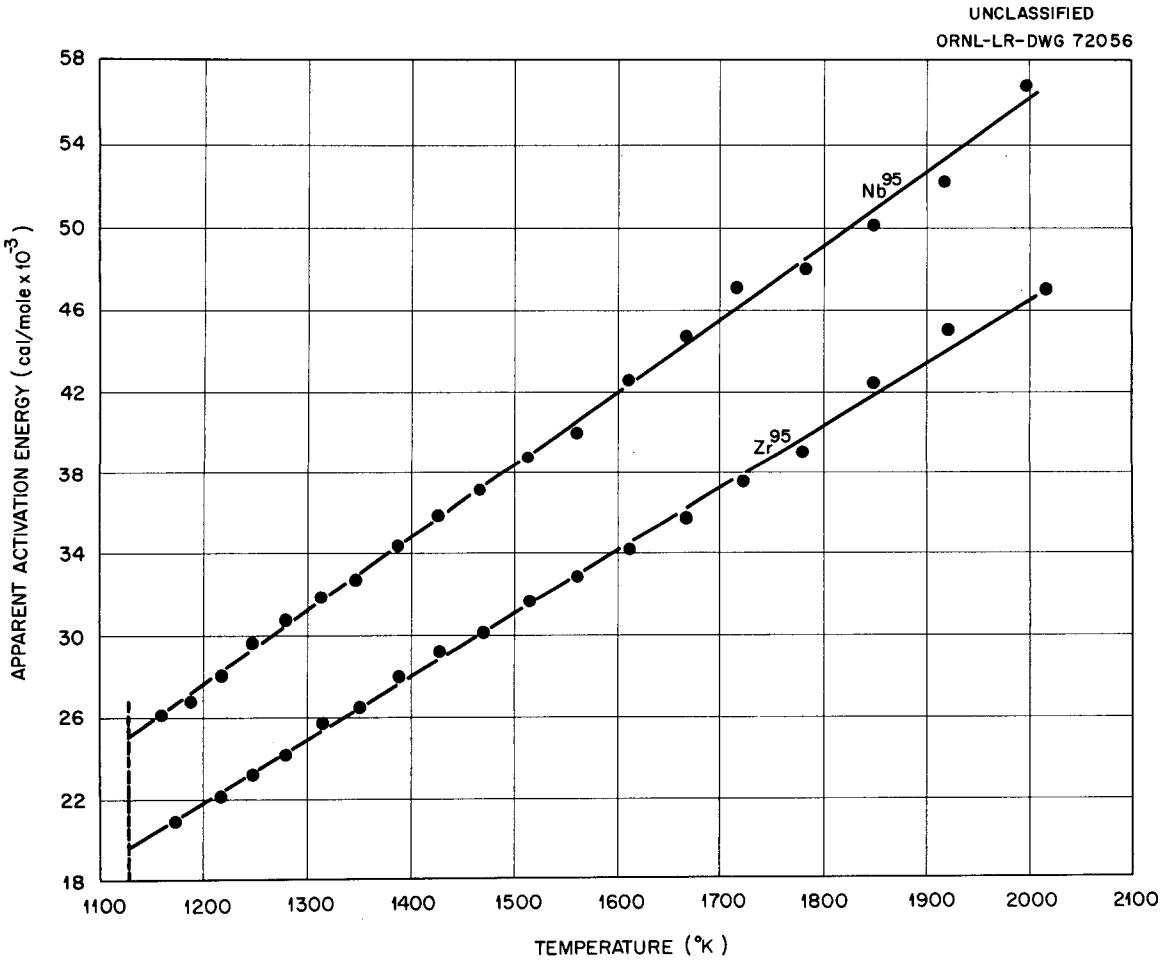

Figure 14. Temperature variation of the apparent activation energies for diffusion of zirconium-95 and niobium-95 in beta zirconium.

predicted by equation 66, page 87, with a power of temperature as illustrated in Figure 15. In this figure, the symbol T_t stands for the alpha to beta transformation temperature of zirconium (T_t = 1136°K). Equations derived by following the above procedures for describing the temperature dependence of diffusion coefficients for these sytems are

$$D_{Zr^{95}} = 3 \times 10^{-6} \left(\frac{T}{1136} \right)^{15.6} \exp \left(- \frac{19,600 + 30.9\ (T-1136)}{RT} \right) \qquad (67)$$

square centimeters per second

and

$$D_{Nb^{95}} = 9 \times 10^{-6} \left(\frac{T}{1136} \right)^{18.1} \exp \left(- \frac{25,100 + 35.5\ (T-1136)}{RT} \right) \qquad (68)$$

square centimeters per second .

Other possible explanations of the curvature in the Arrhenius-type plots for diffusion are based on the possibility that two or more mechanisms of diffusion operate simultaneously. It is generally believed, for example, that short-circuiting along grain boundaries and dislocation pipes acts to enhance values of diffusion coefficients at low temperatures. For diffusion in beta zirconium, it is also possible that defects introduced by the alpha to beta transformation may enhance diffusion rates at low temperatures. In the present study, as will be seen, results on the diffusion of vanadium-48 in vanadium show that low-temperature enhancements are not due entirely to such defects. Transformation effects were also checked by Kidson and McGurn (42) who annealed specimens in the beta range, deposited the

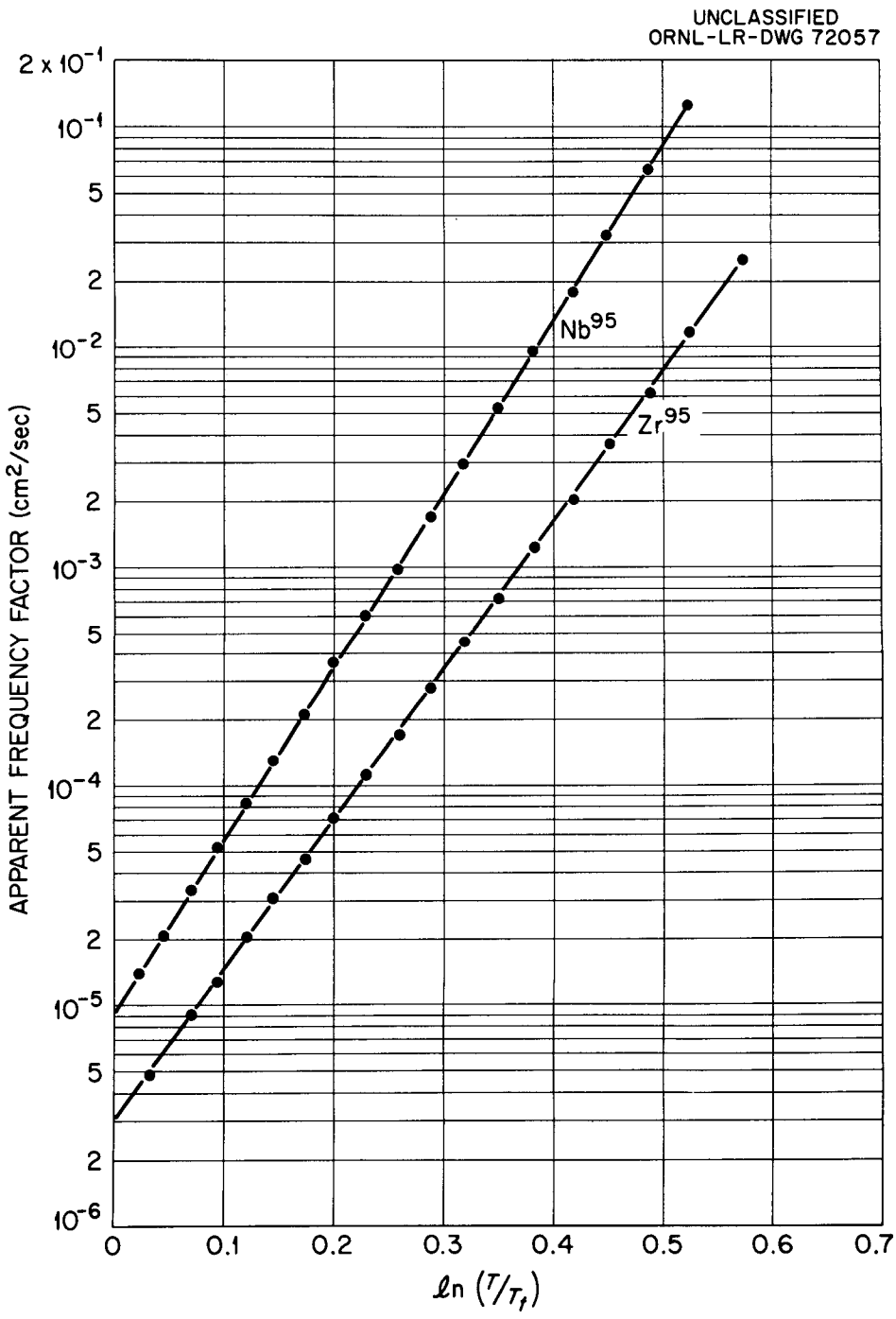

Figure 15. Temperature variation of the apparent frequency factors for diffusion of zirconium-95 and niobium-95 in beta zirconium.

zirconium isotope, and performed diffusion anneals prior to cooling through the transformation. No significant differences were found between these specimens and others heated through the transformation temperature for diffusion annealing after deposition of the isotope. During this study, efforts were made to determine differences in penetration behavior for niobium-95 diffusing into tantalum with different dislocation concentrations. Different dislocation densities were achieved by using well-annealed single crystals and crystals deformed up to about 50 per cent in compression. Diffusion anneals were done at temperatures below 1200°C so that dislocation densities remained fairly constant. Penetration behavior was not detectably different for the different specimens; therefore, short-circuiting down dislocation pipes cannot be taken as the sole reason for nonlinear Arrhenius-type plots.

More than one volume mechanism of diffusion may be operating over the whole range of temperature for zirconium. For example, the values of D_o and Q for the lowest temperatures are consistent with those proposed for the four-atom ring mechanism (53), while the values near the melting point are consistent with those one might expect for the vacancy mechanism (54). The existence of a Kirkendall effect in several body-centered cubic systems, however, tends to dispute the idea that the ring mechanism may operate.

Kidson (55) has proposed that the nonlinear Arrhenius-type plots for diffusion in zirconium may be described as being due to a summation of intrinsic and extrinsic vacancy mechanisms — with each

mechanism being described by a unique activation energy. For the low-temperature data, where the activation energy is also low, he postulates that diffusion occurs primarily by motion of a temperature-independent concentration of vacancies associated with oxygen impurities; at high temperatures the mechanism becomes primarily one of motion of thermally formed vacancies. Using this idea, the determined activation energy at low temperatures is simply that for motion of a vacancy; at high temperatures the activation energy is the sum of the energies of formation and migration of a vacancy. We have checked this possibility experimentally, at least for niobium, by using material of varying oxygen content and, as will be described later, have found little or no enhancement of diffusion due to increasing amounts of oxygen.

II. VANADIUM-48 IN VANADIUM

Diffusion experiments of vanadium-48 in vanadium were performed using vanadium single crystals. The crystals, however, had a high oxygen content (about 880 parts per million) so that Kidson's (55) suggestion with regard to impurity effects could not be evaluated. Vanadium has no crystal structure change between room temperature and its melting point; therefore, difficulties similar to those associated with the transformation in zirconium were not encountered.

Penetration profiles for vanadium (Figures 24–27, Appendix C) are of reasonably normal character. Scatter in the data does become quite large at low temperatures where the grinding technique was used

in sectioning. The Arrhenius-type plot, Figure 11, page 75, illustrates definite deviations from linearity, but the low-temperature diffusion coefficients are quite uncertain and the elaborate technique of fitting the data by equation 66, page 87, in order to obtain a temperature dependence of activation energy is not justified. The high-temperature data (above 1600°C) may be described by

$$D = 58 \exp\left(-\frac{91,500}{RT}\right) \text{ square centimeters per second,}$$

while the low-temperature data (below 1400°C) follow

$$D = 1.1 \times 10^{-2} \exp\left(-\frac{61,000}{RT}\right) \text{ square centimeters per second.}$$

Three specimens were run at 1200°C in evacuated quartz ampoules. Reaction occurred between silicon in the quartz and the specimens. High silicon content on the surfaces of the vanadium was confirmed by analysis. Principal effect of this reaction was to drastically decrease the measured diffusion coefficient. Whether this effect was due to a tying-up of the vanadium-48 by chemical reaction or to a decrease in the vacancy concentration is a matter of speculation. The effect was not marked at lower temperatures.

In summary, the diffusion coefficient of vanadium-48 in vanadium does not obey a simple Arrhenius-type expression. It may follow an equation similar to those derived for diffusion in zirconium or it may be divided into two distinct parts with one Arrhenius-type expression above 1300°C and another below this temperature. The data do not justify choosing between these two alternatives.

III. NIOBIUM-95 AND TANTALUM-182 IN NIOBIUM

As previously discussed, these experiments on diffusion in niobium were performed using three kinds of materials and three different techniques of sectioning. Large-grained polycrystalline niobium was used for all the high-temperature specimens where sectioning was done by lathe techniques and grinding. Some of the same material was used at lower temperatures where sectioning was accomplished by anodizing and stripping, but most of the work using this technique was done with single crystals having three different oxygen contents.

The penetration profiles for seven polycrystalline specimens were determined by lathe sectioning. The profiles, typically Gaussian as illustrated in Figures 28–30, Appendix D, were determined for specimens annealed above about 2000°C. Illustration of diffusion coefficients calculated from these data is made in Figure 12, page 80. There seems to be no deviation from linearity in the Arrhenius-type plot and good agreement with data by Resnick and Castleman (43).

The next five data points from this study, as shown in Figure 12, page 80, were found using the grinding technique with polycrystalline specimens. Penetration profiles for these specimens are given in Figures 31 and 32, Appendix D. There is considerable scatter in the data for these specimens, but the overall profiles are still Gaussian. Examination of these diffusion coefficients in Figure 12, page 80, reveals fair consistency with data of Resnick and Castleman (43), but also illustrates another interesting point. If only these five data

points had been determined and if the data had been fitted with an Arrhenius-type expression, drastic differences would have been found from the overall picture given in Figure 12, page 80. That is, these data might be fitted by

$$D = 1.68 \times 10^{-4} \exp\left(-\frac{61,000}{RT}\right) \text{ square centimeters per second}$$

which, as will be seen, is considerably different from the equation describing the data between 1200 and 2400°C.

The remaining penetration profiles were determined using the anodizing and stripping technique. Two polycrystalline specimens, annealed at 1312 and 1315°C, gave normal penetration profiles (shown in Figure 33, Appendix D) and diffusion coefficients that fit a linear extrapolation on the Arrhenius-type plot in Figure 12, page 80. Diffusion coefficients at 1501°C for oxygen-doped single crystals, as determined from the profiles in Figure 34, Appendix D, are considerably lower than that determined by grinding a specimen annealed at 1502°C. This difference, if real, indicates that oxygen decreases the diffusion coefficient of niobium-95 in niobium. Subsequent results will differ with this possibility. Another reason for this difference might be that, when the technique was changed from rather thick sectioning by grinding to very thin sectioning by anodizing and stripping, volume diffusion (region II in Figure 3, page 34) was no longer dominating but near-surface diffusion (region I in Figure 3, page 34) was measured. This possibility deserves further exploration. Other penetration profiles for diffusion of niobium-95 in undoped niobium are shown in

Figures 35–37, Appendix D. The profile for the specimen annealed at 1003 °C and listed in Table XII, page 76, is omitted.

Figures 36 and 38, Appendix D, show penetration profiles for specimens of different oxygen content subjected to identical diffusion anneals. Increasing the oxygen content seemed to have little effect on the slopes of the lines, but the "tails" (representing region III of diffusion – see Figure 3, page 34) may have been enlarged by higher oxygen. Thus, it is seen that varying the oxygen content has no effect on the volume diffusion coefficient of niobium-95 in niobium but increased oxygen enhances short-circuiting.

Only two specimens were run with both niobium-95 and tantalum-182 isotopes. Penetration profiles for these specimens are shown in Figures 35 and 37, Appendix D. In both instances, it is obvious that tantalum-182 is the slower moving isotope. It is also noteworthy that little or no differences were found in near-surface effects for the two isotopes. The tantalum diffusion coefficients are not plotted but are listed in Table XV, page 79. More data are required before the temperature dependence of the diffusion of tantalum in niobium can be adequately described.

The overall temperature dependence for the diffusion of niobium-95 in niobium may be pictured as obeying the Arrhenius-type expression

$$D = 1.66 \exp\left(-\frac{97{,}600}{RT}\right) \text{ square centimeters per second}$$

for all temperatures above about 1200 °C. The enhancement of diffusion

rates at lower temperatures is real and may be considered to agree qualitatively with data for diffusion in beta zirconium and vanadium.

IV. NIOBIUM-95 IN TANTALUM

Penetration profiles for diffusion of niobium-95 in tantalum (Figures 39–41, Appendix E) are non-Gaussian. They consist of a near-surface region and a volume region (regions I and II, respectively, in Figure 3, page 34). Apparent diffusion coefficients calculated in regions I and II differ by large factors as summarized in Table XVI, page 84, and Figure 13, page 83. Agreement between the coefficients in region II and previous experiments on diffusion of tantalum-182 and niobium in tantalum is also given in Figure 13, page 83. Note that the depths of the surface-affected regions are less than one micron in all cases. Thus, conventional sectioning methods would probably completely mask the near-surface region while anodizing and stripping allowed an accurate characterization.

The existence of near-surface effects may be used to explain some anomalous results reported in the literature. For example, comparison of the data by Hirano, Cohen, and Averbach (7) on impurity diffusion in silver with data from works by Mullen (56), Hirone, Muira, and Suzuoka (57), and Hirone and Yamamoto (58) reveals large and previously unexplained differences. These differences may readily be resolved in terms of the near-surface effect. The first workers (7) sectioned specimens by grinding thin layers and thus studied the near-surface effect; the other workers (56–58) used longer annealing times,

and thicker sectioning techniques, and neglected near-surface effects in computing diffusion coefficients. A similar argument may be used to explain the peculiar results for impurity diffusion in aluminum (59). It may tentatively be concluded from the data of Hirano et al. (7,59) that the temperature dependence of diffusion in the near-surface region is characterized by very low D_o and Q values in the Arrhenius-type expression.

Although further work is needed to explain near-surface effects, some thoughts as to their origin may be helpful. At first, one might consider the isotope layer to have been too thick for the assumed boundary conditions to apply. However, as pointed out on page 5, too thick an isotope layer causes the penetration profile (on a plot of $\ell n\ A(x)$ versus x^2) to be concave downward near $x = 0$. Thus, such conditions would cause the opposite deviation from "normality" from that encountered here. A second possibility is that a barrier to diffusion exists which is somehow related to the method of isotope deposition. In these experiments, both dropwise deposition and electroplating of the isotope were tried without significant differences in the resulting penetration profiles. This idea is, therefore, not believed to give the correct answer. It has been suggested that interaction of the isotope atoms with some impurity atoms concentrated near the specimen surface might cause reduced diffusion rates. The fact that near-surface effects are quite pronounced for diffusion of both niobium-95 and tantalum-182 in tantalum seems to rule out this possibility, because one should expect little or no difference in interaction

of tantalum-182 with such impurities and interaction of normal tantalum with them. If one assumes a vacancy mechanism of diffusion, the reduced mobility near a surface may be considered due to a reduced vacancy concentration. It is possible, though quite unlikely, that surface tension effects may cause such a state to exist. Another possibility is that the vacancy concentration near a surface is lowered by the physical presence of impurity atoms that are known to segregate to regions near boundaries. This last idea seems to be at least partially discounted by the almost complete absence of these effects for diffusion in niobium which had a purity somewhat comparable to that for the tantalum. Use of high purity aluminum (59), copper (31), and silver (30) in other works where near-surface effects were observed also tends to discount this possibility. In short, none of the considered explanations for the near-surface effect stand out as being likely. Other possibilities must exist and further experimental work is needed to clarify the situation.

V. DIFFUSION MODELS

Two models representing possible mechanisms of substitutional-type diffusion have been widely considered. These models, briefly described in Chapter I, are called the vacancy model and the n-atom ring model. As previously stated, the most likely value of n for describing diffusion in body-centered cubic metals is four (9).

Calculations have generally supported the vacancy model for diffusion in face-centered cubic metals. Moreover, there have been a

number of experiments on other aspects of vacancies in these metals to provide data for checking the model. It was previously stated for this model that the activation energy Q for diffusion should equal the sum of the energies of formation Q_f and migration Q_m of vacancies. Shewmon (19) tabulated these values for diffusion in gold, silver, aluminum, and copper. In all cases, the energies of formation of vacancies as found by two methods — thermal expansion and quenching experiments — are in good agreement. The sum of these values with values of Q_m, also obtained from quenching experiments, is in reasonable agreement with experimentally determined activation energies of diffusion. For example, Desorbo and Turnbull (60) found Q_f and Q_m to be 18,200 and 12,000 calories per mole, respectively, for aluminum; Lundy and Murdock (61) determined the activation energy for diffusion of aluminum-26 in aluminum to be 34,000 calories per mole. The data for face-centered cubic metals are all consistent with $Q_f \approx 0.6\ Q$ and $Q_m \approx 0.4\ Q$.

The situation with regard to the vacancy model for diffusion in body-centered cubic metals is considerably different. The fact that a Kirkendall effect has been observed in several systems having this crystal structure does support the vacancy model. This effect, however, is observed only in cases where large chemical gradients exist and the large extrapolation to isotope diffusion in pure metals may not be justified. Quenching experiments have shown no excess resistivity that might be related to vacancy concentrations. This means that such point defects are present in very small numbers either because few existed at the annealing temperature (hence, a high value

for Q_f) or because they escaped to traps during the quenching (thus, a very low value of Q_m). Attempts to find Q_m from annealing experiments on cold-worked or irradiated specimens are open to serious questions because of the variety of defects produced and because of "damage" to the matrix itself. Such data as are available are listed in Table XVII.

Mehl, Swanson, and Pound (65) calculated formation energies for vacancies by using $Q_f = 0.4\ (V/\Delta V)\ \Delta H_f$ where $\Delta V/V$ and ΔH_f represent the solidification shrinkage and the heat of fusion, respectively. If one assumes, in accordance with Darken and Gurry (66), that $\Delta V/V$ is about 0.03 for body-centered cubic metals and uses standard references (67,68) to obtain values of ΔH_f, one obtains values for formation energies of vacancies. These are summarized in Table XVIII.

If results listed in Tables XVII and XVIII are combined, values of $Q_m + Q_f$ may be compared with experimentally determined activation energies of diffusion. Such comparisons are given in Table XIX where values of Q_m for zirconium, titanium, and vanadium were estimated from $Q_m \approx 0.25\ Q_f$ as suggested by Brooks (69). Agreement between predictions based on the simple vacancy model and measured activation energies of diffusion is fair except for zirconium and titanium. Estimated values are on the high side in almost all cases but are considerably higher for these two metals. Using this comparison, one might conclude that diffusion occurs by a vacancy mechanism for niobium, molybdenum, tantalum, tungsten, and vanadium. The situation remains unclear for deciding on the mechanism in zirconium and titanium.

TABLE XVII

SUMMARY OF AVAILABLE DATA ON THE ENERGY OF MOTION OF VACANCIES IN BODY-CENTERED CUBIC METALS

Metal	Q_m (cal/mole)	Type of Experiment	Reference
Niobium	28,000	Neutron Irradiation	(62)
Molybdenum	28,800	Neutron Irradiation	(62)
Tantalum	31,000	Neutron Irradiation	(63)
Tungsten	39,000	Cold Work	(64)

TABLE XVIII

VALUES OF THE ENERGY OF FORMATION OF VACANCIES AS COMPUTED BY THE METHOD OF MEHL, SWANSON, AND POUND (65)

Metal	ΔH_f (cal/mole)	Q_f (cal/mole)
Niobium	6400	85,300
Molybdenum	6700	89,400
Tantalum	6900	92,000
Tungsten	8100	108,000
Zirconium	5500	73,300
Titanium	5000	66,700
Vanadium	4000	53,300

TABLE XIX

COMPARISON OF PREDICTED AND MEASURED ACTIVATION ENERGIES FOR DIFFUSION IN CERTAIN BODY-CENTERED CUBIC METALS

Metal	Predicted			Measured	
	Q_f (cal/mole)	Q_m (cal/mole)	$Q_f + Q_m$ (cal/mole)	Q (cal/mole)	Reference
Niobium	85,300	28,000	113,300	97,600	This Work
Molybdenum	89,400	28,800	118,200	92,200	(48)
Tantalum	92,000	31,000	123,000	110,000	(45)
Tungsten	108,000	39,000	147,000	120,500	(70)
Zirconium	73,300	18,300	91,600	20,700–46,900	This Work
Titanium	66,700	16,700	83,400	31,200–60,000	(41)
Vanadium	53,300	13,300	66,600	61,000–91,500	This Work

At least three attempts have been made to relate the magnitude of the pre-exponential factor D_o in the Arrhenius-type expression to the mechanism of diffusion (53,71,72). Even though inaccuracies in experimental determinations of D_o are quite large, a comparison of experimental values with those predicted by theoretical models may be helpful in choosing a likely mechanism.

Zener (71) derived the expression

$$D_o = \gamma\, a^2\, \nu \exp(\Delta S/R) \tag{69}$$

where

γ = a geometrical factor related to the crystal structure,

a = the lattice parameter,

ν = the vibrational frequency, and

ΔS = the entropy of activation.

He related the entropy of activation to other factors by

$$\Delta S = \frac{\lambda\, \beta\, Q}{T_m} \tag{70}$$

where

λ = a numerical coefficient related to the fraction of energy used in straining the lattice during a diffusion jump,

β = the negative of the normalized rate of change of elastic modulus with temperature,

Q = the activation energy for diffusion, and

T_m = the melting temperature.

He then demonstrated that λ should be about 0.55 for vacancy diffusion and about 1.0 for ring diffusion. Zener emphasized that it was "highly improbable" that ΔS could have a negative sign because β is expected to always be positive. By combining equations 69 and 70, page 105, one finds

$$D_o = \gamma\ a^2\ \nu\ \exp\ (\lambda\ \beta\ Q/RT_m)\ . \qquad (71)$$

Now, either a vacancy mechanism (for which $\lambda = 0.55$ and $\gamma = 1.0$) or a four-atom ring mechanism (for which $\lambda = 1.0$ and $\gamma = 6.0$) may be assumed. Then, D_o values computed using equation 71 may be compared with those found experimentally. Such comparisons are given in Tables XX and XXI for niobium, zirconium, vanadium, and titanium. Except for the case of vanadium, these comparisons support the idea that diffusion in body-centered cubic metals occurs by a vacancy mechanism. Such support, however, is not altogether convincing.

LeClaire (72) extended the theory of Zener by assuming correlations between the various quantities occurring in the theoretical expressions for the diffusion coefficient and other properties of the lattice. He showed that experimentally observed values of D_o and Q were consistent only with the supposition of a vacancy mechanism in face-centered cubic metals and with a ring mechanism in the body-centered cubic metals, alpha iron and tungsten. Theoretical expressions for the diffusion coefficients were based on Zener's relation for D_o.

Pound, Bitler, and Paxton (53) treated kinetics of diffusion in cubic metals in terms of statistical mechanics from the point of view

TABLE XX

COMPARISON OF EXPERIMENTAL D_o VALUES WITH D_o VALUES CALCULATED BY THE ZENER METHOD USING THE VACANCY MODEL

Metal	Temperature (°C)	D_o (cm^2/sec) Calculated	D_o (cm^2/sec) Experimental
Niobium	T > 1200	0.46	1.66
Zirconium	T ≈ 1650	3.9	2.5×10^{-2}
Zirconium	T ≈ 900	0.13	4.8×10^{-6}
Vanadium	T > 1300	0.43	58
Titanium	T ≈ 1550	12	0.1*
Titanium	T ≈ 900	1.1	3.6×10^{-4}*

*See reference 41.

TABLE XXI

COMPARISON OF EXPERIMENTAL D_o VALUES WITH D_o VALUES CALCULATED BY THE ZENER METHOD USING THE RING MODEL

Metal	Temperature (°C)	D_o (cm^2/sec) Calculated	D_o (cm^2/sec) Experimental
Niobium	T > 1200	20	1.66
Zirconium	T ≈ 1650	3,600	2.5×10^{-2}
Zirconium	T ≈ 900	7	4.8×10^{-6}
Vanadium	T > 1300	80	58
Titanium	T ≈ 1550	26,000	0.1*
Titanium	T ≈ 900	340	3.6×10^{-4}*

*See reference 41.

of absolute rate theory. They concluded, in conflict with Zener's argument, that there is a negative contribution to the entropy of activation for diffusion in solids. This negative contribution is negligible for the vacancy mechanism but very significant for the ring mechanism. They found that a low experimental D_o (of the order of 10^{-4} square centimeters per second) could be a criterion for the existence of the four-atom ring mechanism of diffusion and suggested that self-diffusion in pure chromium and in gamma uranium might occur by this mechanism. This idea might be extended to describe diffusion at low temperatures in beta zirconium and titanium and in niobium and vanadium.

All of the proposed models of diffusion suffer from the fact that they represent drastic oversimplification of very complex phenomena. For example, many are based on the assumption that one can use equilibrium thermodynamics to describe the relation between the normal and the activated state. The existence of such a state for long enough times to allow adjustment of the surrounding lattice has not been adequately demonstrated. Even if this type approach is allowed, the answers to such questions as what vibrational frequency should one use in the theoretical expressions are not altogether clear. Certainly, the frequency of an atom adjacent to a vacancy is different from that of an atom in the perfect lattice. Thus, we see that it is essentially impossible to make exact calculations from first principles for describing the diffusion process. Attempts such as those described

in this section have been instructive in understanding the process, and extension of such attempts to cover new ideas and new experimental data is of utmost importance.

CHAPTER V

CONCLUSIONS AND RECOMMENDATIONS

Based on the findings of this investigation, the following conclusions and recommendations are stated:

1. The Arrhenius-type expression with constants D_o and Q cannot be generally used to describe the temperature dependence of diffusion coefficients in body-centered cubic metals over wide temperature ranges. Extrapolations beyond the temperature interval covered by experimental data must be done with caution. Further experiments should be performed on face-centered cubic systems to extend temperature ranges covered by diffusion data and determine the applicability of the Arrhenius-type expression. It is suggested that such experiments be done using copper, gold, nickel, and/or silver.
2. For diffusion in beta zirconium, expressions of the form $D = AT^B \exp(C/T)$ were found to accurately describe the experimental data over the whole temperature interval. This expression is of the same form as that sometimes used to accurately describe the temperature dependence of vapor pressure data.

3. Deviations from linearity in ℓn D versus T^{-1} plots were also observed for diffusion in single crystals of vanadium and niobium. Thus, low-temperature enhancements of diffusion coefficients cannot be explained entirely on the basis of the phase transformation that occurs in zirconium or of diffusion along grain boundaries.

4. Experiments with niobium having different oxygen contents have shown that low-temperature deviations from Arrhenius-type behavior cannot be explained, at least for niobium, on the basis of oxygen content effects on the vacancy concentration. These experiments gave some rather inconclusive evidence that oxygen does affect region III of diffusion. Such effects should be more thoroughly investigated.

5. Experiments to determine the effect of dislocation concentration changes on diffusion rates of niobium-95 in tantalum showed no large effect. Such tests should be repeated and extended to other systems to clarify the role of dislocations in diffusion.

6. It is not possible to decide if the non-Arrhenius behavior observed in several body-centered cubic systems is due to a temperature dependent activation energy for a single process or to the action of multiple mechanisms with each having a unique activation energy. Further experimental and theoretical

efforts should be made to resolve the question. In particular, more information on the energies of formation and migration of vacancies is needed for body-centered cubic metals. Since quenching methods were inconclusive, it is suggested that another method such as that using field ion microscopy be used in such determinations.

7. The newly developed anodizing and stripping technique is a valuable tool for determining small diffusion coefficients and for studying surface effects on diffusion rates. The technique should be developed further, so that it might be used with metals other than niobium and tantalum.

8. Near-surface effects dominated the data on diffusion of niobium-95 in tantalum. However, data far from the surface could be related to volume diffusion. These effects are of extreme importance both in diffusion work and in surface studies and should be investigated thoroughly.

9. Examination of the vacancy and ring models of diffusion in terms of data from this work revealed general agreement with the vacancy mechanism of diffusion. However, the possibility that another mechanism may dominate in a certain temperature range cannot be excluded with the present state of development of the theory.

LIST OF REFERENCES

1. Webster's New Collegiate Dictionary. Springfield, Massachusetts: G. & C. Merriam Company, 1956.

2. Crank, J. The Mathematics of Diffusion. London: Oxford University Press, 1956.

3. Jost, W. Diffusion in Solids, Liquids, Gases. New York: Academic Press, Incorporated, 1960.

4. Seith, W. and T. Heumann. Diffusion in Metallen. Berlin/Goettingen/Heidelberg: Springer-Verlag, 1955.

5. Roberts-Austen, W. C. "On the Diffusion of Metals," Phil. Trans. Roy. Soc. London, Ser. A, 187 (1896), 404.

6. Hirone, Tokutaro, et al. "Diffusion of Iron Group Elements in Silver," Conf. J. Phys. Soc. Japan, 18, Suppl. II (1963), 213.

7. Hirano, Ken-ichi, Morris Cohen, and B. L. Averbach. "Diffusion of Iron, Cobalt and Nickel in Silver," Acta Met., 11 (May, 1963), 463.

8. Biermann, W., F. R. Winslow, and T. S. Lundy. "Concerning Diffusion of Iron, Cobalt and Nickel in Silver," Acta Met., 12 (March, 1964), 328.

9. Zener, C. "Ring Diffusion in Metals," Acta Cryst., 3 (1950), 346.

10. Mortlock, A. J., and D. H. Tomlin. "The Atomic Diffusion of Chromium in the Titanium-Chromium System," Phil. Mag., 4 (1959), 628.

11. Paxton, H. W., and T. Kunitake. "Diffusion in the Iron-Chromium System," Trans. AIME, 218 (December, 1960), 1003.

12. Peart, R. F., and D. H. Tomlin. "Diffusion of Solute Elements in Beta-Titanium," Acta Met., 10 (February, 1962), 123.

13. Gibbs, G. B., D. Graham, and D. H. Tomlin. "Diffusion in Titanium and Titanium-Niobium Alloys," Phil. Mag., 8 (August, 1963), 1269.

14. LeClaire, A. D. "Diffusion of Metals in Metals," Progress in Metal Physics, Vol. 1, pp. 306–79. New York: Interscience Publishers, Incorporated, 1949.

15. Seitz, Frederick. "Fundamental Aspects of Diffusion in Solids," Phase Transformations in Solids, pp. 77–148. New York: John Wiley and Sons, Incorporated, 1951.

16. Smallman, R. E. Modern Physical Metallurgy. London: Butterworths and Company, 1962.

17. Glasstone, Samuel, Keith J. Laidler, and Henry Eyring. The Theory of Rate Processes. New York and London: McGraw-Hill Book Company, Incorporated, 1941.

18. Fisher, J. C., J. H. Holloman, and D. Turnbull. "Absolute Reaction Rate Theory for Diffusion in Metals," Trans. AIME, 175 (1948), 202.

19. Shewmon, P. G. Diffusion in Solids. New York: McGraw-Hill Book Company, Incorporated, 1963.

20. LeClaire, A. D., and A. B. Lidiard. "Correlation Effects in Diffusion in Crystals," Phil. Mag., 1, Ser. 8 (1956), 518.

21. Mackliet, C. A. "Diffusion of Iron, Cobalt and Nickel in Single Crystals of Pure Copper," Phys. Rev., 109 (1958), 1964.

22. Arrhenius, Svante. "Uber die Reaktionsgeschwindigkeit bei der Inversion von Rohrzucker durch Sauren," Z. phy. chemie, 4 (1889), 226.

23. van't Hoff. "Etudes de dynamique chemique," as cited by Svante Arrhenius, Z. phy. chemie, 4 (1889), 226.

24. Perrin. Ann. Phys. (Paris) II, 5 (1919), as cited by Richard C. Tolman, J. Am. Chem. Soc., 42 (1920), 2506.

25. Tolman, Richard C. "Statistical Mechanics Applied to Chemical Kinetics," J. Am. Chem. Soc., 42 (1920), 2506.

26. Daniels, Farrington, and E. H. Johnston. "The Thermal Decomposition of Gaseous Nitrogen Pentoxide. A Monomolecular Reaction," J. Am. Chem. Soc., 43 (1921), 53.

27. Dushman, S., and I. Langmuir. "The Diffusion Coefficient in Solids and its Temperature Coefficient," Phys. Rev., 20 (1922), 113.

28. Langmuir, I. "The Electron Emission from Thoriated Tungsten Filaments," Phys. Rev., 22 (1923), 357.

29. Wert, C., and C. Zener. "Interstitial Atomic Diffusion Coefficients," Phys. Rev., 76 (1949), 1169.

30. Williams, G. P., Jr., and L. Slifkin. "Tracer Insolubility and the Anomalous Diffusion of Rare Earths in Silver and Lead," Acta Met., 11 (May, 1963), 319.

31. Styris, D. L., and C. T. Tomizuka. "Anomalous Diffusion Rate for Small Penetration Distance in Copper," J. Appl. Phys., 34 (1963), 1001.

32. Kosenko, V. E. "Two Simultaneous Mechanisms of Diffusion in Germanium," Fizika Tverdovo Tela, III (1961), 2102.

33. Ignatkov, V. D., and V. E. Kosenko. "Diffusion of Tellurium in Germanium," Fizika Tverdovo Tela, 4 (1962), 1627.

34. Peterson, N. L. "Diffusion in Refractory Metals," Wright Air Development Division Technical Report 60-793 (March, 1961).

35. Federov, G. B., and V. D. Gulyakin. "Diffusion of Zirconium and Tin in Tin Alloys of Beta-Zirconium," Met. i Met. Chist. Met., 1 (1959), 170.

36. Kidson, G., and J. McGurn. "Self-Diffusion in Body-Centered Cubic Zirconium," Can. J. Phys., 39 (1961), 1146.

37. Lyashenko, V. S., V. N. Bykov, and L. V. Pavlinov. "A Study of Self-Diffusion in Zirconium and its Alloys with Tin," Fiz. Metal. Metalloved., 8 (1959), 362.

38. Volokoff, D., Serge May, and Yves Adda. "Étude de l'autodiffusion du zirconium en phase β cubique centrée," Compt. Rend., 251 (1960), 2341.

39. Borisov, Ye. V., et al. "Study of Diffusion in Zirconium and in Certain Alloys with a Zirconium Base," Metallurgiya i Metallovedeniye, Izdatel'stvo Akademii Nauk USSR, Moscow, 1948 (NP-TR-448, F-TS-9849/V), 196.

40. Lundy, T. S., and J. I. Federer. "Diffusion of Zr^{95} in Body-Centered Cubic Iodide Zirconium." Paper read at the Fall Meeting of The Metallurgical Society of AIME, New York, New York, October 29, 1962.

41. Murdock, J. F., and T. S. Lundy. "Diffusion of Ti^{44} and V^{48} in Body-Centered Cubic Titanium." Paper read at the AIME Annual Meeting, Dallas, Texas, February 25, 1963.

42. Peart, R. F. Personal communication, 1963.

43. Resnick, R., and L. S. Castleman, "The Self-Diffusion of Columbium," Trans. AIME, 218 (April, 1960), 307.

44. Peart, R. F., D. Graham, and D. H. Tomlin. "Tracer Diffusion in Niobium and Molybdenum," Acta Met., 10 (May, 1962), 519.

45. Gruzin, P. L., and V. I. Meshkov. Problemy Metallovedeniza i Fiziki Metallov., 4 (1955), 570, as cited by N. L. Peterson, "Diffusion in Refractory Metals," Wright Air Development Division Technical Report 60-793 (March, 1961).

46. Hagel, W. C. "Self-Diffusion in Solid Chromium," Trans. AIME, 224 (June, 1962), 430.

47. Paxton, H. W., and E. G. Gondolf. "The Rate of Self-Diffusion in Pure Chromium," Arch. Eisenhüttenw., 30 (1959), 55.

48. Askill, J., and D. H. Tomlin. "Self-Diffusion in Molybdenum," Phil. Mag., 8 (June, 1963), 997.

49. Betterton, J. O. Personal communication, 1961.

50. Young, L. Anodic Oxide Films, New York: Academic Press, 1961.

51. Winslow, F. R. A FORTRAN Program for Calculating Diffusion Coefficients and Plotting Penetration Curves, Oak Ridge National Laboratory TM-726 (1963).

52. Daniels, Farrington. Outlines of Physical Chemistry. New York: John Wiley and Sons, Incorporated, 1952.

53. Pound, G. M., W. R. Bitler, and H. W. Paxton. "Theory of the Self-Diffusion Coefficient in Cubic Metals," Phil. Mag., 6 (April, 1961), 473.

54. Seitz, Frederick. "On the Theory of Diffusion in Metals," Acta Cryst., 3 (1950), 355.

55. Kidson, G. V. "On the Anomalous Diffusion Rates in B.C.C. Zirconium and Titanium," Can. J. Phys., 41 (1963), 1563.

56. Mullen, J. G. "Isotope Effect in Intermetallic Diffusion," Phys. Rev., 121 (1961), 1649.

57. Hirone, Tokutaro, Shigeto Miura, and Toshiro Suzuoka. "Diffusion of Nickel in Silver," J. Phys. Soc. Japan, 16 (December, 1961), 2456.

58. Hirone, Tokotaro, and Hisao Yamamoto. "Diffusion of Cobalt into Silver," J. Phys. Soc. Japan, 16 (March, 1961), 455.

59. Hirano, Ken-ichi, R. P. Agarwala, and Morris Cohen. "Diffusion of Iron, Nickel and Cobalt in Aluminum," Acta Met., 10 (September, 1962), 857.

60. DeSorbo, W., and D. Turnbull. "Quenching of Imperfections in Aluminum," Acta Met., 7 (1959), 83.

61. Lundy, T. S., and J. F. Murdock. "Diffusion of Al^{26} and Mn^{54} in Aluminum," J. Appl. Phys., 33 (1962), 1671.

62. Peacock, D. E., and A. A. Johnson. "Stage III Recovery in Neutron Irradiated Molybdenum and Niobium," Phil. Mag., 8 (1963), 563.

63. Peacock, D. E., and A. A. Johnson. "Point Defects in Niobium, Molybdenum and Tantalum," Nature, 195 (1962), 169.

64. Niemark, L. A., and R. A. Swalin. "Annealing of Point Defects in Cold-Worked Tungsten and the Influence of Impurities on the Kinetics," Trans. AIME, 218 (1960), 82.

65. Mehl, R. F., M. Swanson, and G. M. Pound. "Estimation of equilibrium vacancy concentration in solid metals," Acta Met., 9 (1961), 256.

66. Darken, Lawrence S., and Robert W. Gurry. Physical Chemistry of Metals. New York/Toronto/London: McGraw-Hill Book Company, Incorporated, 1953.

67. Metals Handbook (8th Edition), Vol. 1. Novelty, Ohio: American Society for Metals, 1961.

68. Hampel, Clifford A. Rare Metals Handbook (Second Edition). London: Reinhold Publishing Corporation, 1961.

69. Brooks, Harvey. "Lattice Vacancies and Interstitials in Metals," Impurities and Imperfections. Cleveland, Ohio: American Society for Metals, 1955.

70. Danneberg, W. "Selbstdiffusionsuntersuchungen an Wolfram," Metallwissenschaft und Technik, 15 (1961), 11.

71. Zener, Clarence. "Theory of D_o for Atomic Diffusion in Metals," J. Appl. Phys. 22 (1951), 372.

72. LeClaire, A. D. "The Theory of D_o in the Arrhenius Equation for Self-Diffusion in Cubic Metals," Acta Met., 1 (1953), 438.

APPENDIX A

PENETRATION PROFILES FOR DIFFUSION OF ZIRCONIUM-95 IN ZIRCONIUM

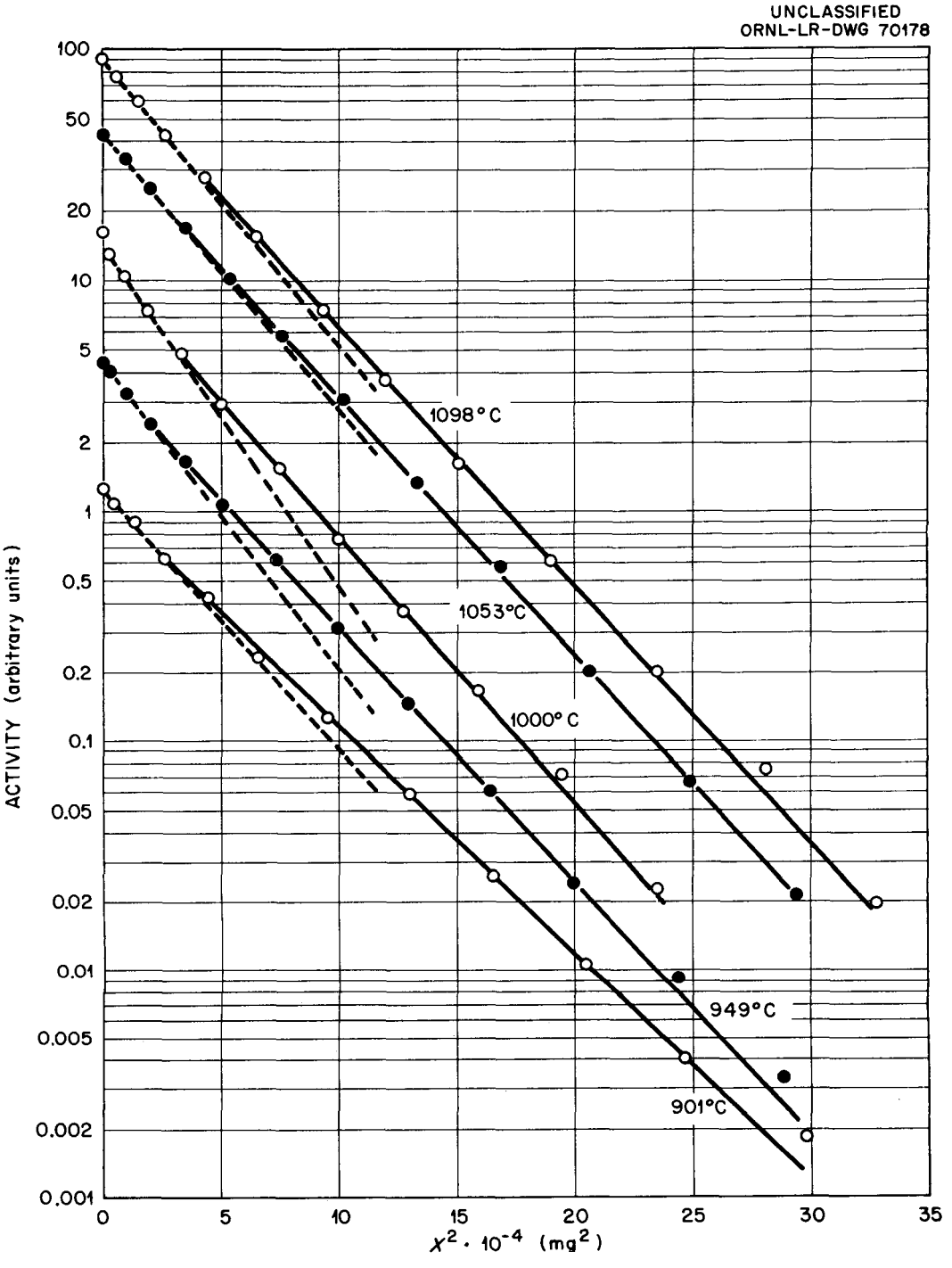

Figure 16. Penetration profiles for diffusion of zirconium-95 in zirconium at 901, 949, 1000, 1053, and 1098°C.

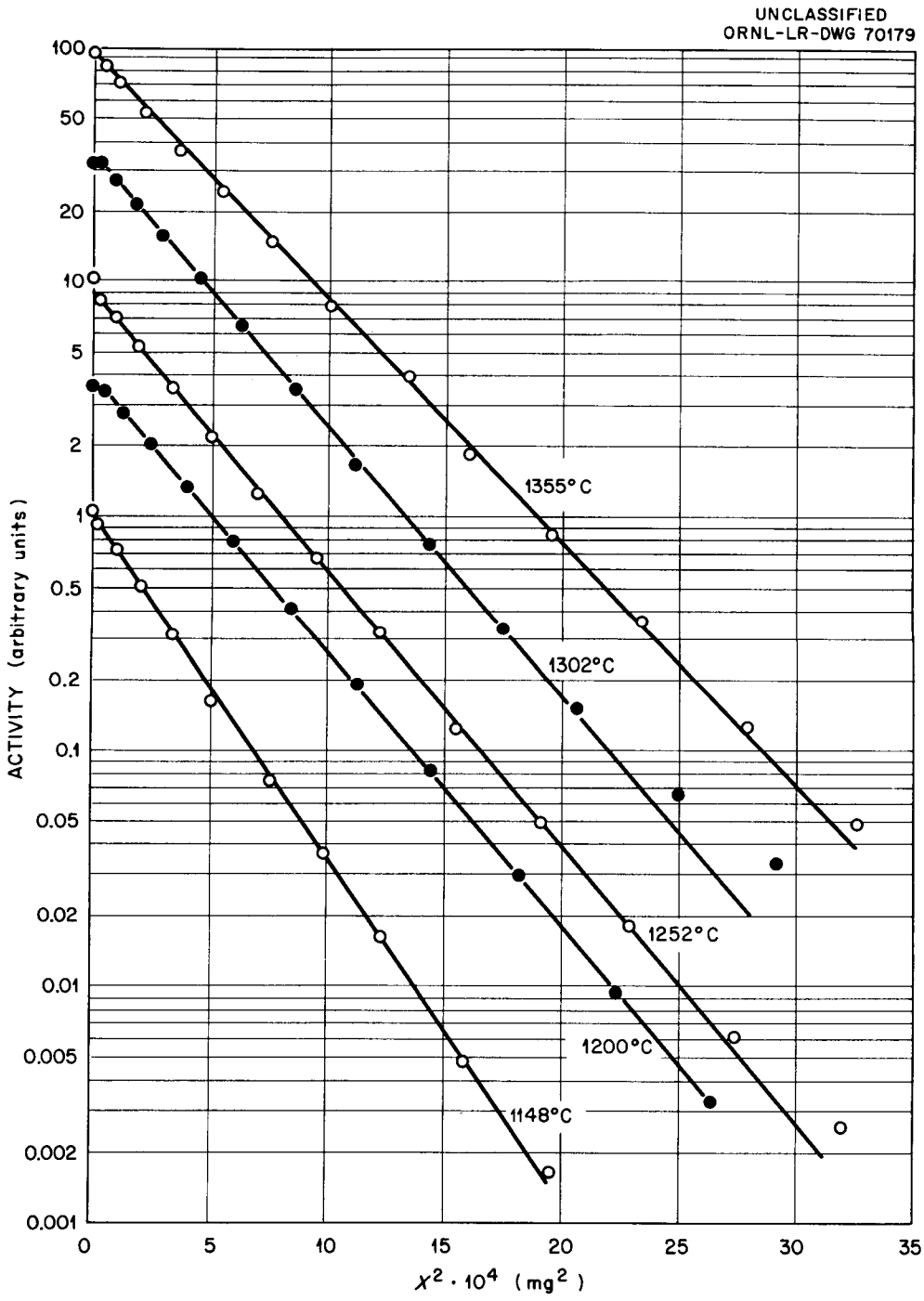

Figure 17. Penetration profiles for diffusion of zirconium-95 in zirconium at 1148, 1200, 1252, 1302, and 1355°C.

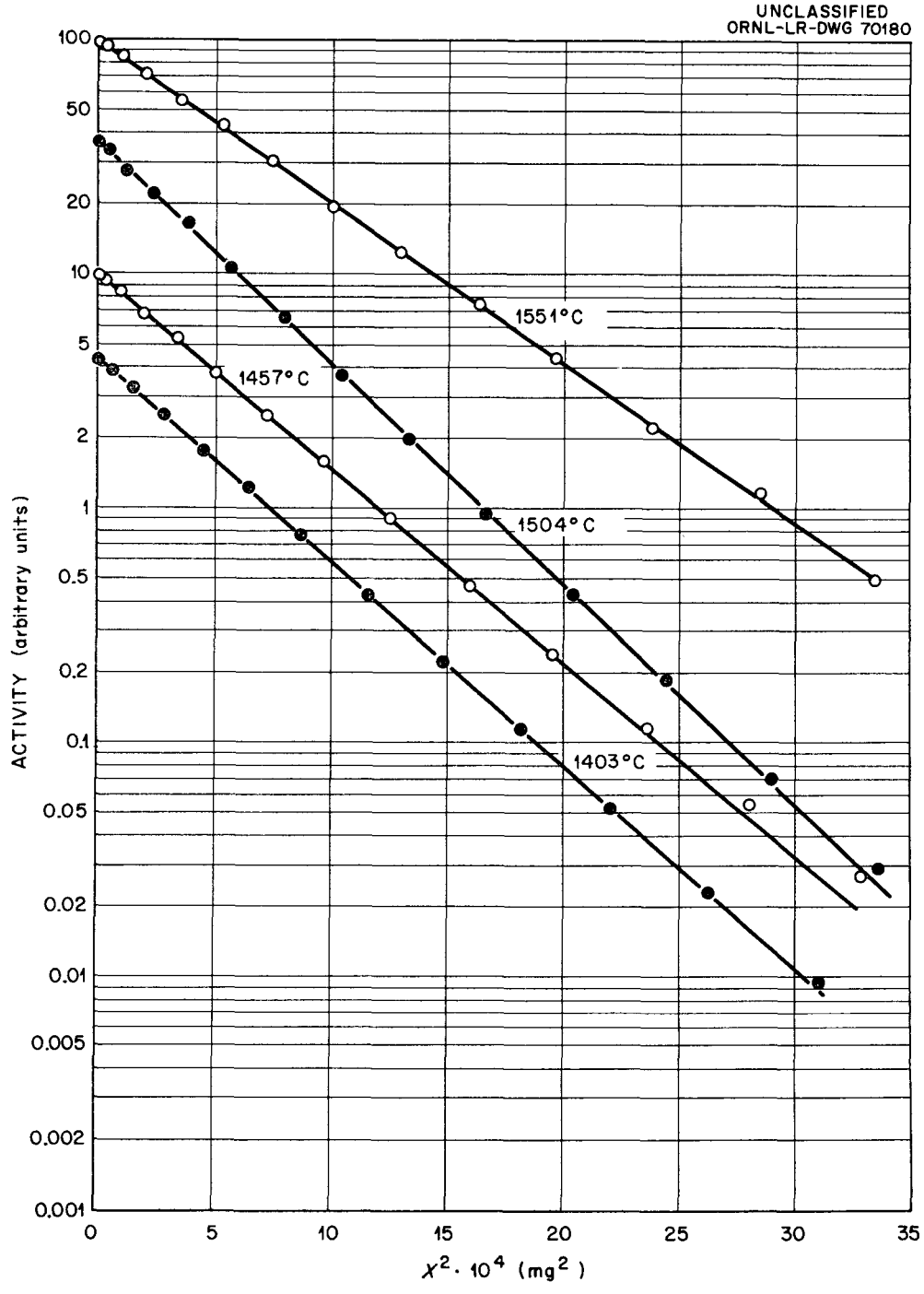

Figure 18. Penetration profiles for diffusion of zirconium-95 in zirconium at 1403, 1457, 1504, and 1551°C.

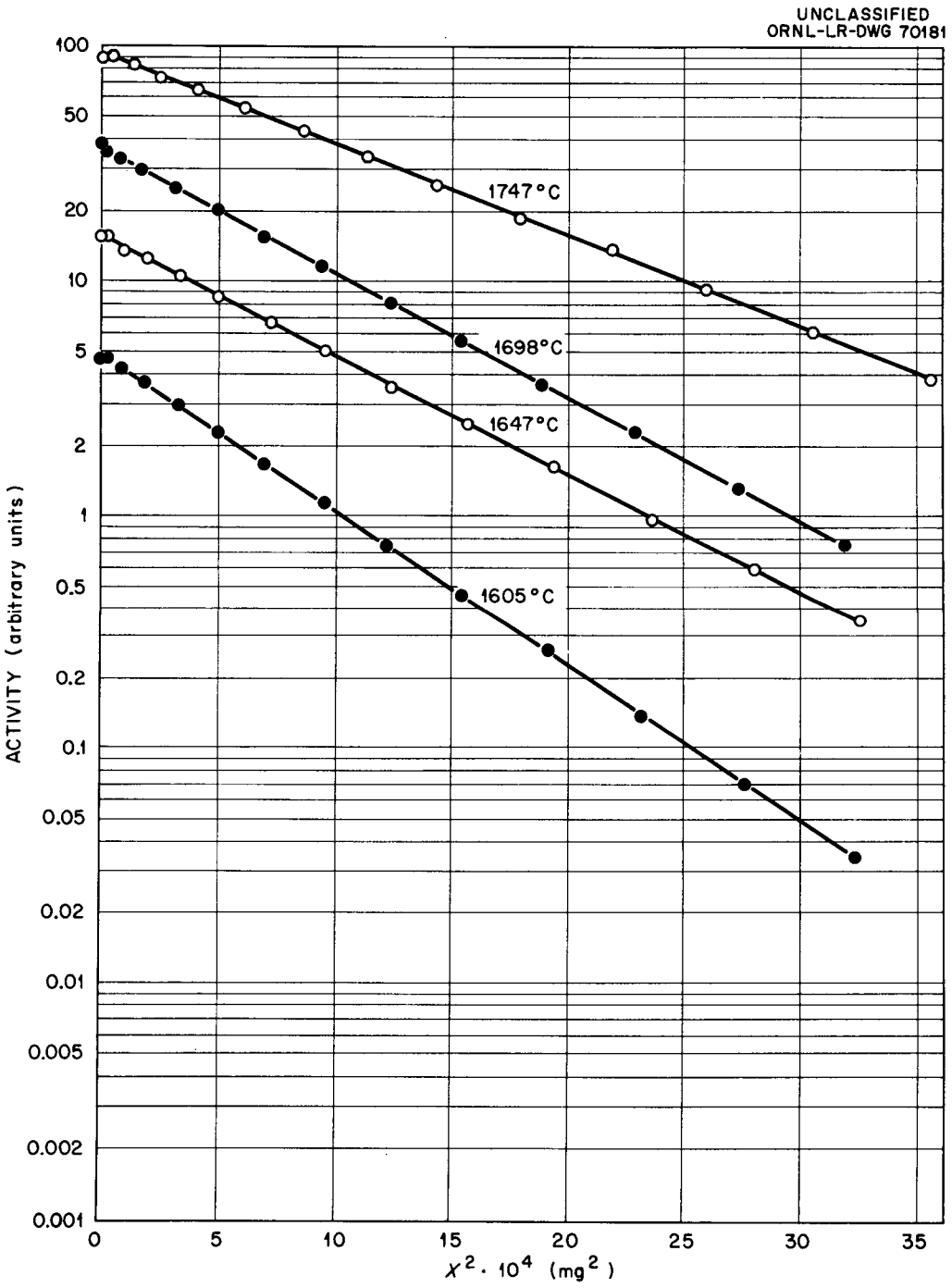

Figure 19. Penetration profiles for diffusion of zirconium-95 in zirconium at 1605, 1647, 1698, and 1747°C.

APPENDIX B

PENETRATION PROFILES FOR DIFFUSION OF NIOBIUM-95 IN ZIRCONIUM

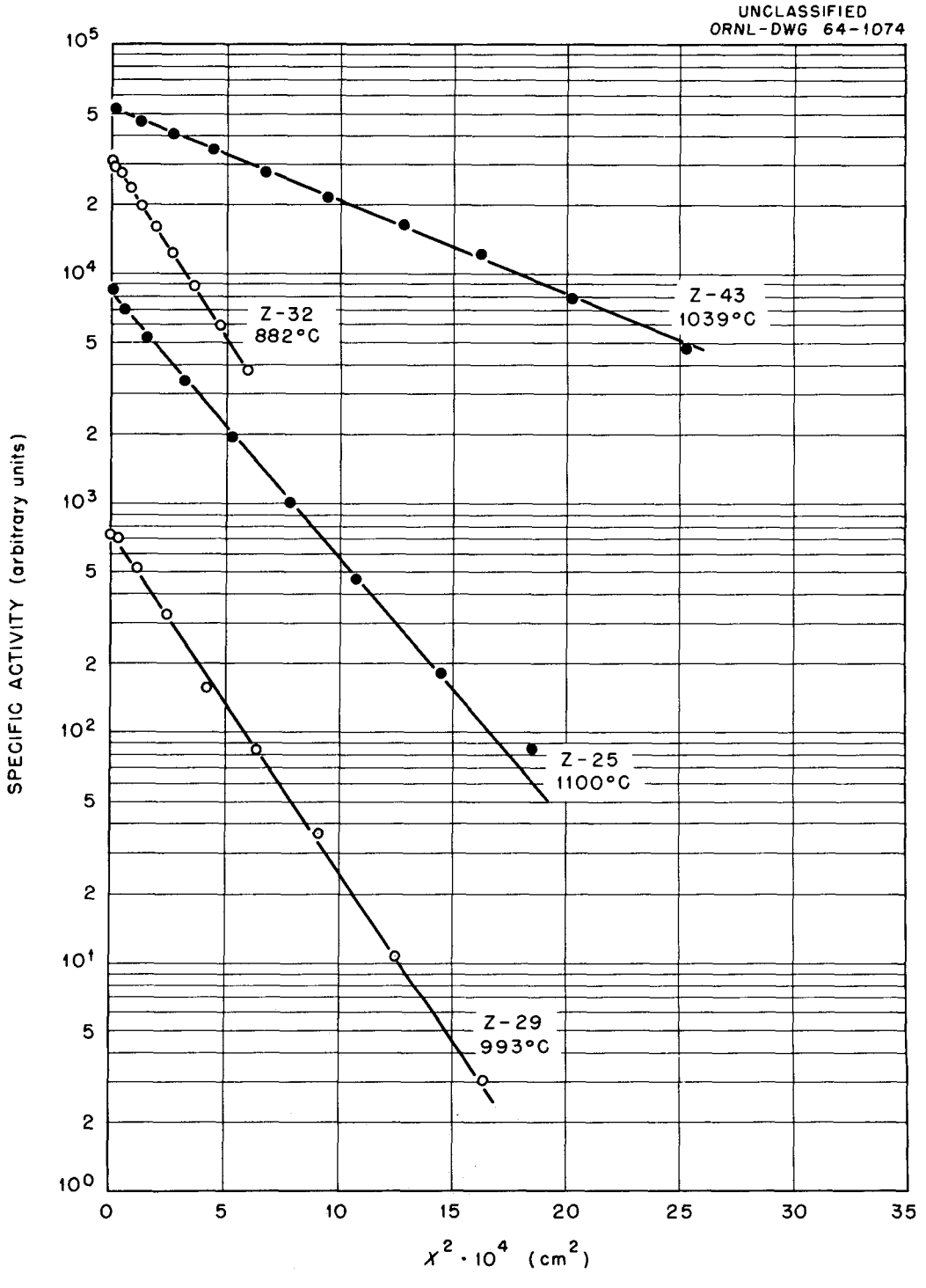

Figure 20. Penetration profiles for diffusion of niobium-95 in zirconium at 882, 993, 1039, and 1100°C.

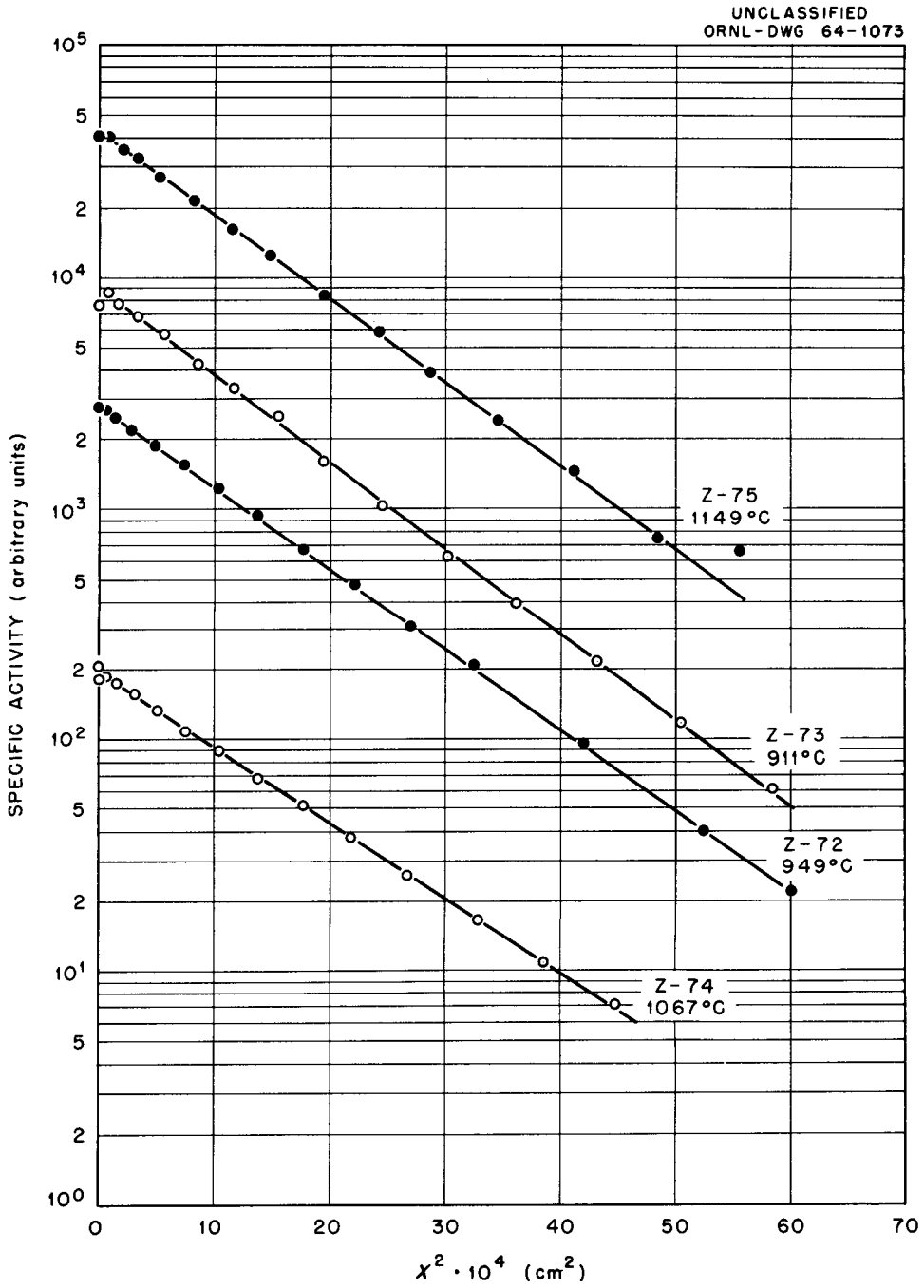

Figure 21. Penetration profiles for diffusion of niobium-95 in zirconium at 911, 949, 1067, and 1149°C.

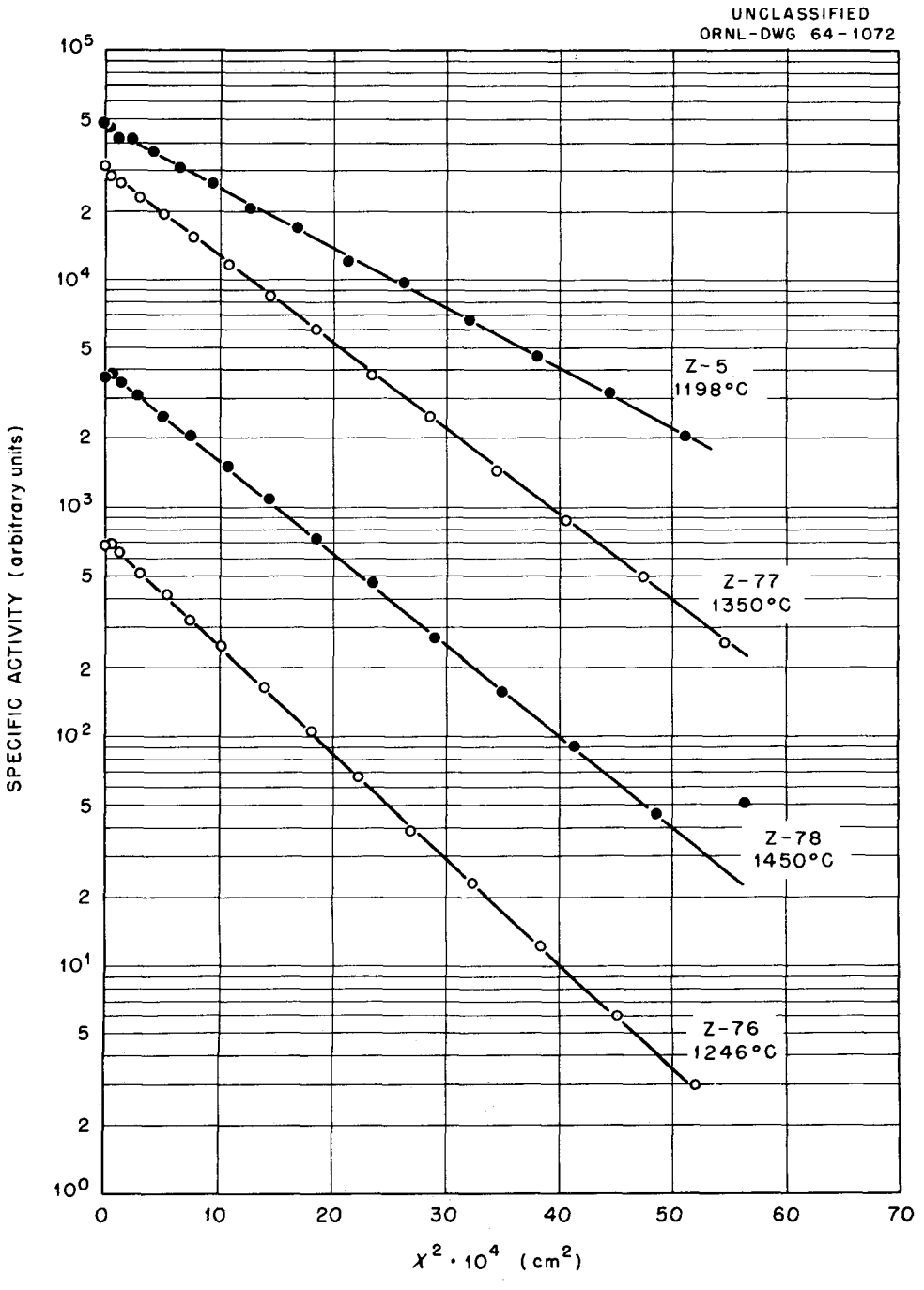

Figure 22. Penetration profiles for diffusion of niobium-95 in zirconium at 1198, 1246, 1350, and 1450°C.

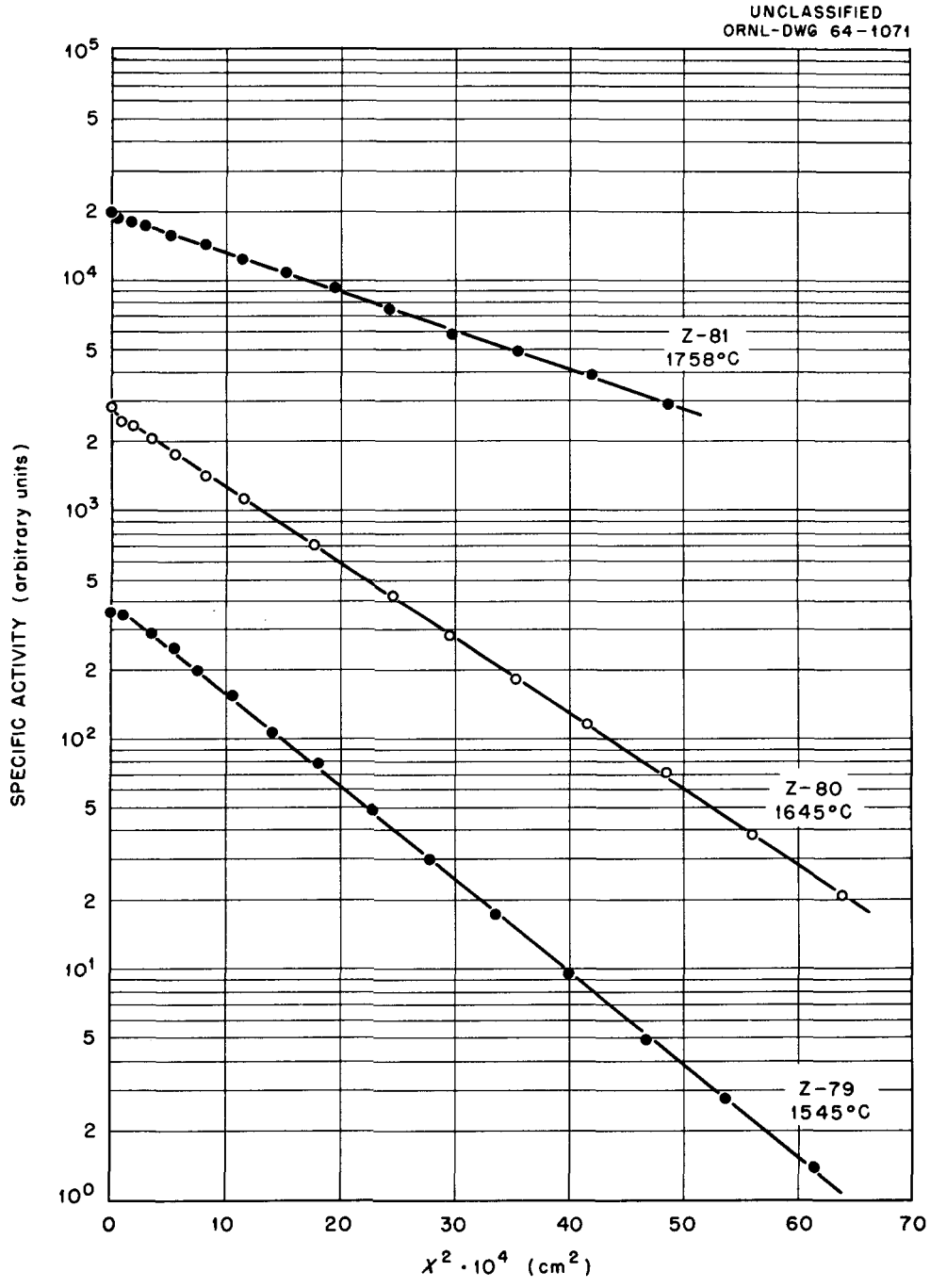

Figure 23. Penetration profiles for diffusion of niobium-95 in zirconium at 1545, 1645, and 1758°C.

APPENDIX C

PENETRATION PROFILES FOR DIFFUSION OF VANADIUM-48 IN VANADIUM

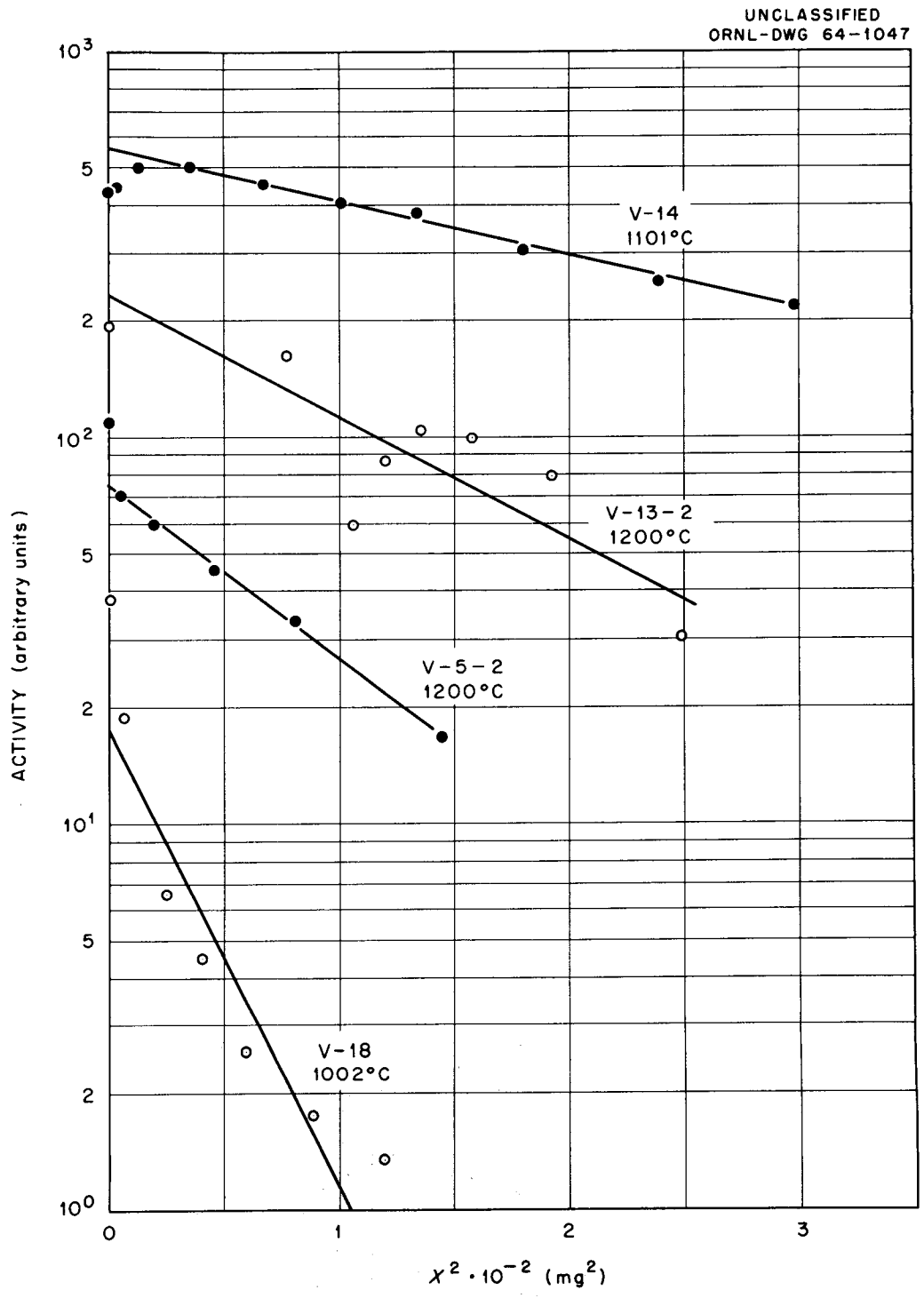

Figure 24. Penetration profiles for diffusion of vanadium-48 in vanadium at 1002, 1101, and 1200°C.

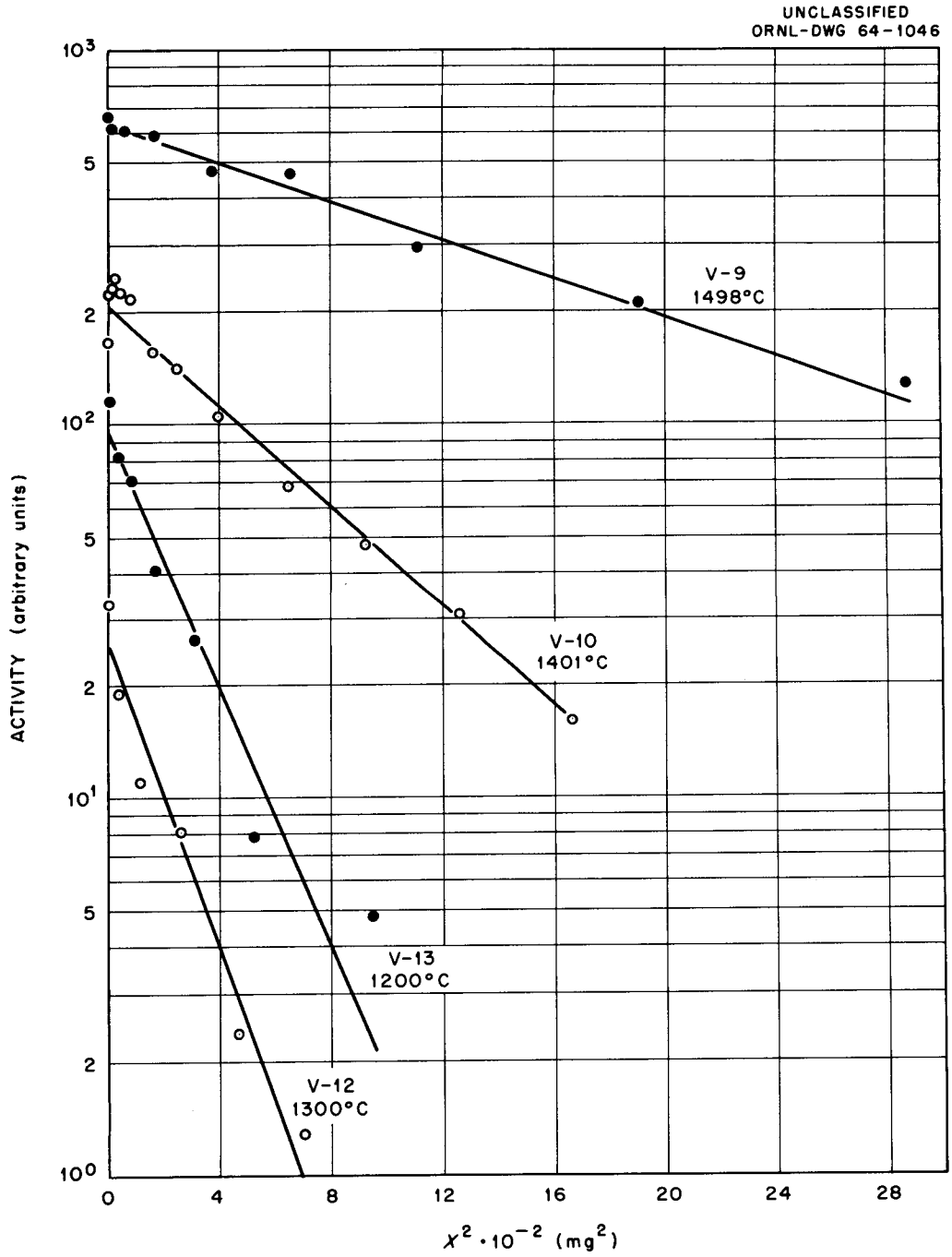

Figure 25. Penetration profiles for diffusion of vanadium-48 in vanadium at 1200, 1300, 1401, and 1498°C.

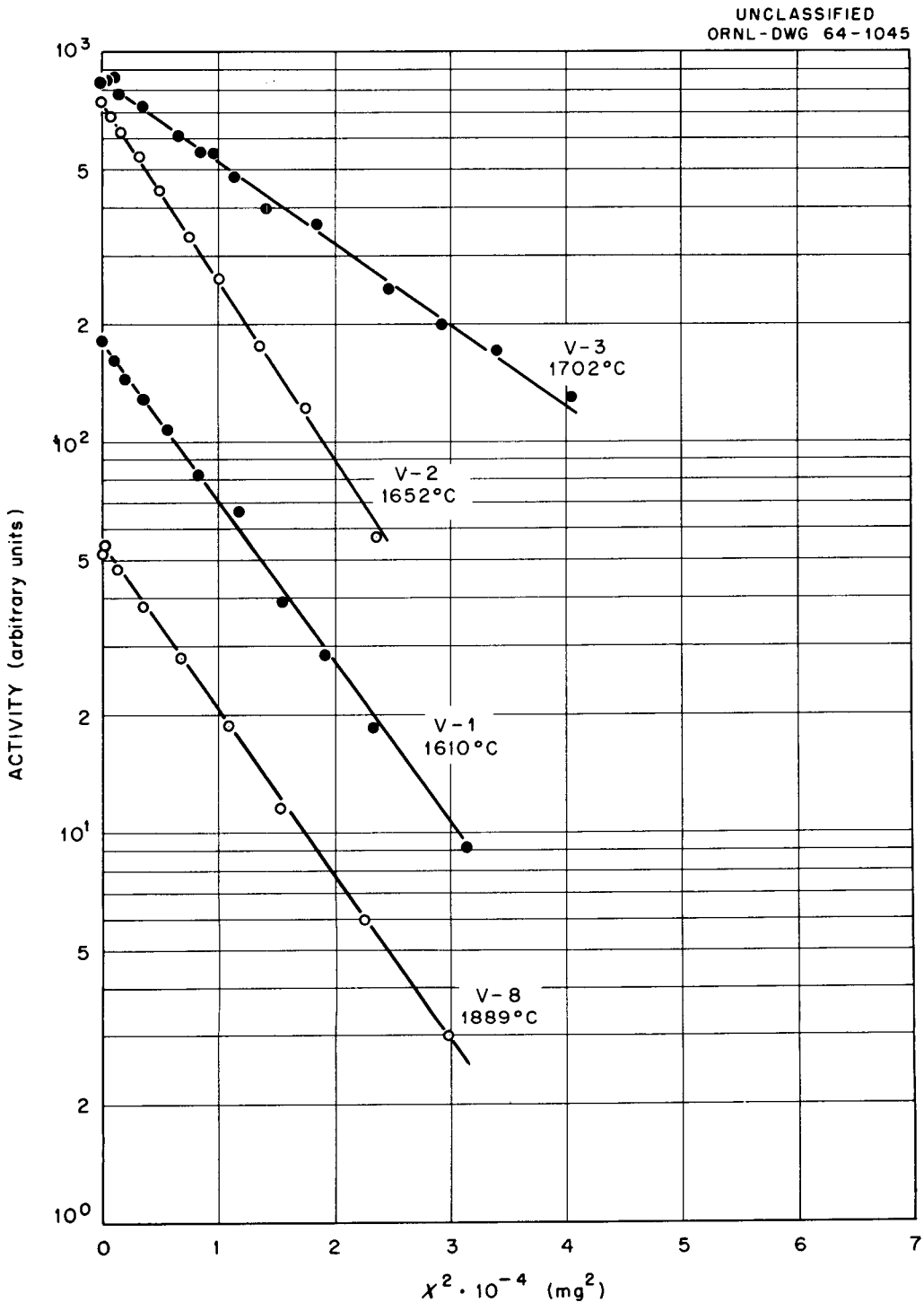

Figure 26. Penetration profiles for diffusion of vanadium-48 in vanadium at 1610, 1652, 1702, and 1889°C.

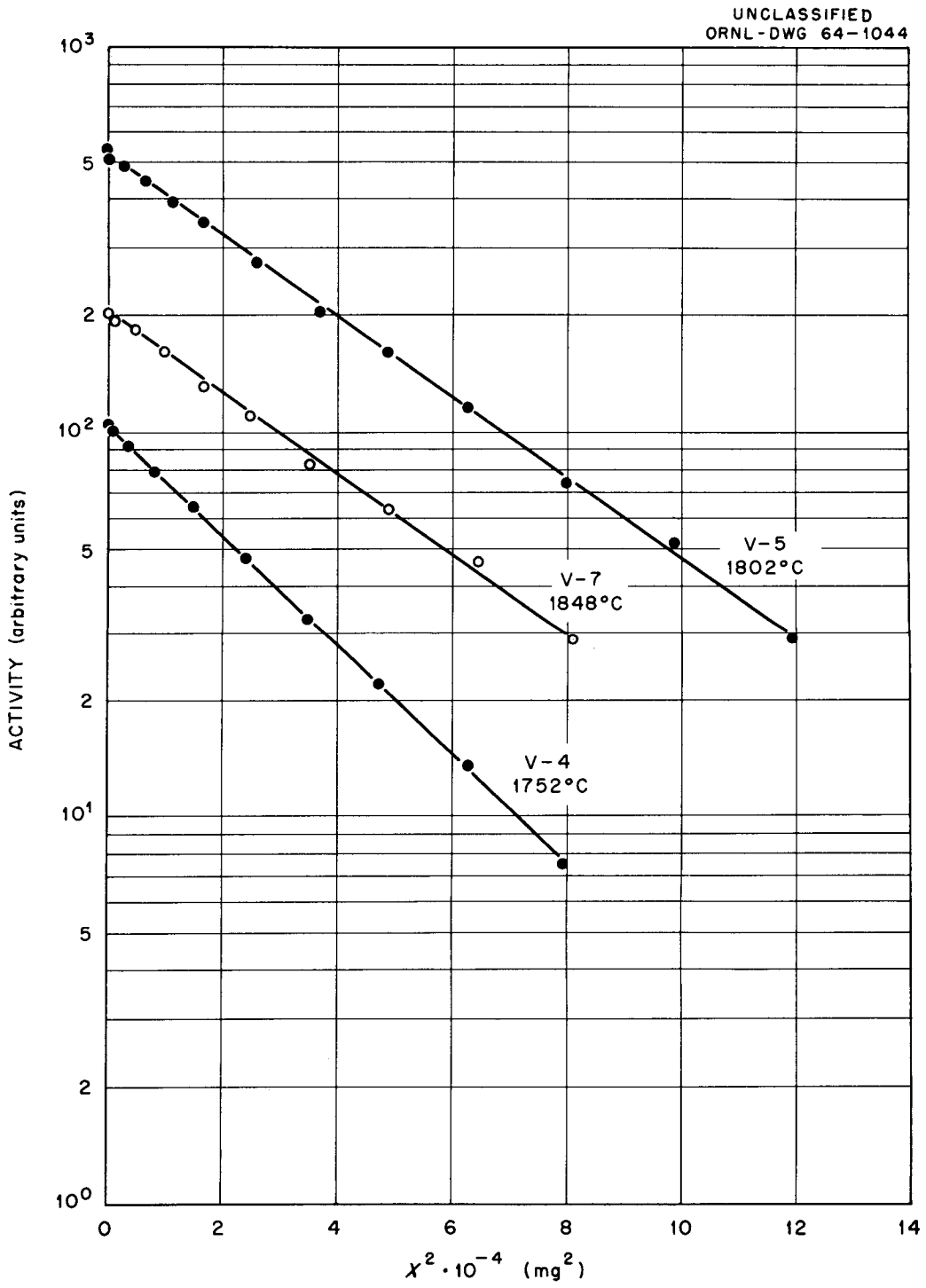

Figure 27. Penetration profiles for diffusion of vanadium-48 in vanadium at 1752, 1802, and 1848 °C.

APPENDIX D

PENETRATION PROFILES FOR DIFFUSION OF NIOBIUM-95 AND TANTALUM-182 IN NIOBIUM

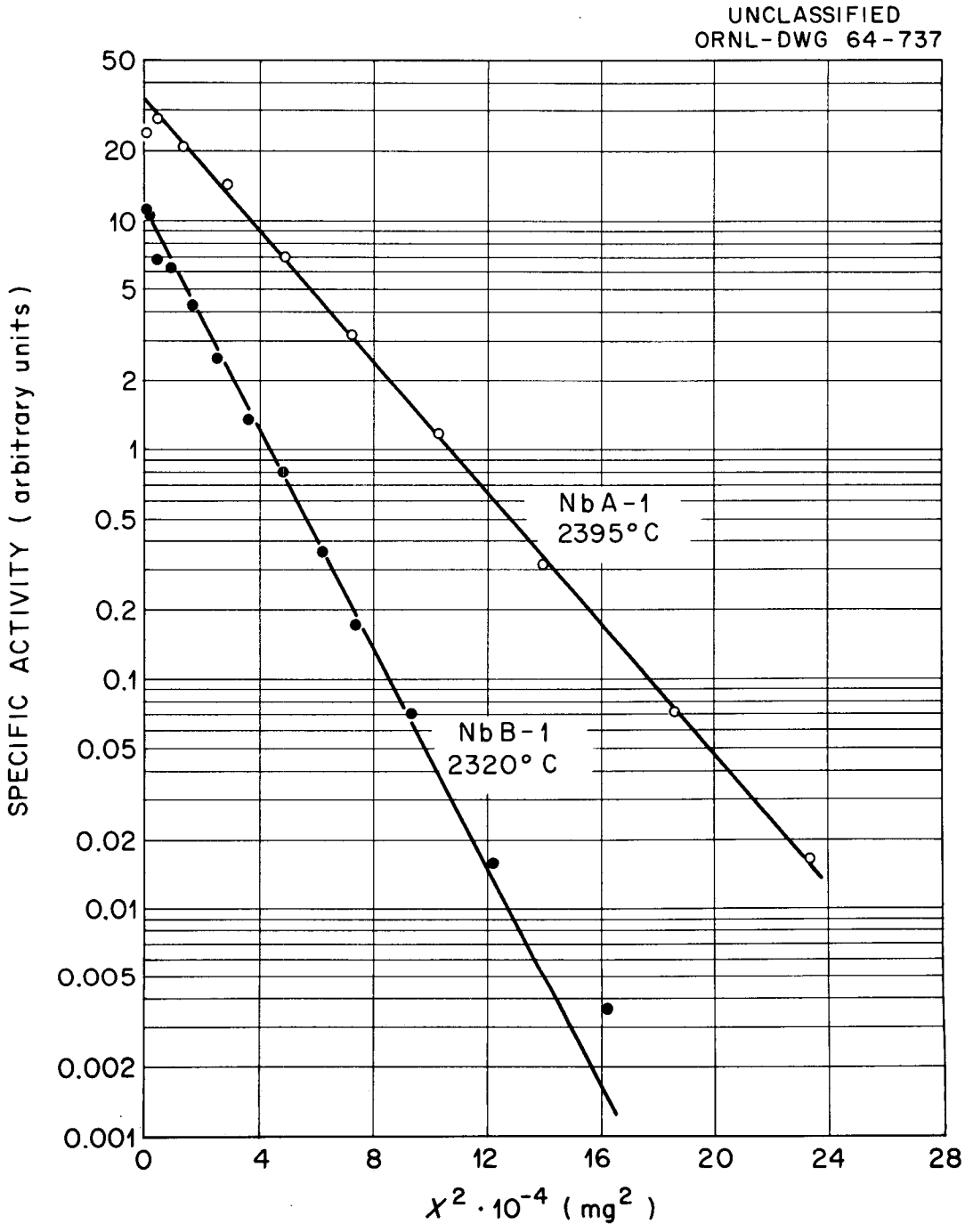

Figure 28. Penetration profiles for diffusion of niobium-95 in niobium at 2320 and 2395°C.

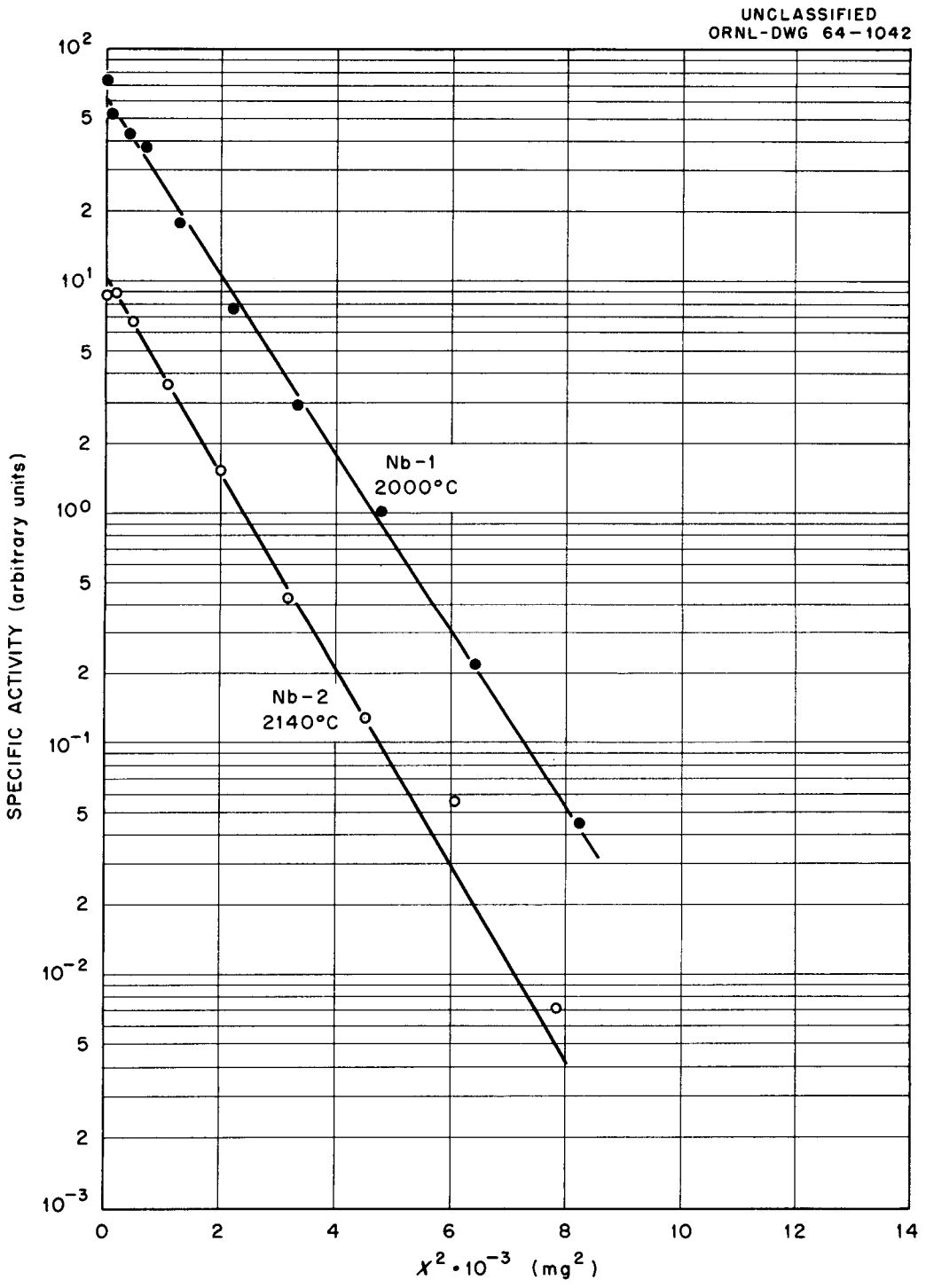

Figure 29. Penetration profiles for diffusion of niobium-95 in niobium at 2000 and 2140°C.

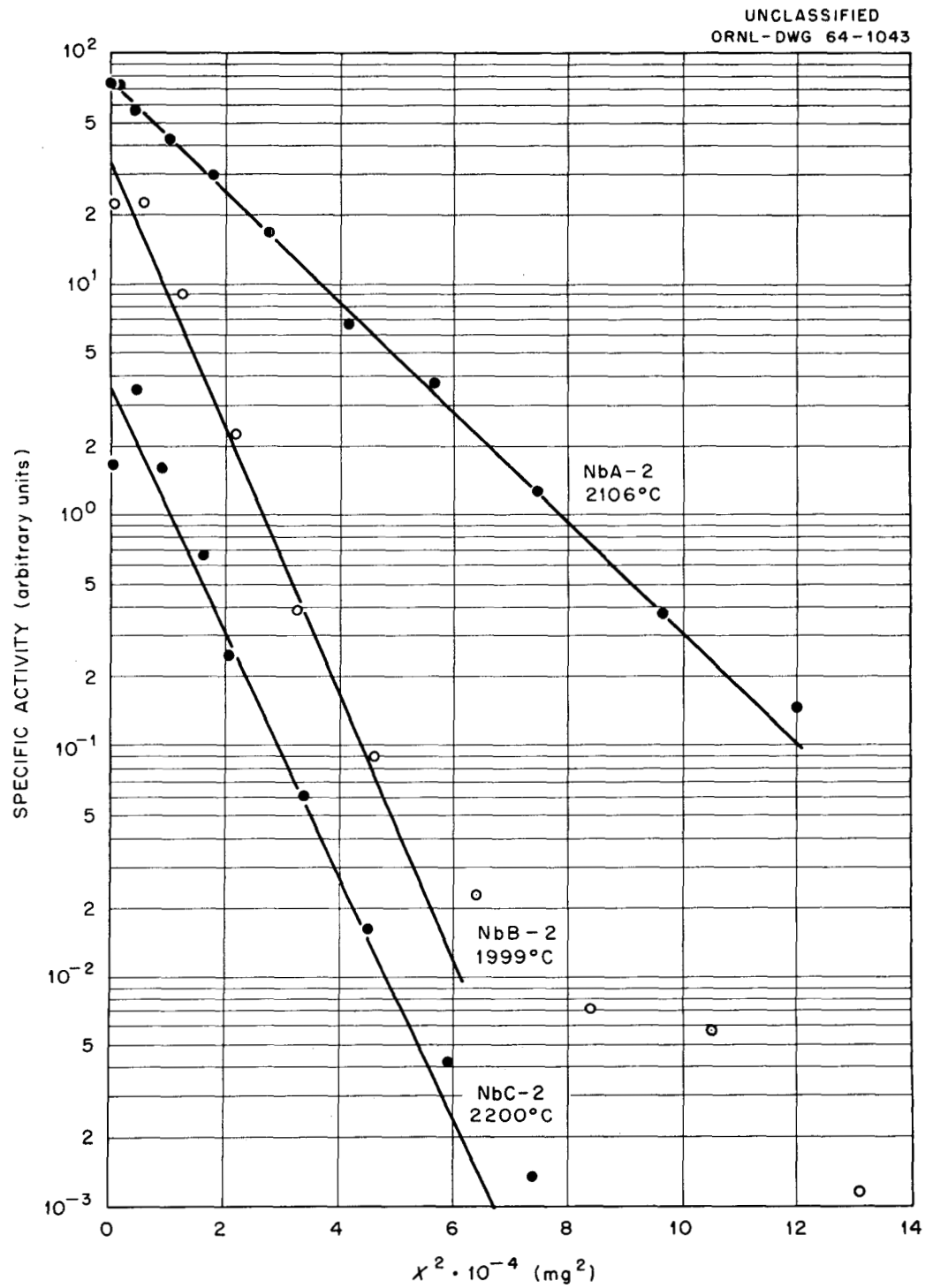

Figure 30. Penetration profiles for diffusion of niobium-95 in niobium at 1999, 2106, and 2200°C.

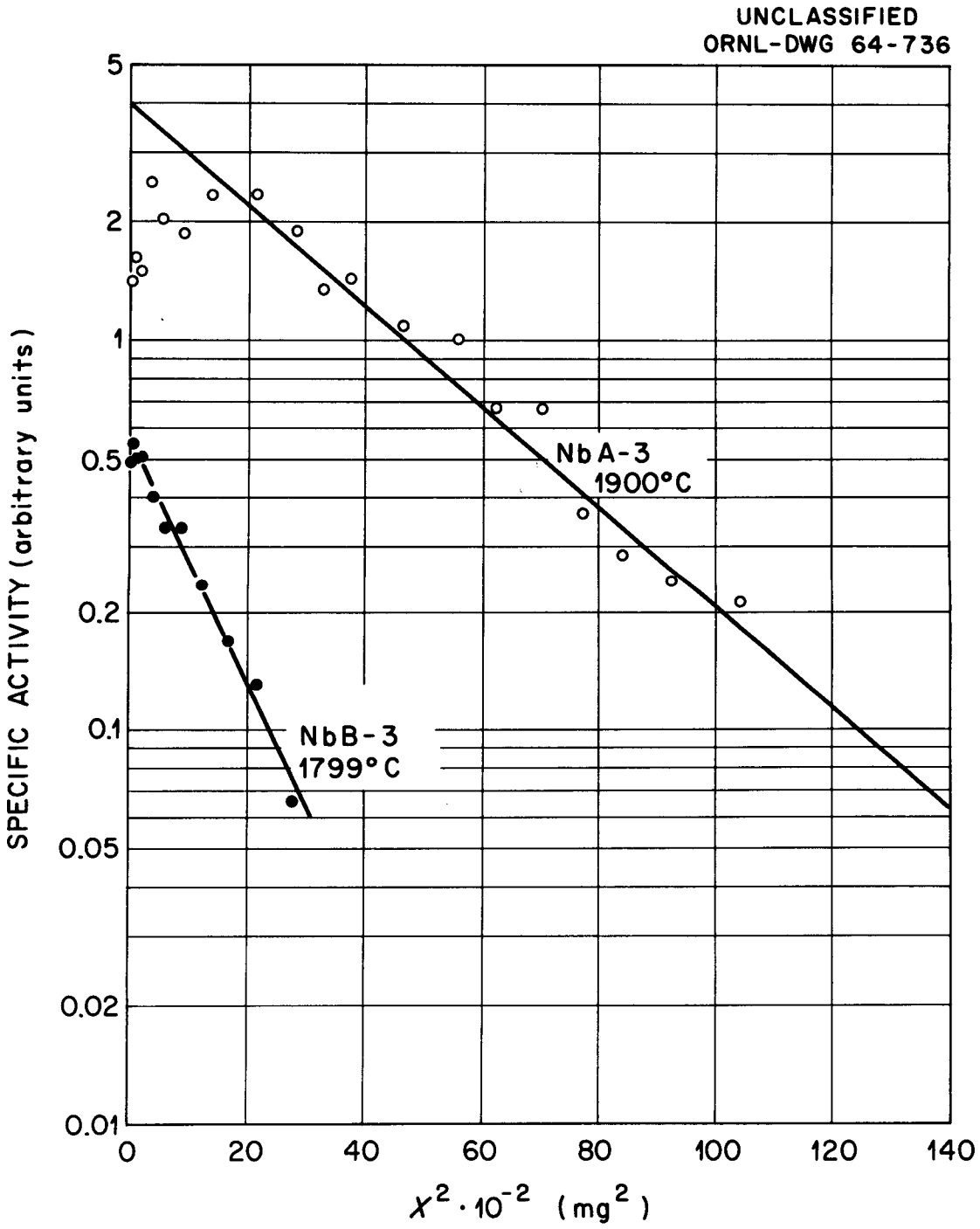

Figure 31. Penetration profiles for diffusion of niobium-95 in niobium at 1799 and 1900°C.

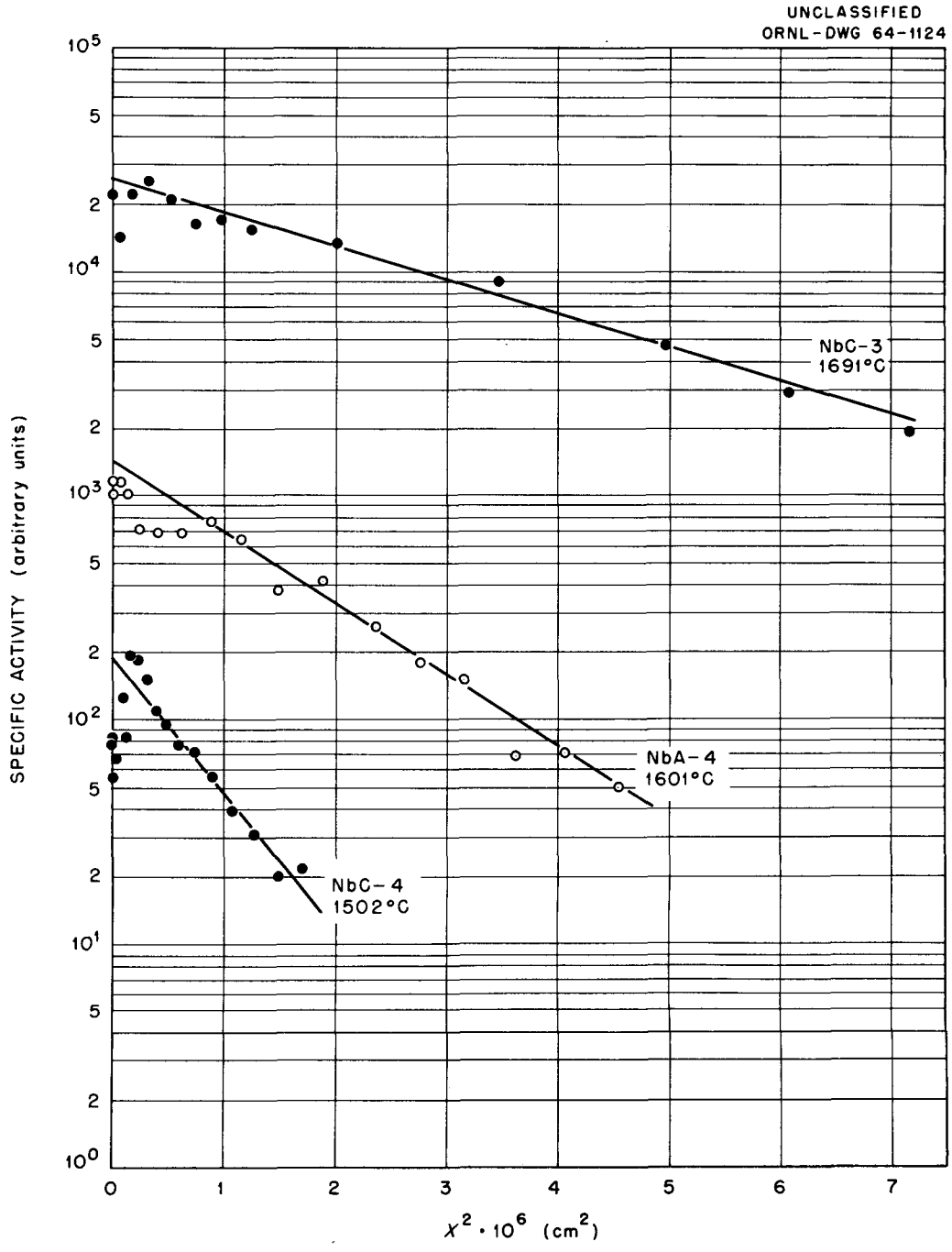

Figure 32. Penetration profiles for diffusion of niobium-95 in niobium at 1502, 1601, and 1691°C.

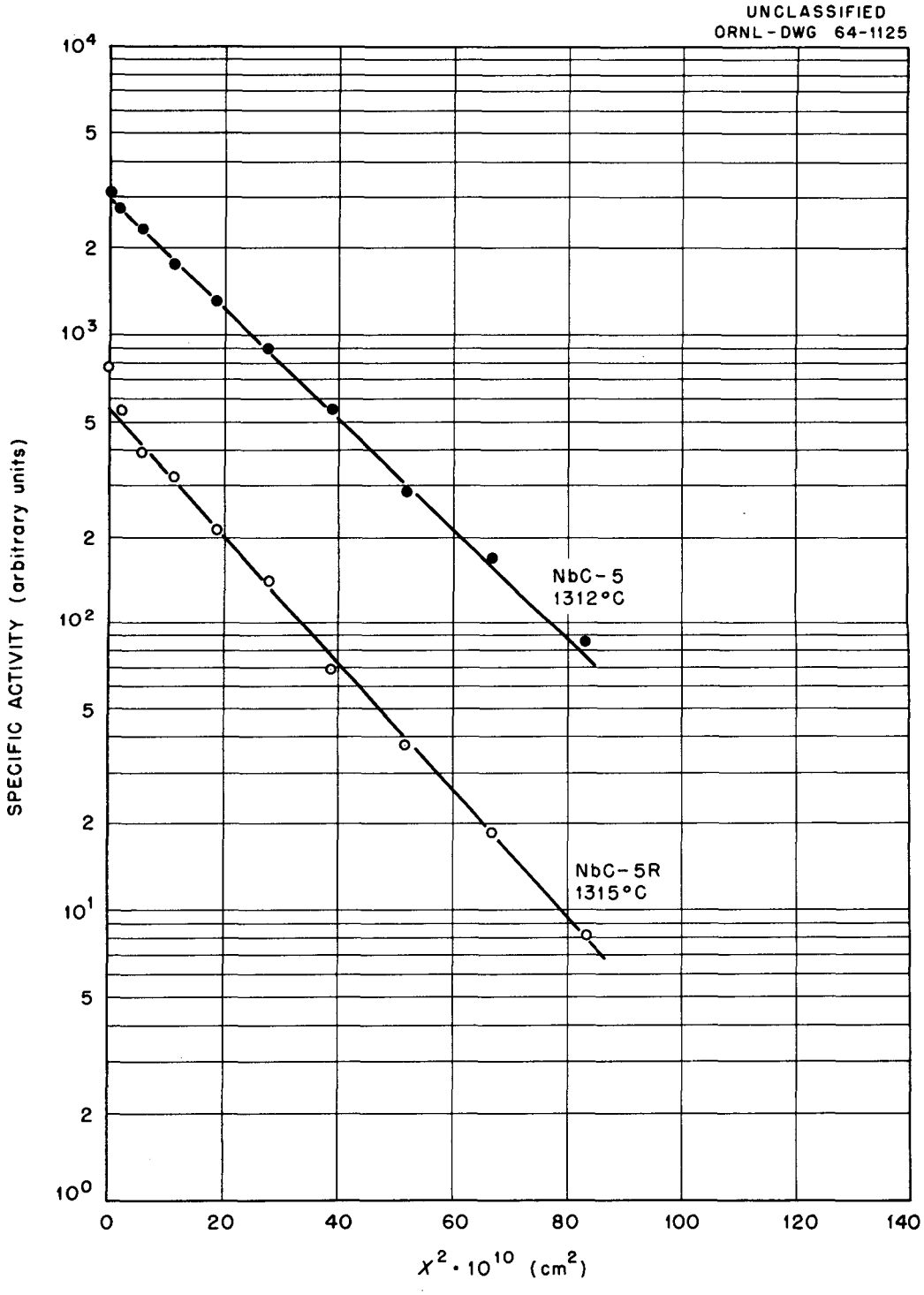

Figure 33. Penetration profiles for diffusion of niobium-95 in niobium at 1312 and 1315°C.

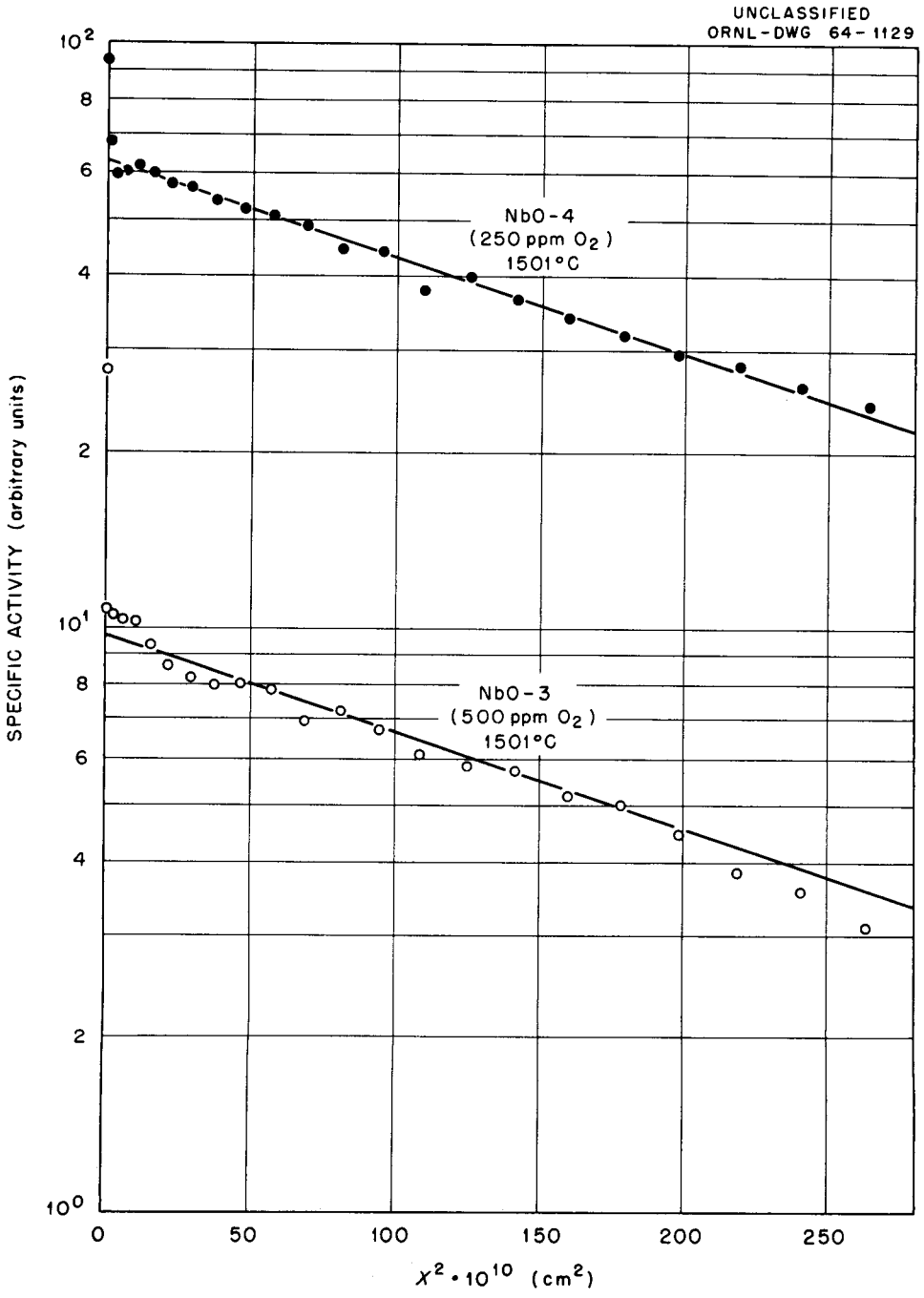

Figure 34. Penetration profiles for diffusion of niobium-95 in oxygen-doped niobium at 1501°C.

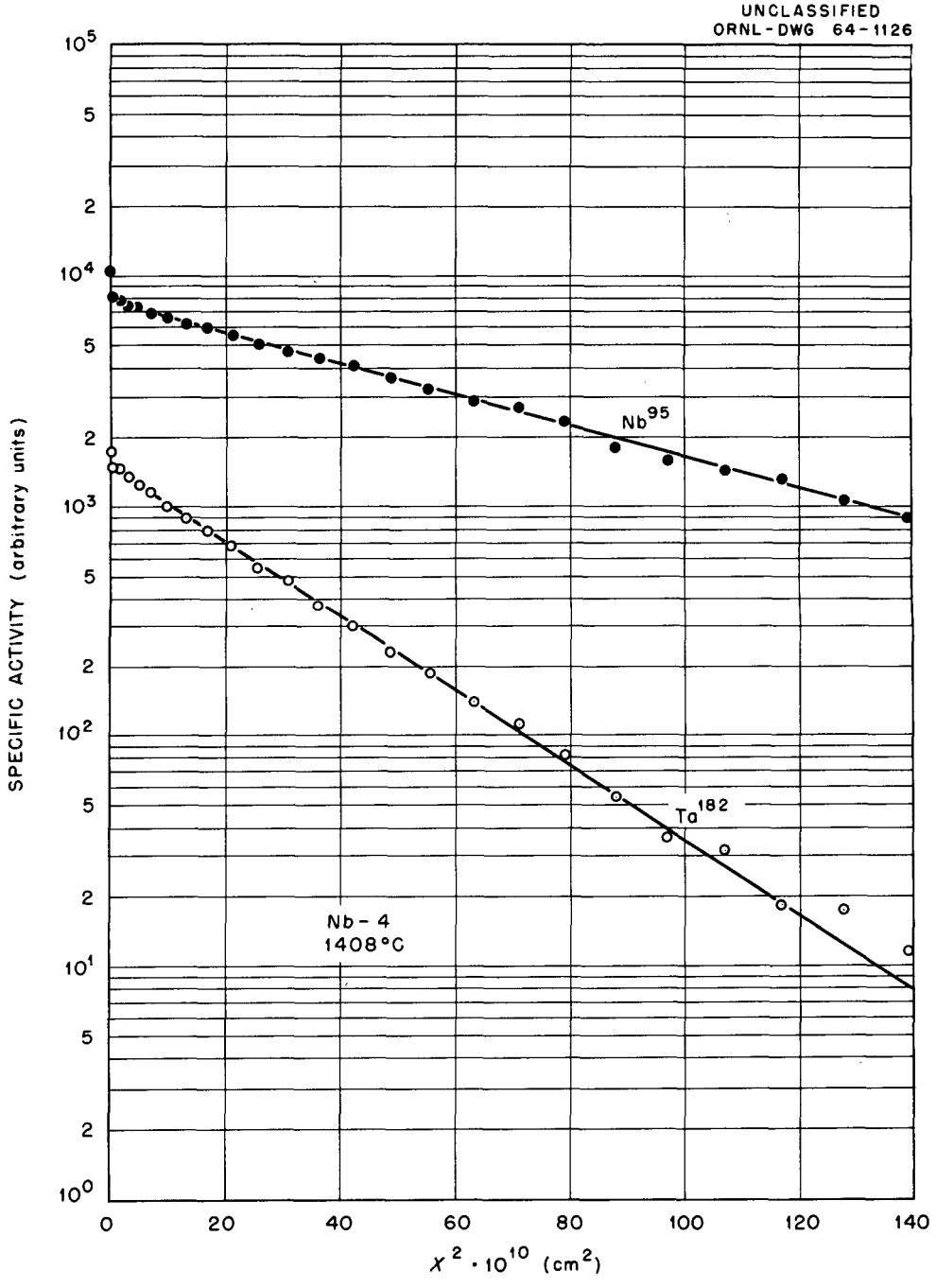

Figure 35. Penetration profiles for diffusion of niobium-95 and tantalum-182 in niobium at 1408°C.

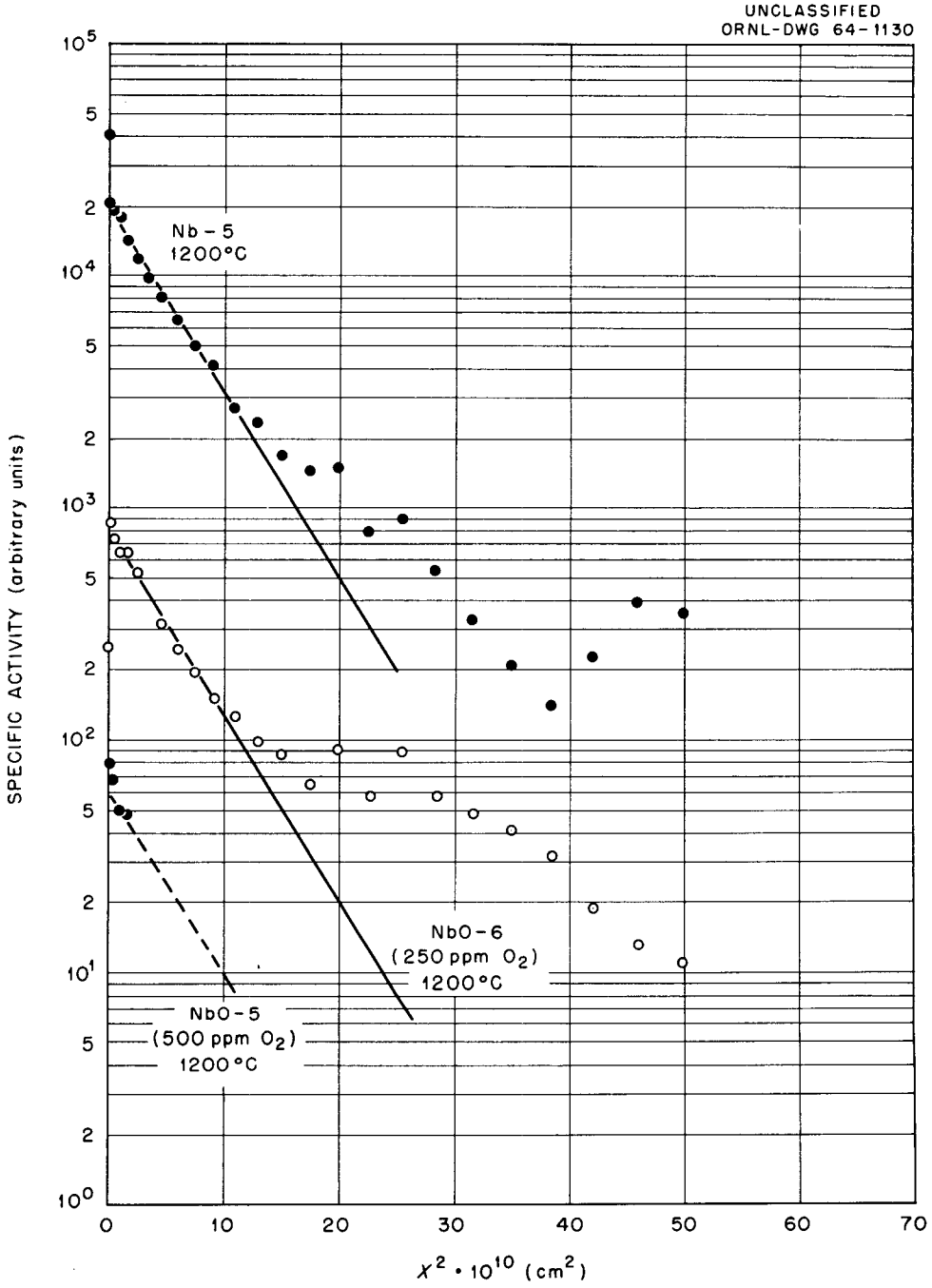

Figure 36. Penetration profiles for diffusion of niobium-95 in niobium and in oxygen-doped niobium at 1200°C.

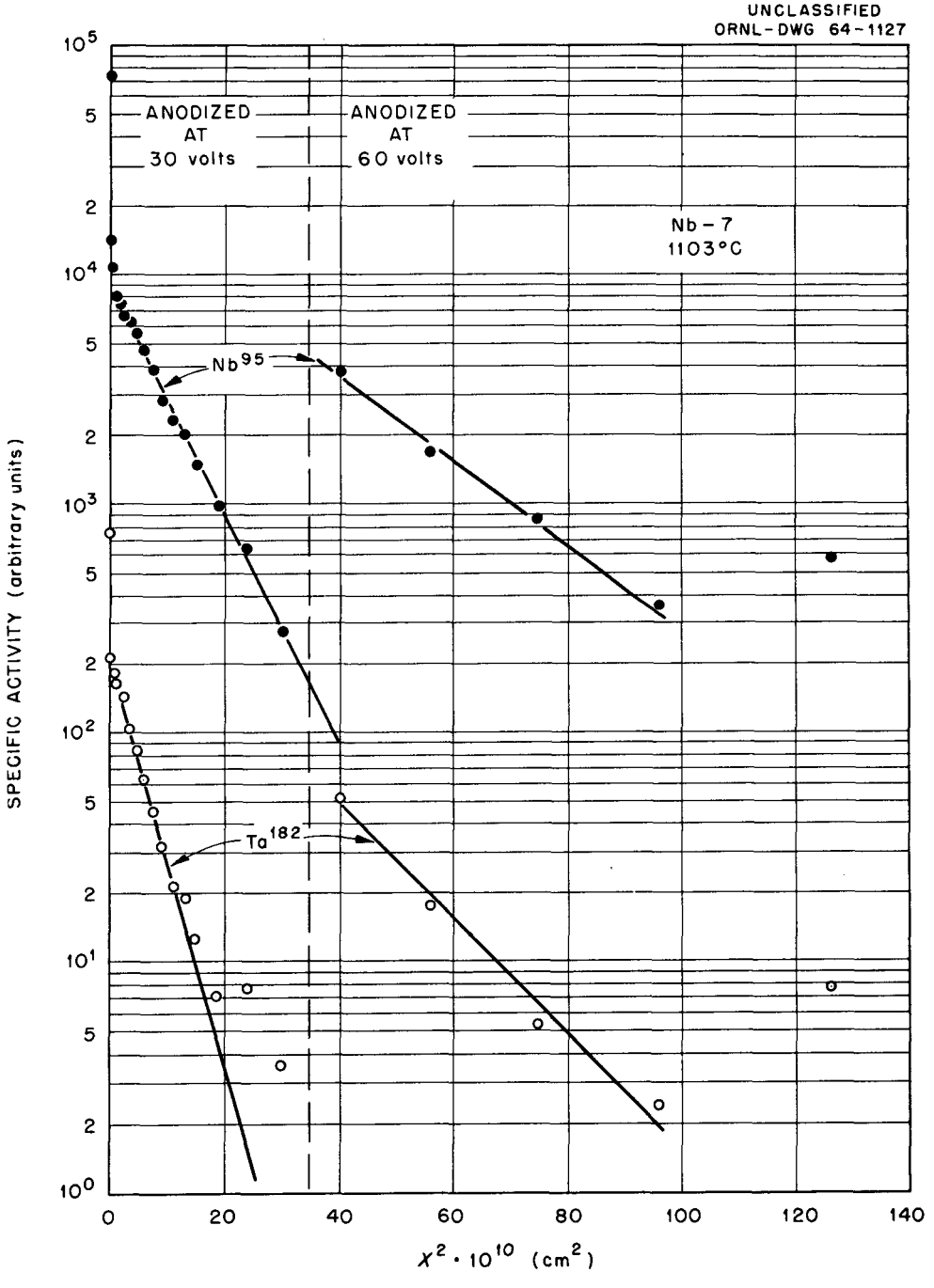

Figure 37. Penetration profiles for diffusion of niobium-95 and tantalum-182 in niobium at 1103°C.

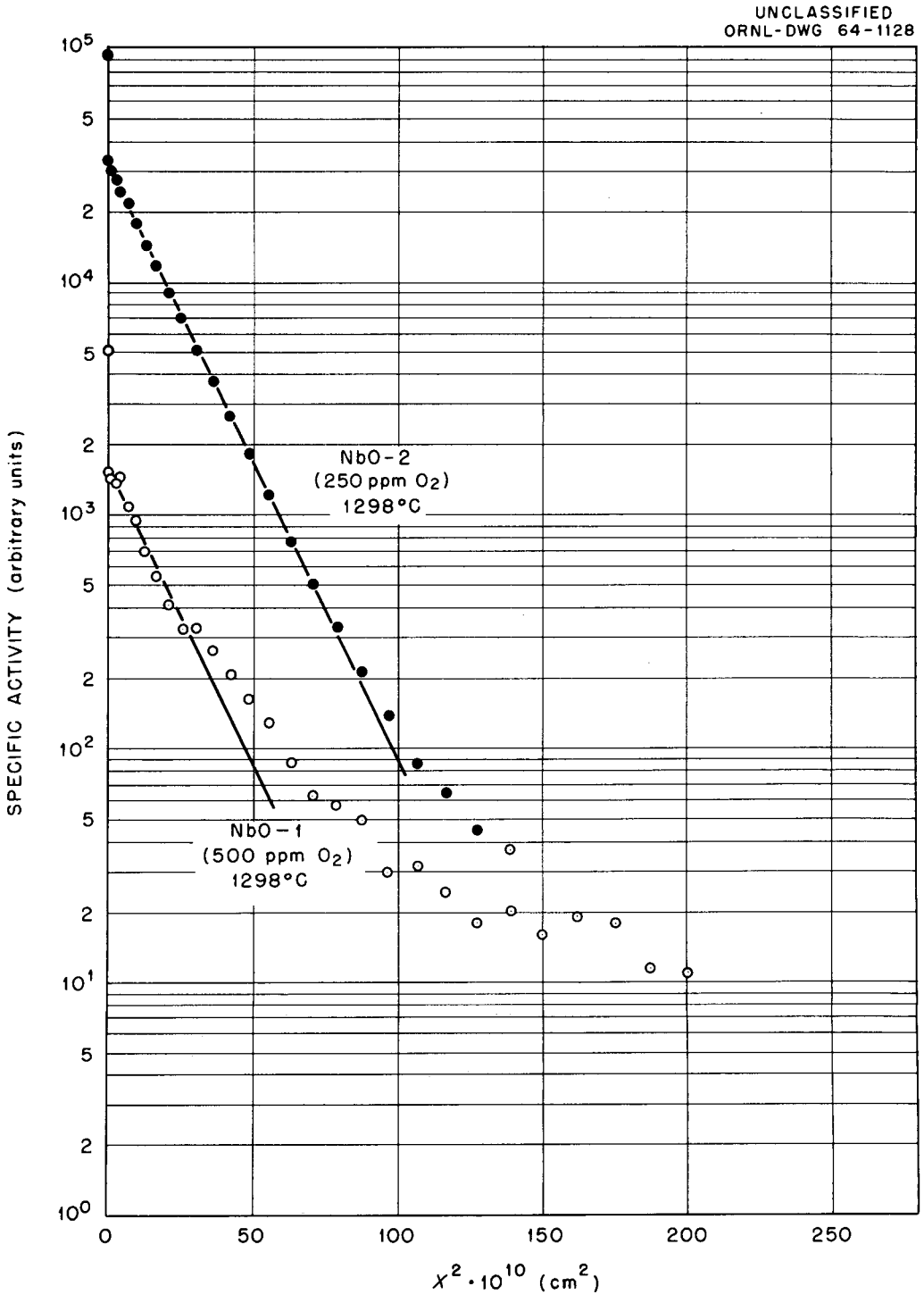

Figure 38. Penetration profiles for diffusion of niobium-95 in oxygen-doped niobium at 1298°C.

APPENDIX E

PENETRATION PROFILES FOR DIFFUSION OF NIOBIUM-95 IN TANTALUM

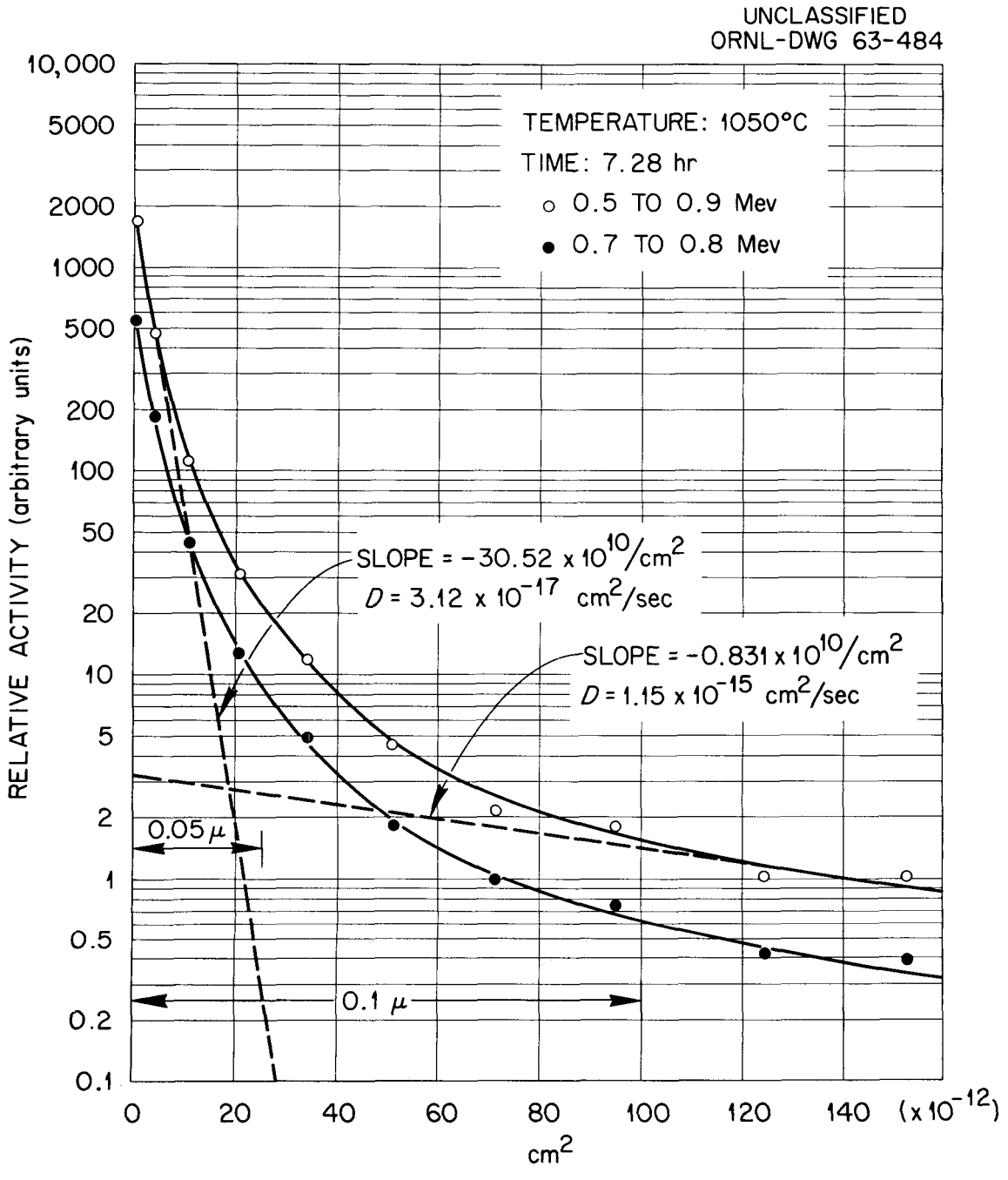

Figure 39. Penetration profiles for diffusion of niobium-95 in tantalum at 1050°C.

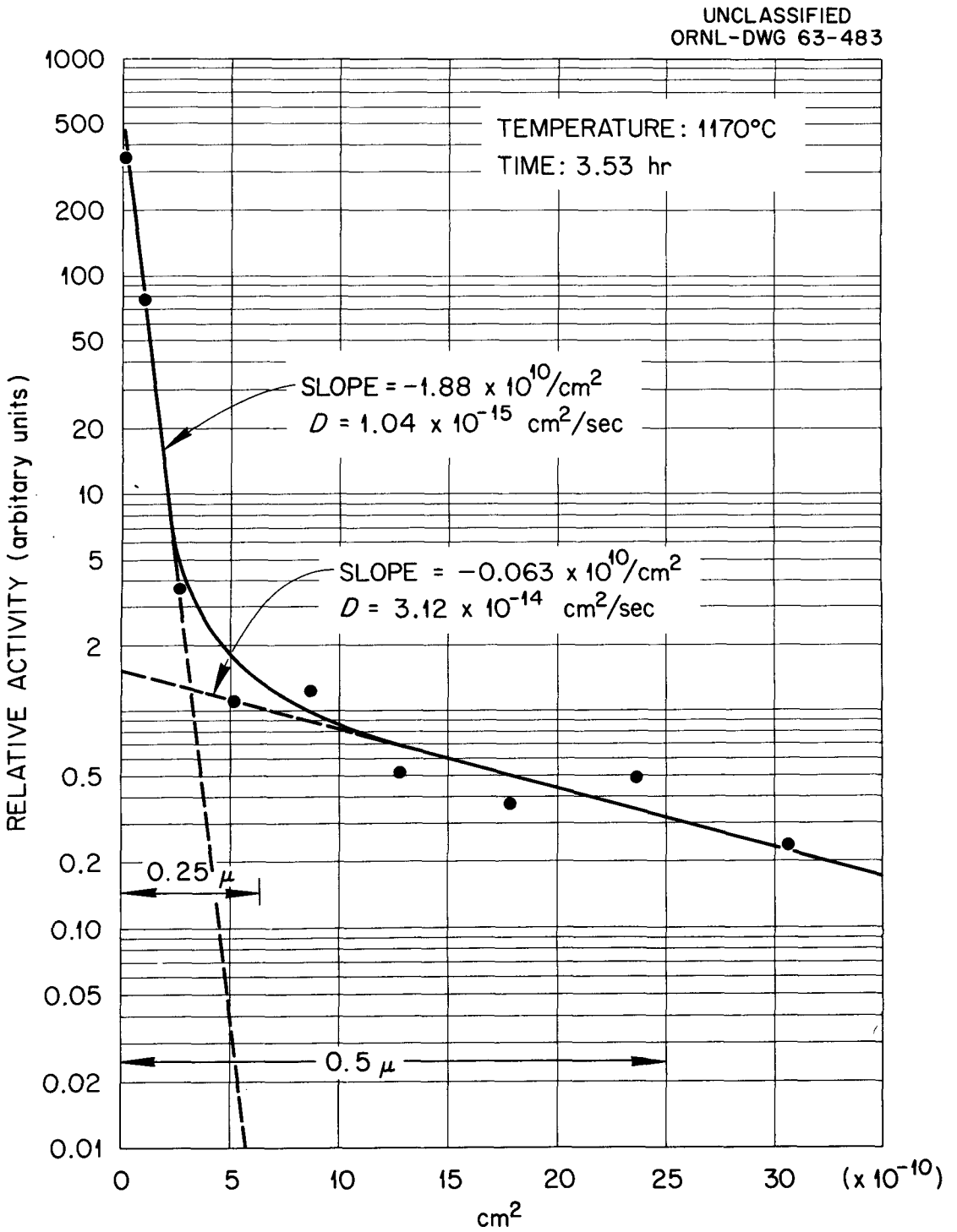

Figure 40. Penetration profile for diffusion of niobium-95 in tantalum at 1170°C.

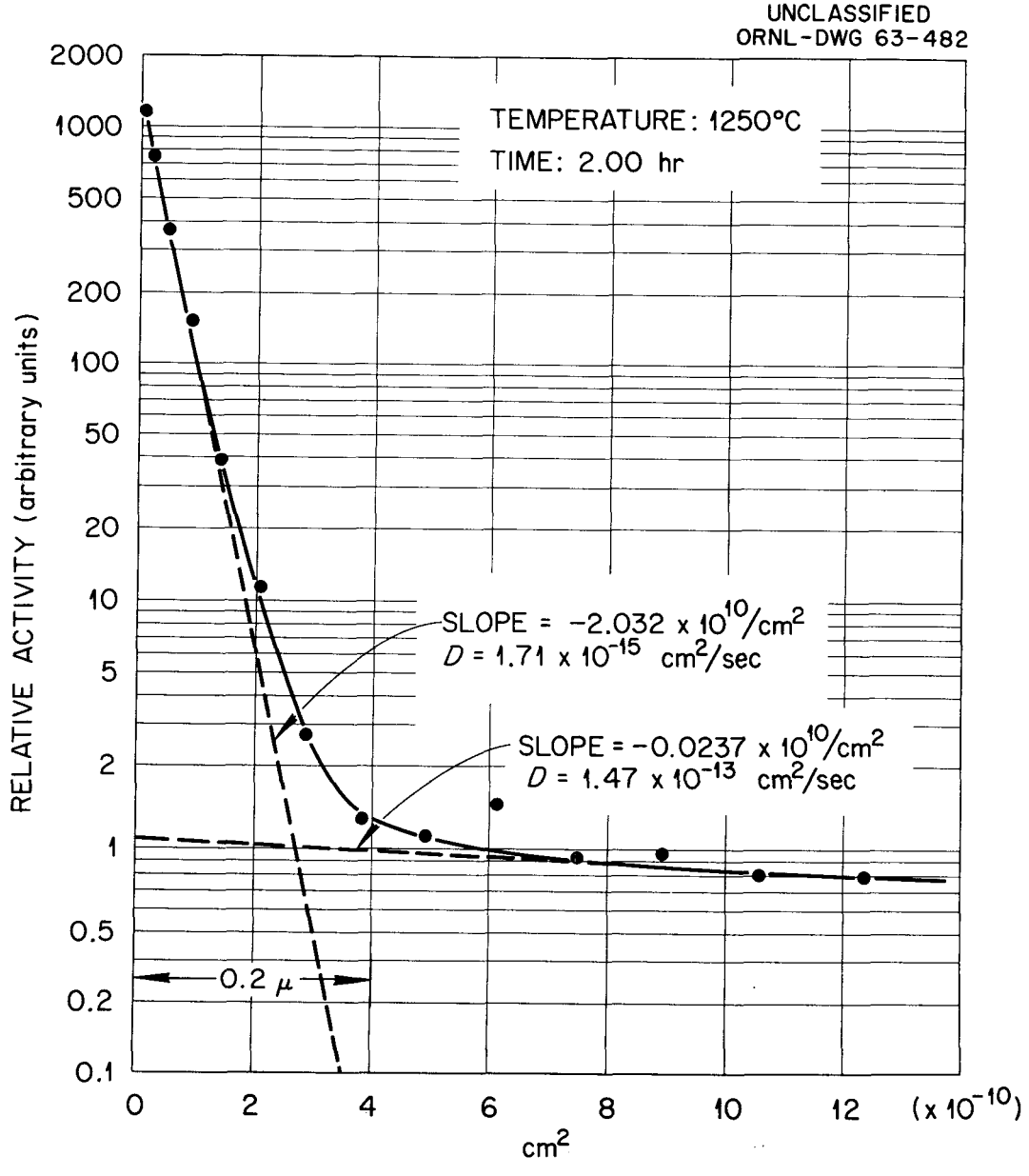

Figure 41. Penetration profile for diffusion of niobium-95 in tantalum at 1250°C.

ORNL-3617
UC-25 – Metals, Ceramics, and Materials
TID-4500 (30th ed.)

INTERNAL DISTRIBUTION

1–3. Central Research Library
4. Reactor Division Library
5–6. ORNL – Y-12 Technical Library
Document Reference Section
7–26. Laboratory Records Department
27. Laboratory Records, ORNL RC
28. ORNL Patent Office
29. R. E. Adams
30. R. G. Berggren
31. W. K. Biermann
32. C. M. Blood
33. W. E. Brundage
34. J. Burka
35. M. M. Chiles
36. E. L. Compere
37. T. F. Connolly
38. J. H. Crawford, Jr.
39. F. L. Culler
40. J. E. Cunningham
41. J. H. DeVan
42. J. R. DiStefano
43. W. S. Ernst, Jr.
44. J. I. Federer
45. J. H Frye, Jr.
46. R. G. Gilliland
47. George Hallerman
48. D. Heitkamp
49–53. M. R. Hill
54. N. E. Hinkle
55. D. O. Hobson
56. G. H. Jenks
57. H. W. Joy
58. G. W. Keilholtz
59. R. H. Lafferty, Jr.
60. C. E. Larson
61. A. Litman
62–76. T. S. Lundy
77. H. G. MacPherson
78. W. R. Martin
79. H. E. McCoy
80. J. F. Murdock
81. F. H. Neill
82. R. E. Pawel
83. M. L. Picklesimer
84. J. C. Pigg
85. J. J. Pinajian
86. S. A. Rabin
87. R. E. Reed, Sr.
88. J. E. Savolainen
89. C. E. Sessions
90. O. Sisman
91. J. T. Stanley
92. W. J. Stelzman
93. R. L. Stephenson
94. J. O. Stiegler
95. J. A. Swartout
96. W. C. Thurber
97–134. D. B. Trauger
135. R. A. Vandermeer
136. M. S. Wechsler
137. A. M. Weinberg
138. J. A. Wheeler, Jr.
139. R. P. Wichner
140. F. R. Winslow
141. A. A. Burr (consultant)
142. J. R. Johnson (consultant)
143. C. S. Smith (consultant)
144. R. Smoluchowski (consultant)

EXTERNAL DISTRIBUTION

145. C. M. Adams, Jr., Massachusetts Institute of Technology
146. D. E. Baker, General Electric, Hanford
147. R. J. Borg, Lawrence Radiation Laboratory
148. C. R. Brooks, University of Tennesssee
149–150. D. F. Cope, AEC, ORO
151. J. A. Davies, Atomic Energy of Canada, Limited
152. W. E. Deeds, University of Tennessee
153. Ersel Evans, General Electric, Hanford
154. Sharon Fischer, University of Cincinnati
155. D. Graham, NASA Lewis Research Center
156. J. L. Gregg, Cornell University
157. A. G. Guy, University of Florida
158. W. C. Hagel, General Electric Company
159. G. W. Kidson, Atomic Energy of Canada, Limited
160. W. D. Klopp, NASA Lewis Research Center
161. R. L. Maxwell, University of Tennessee
162. R. R. Nash, NASA, Washington, D.C.
163. T. Oishi, University of California
164. R. F. Peart, University of Illinois
165. Research and Development, ORO
166. F. N. Rhines, University of Florida
167. S. J. Rothman, Argonne National Laboratory
168. P. G. Sherman, Carnegie Institute of Technology
169. J. Simmons, AEC, Washington, D.C.
170. L. M. Slifkin, University of North Carolina
171. J. Spruiell, University of Tennessee
172. E. E. Stansbury, University of Tennessee
173. D. K. Stevens, AEC, Washington, D.C.
174. R. A. Swalin, University of Minnesota
175. L. I. van Torne, University of California
176. C. A. Wert, University of Illinois
177–677. Given distribution as shown in TID-4500 (30th ed.) under Metals, Ceramics, and Materials category.